

**ATTENTIONAL NETWORKS IN AGING AND STROKE: AN FMRI STUDY**

**Erlend S. Dørum**

The degree philosophiae doctor (PhD)

Department of Psychology

Faculty of Social Sciences

University of Oslo

2024

© Erlend S. Dørum , 2024

*Series of dissertations submitted to the  
Faculty of Social Sciences, University of Oslo  
No. 1013*

ISSN 1504-3991

All rights reserved. No part of this publication may be reproduced or transmitted, in any form or by any means, without permission.

Cover: UiO.

Print production: Graphic center, University of Oslo.

## TABLE OF CONTENT

1. Acknowledgements
2. General summary
3. List of papers
4. Introduction
  - 4.1. fMRI
    - 4.1.1. Resting-state fMRI
    - 4.1.2. Task fMRI
  - 4.2. Visual attention and multiple object tracking
  - 4.3. Brain networks in aging
  - 4.4. Brain networks in stroke
5. Methods and Materials
  - 5.1. Study sample
  - 5.2. MRI acquisition
  - 5.3. fMRI paradigms
  - 5.4. fMRI processing and analysis
  - 5.5. Voxel-wise general linear model (GLM) – Paper I
  - 5.6 Group Independent component analysis (ICA) and network estimation – Papers I, II and III
  - 5.7. Edgewise univariate analyses – Papers II and III
  - 5.8. Multivariate machine learning analysis - Papers II and III
  - 5.9. Eigenvector centrality – Paper II
  - 5.10. Standard deviation of signal amplitude (SDSA) – Paper II and III
  - 5.11. Lesion mask – Paper III
  - 5.12. Clinical assessment – Paper III
  - 5.13. Non-imaging statistical analyses – Papers I, II and III
6. Research questions

7. Summary of papers
8. Ethical considerations
9. Discussion
  - 9.1. Stroke in the context of age
  - 9.2. Over- or underactivation with advancing age
  - 9.3. Effects of age on DAN and DMN dynamics
  - 9.4. BOLD variability: signal disguised as noise
  - 9.5. On the search for imaging biomarkers: machine learning and the value of task
  - 9.6. Methodological considerations
    - 9.6.1. Study sample and selection bias
    - 9.6.2. Study design
    - 9.6.3. BOLD signal alterations in aging and stroke
10. Concluding remarks and future directions
11. References

## 1. ACKNOWLEDGEMENTS

This thesis represents a fraction of the output from the StrokeMRI project carried out at the Norwegian Centre for Mental Disorders Research (NORMENT) and Oslo University Hospital. The project was made possible by funding from the Norwegian ExtraFoundation for Health and Rehabilitation, through Sunnaas Rehabilitation Hospital.

StrokeMRI is a collaborative and cross-disciplinary project that investigates brain health and cognition throughout the life course and in phases of stroke recovery. The research group comprises colleagues from diverse academic and national backgrounds that I have been blessed to encounter and befriend. The experiences and wisdom I've gained from being part of this project have been immeasurable, both academically and on a personal level. I am grateful to everyone one at NORMENT for fostering a dynamic research environment and equally valuable, a fun and inclusive social milieu. Thanks to all the doctors, nurses, radiologists, radiographers and administrative staff at Oslo University Hospital, Ullevål for allowing us the research facilities and aiding in patient recruitment and data collection. Thanks also to the healthy control subjects who enrolled so enthusiastically. Special considerations and gratitude must be afforded to all the stroke patients who volunteered their time and effort to this project. I was both surprised and awed by your selflessness, positivity and determination to participate in this demanding study at such a critical moment of life.

Working on this project, the day-to-day office life and grueling hours spent nights and weekends at the MRI scanner, was made more than bearable thanks to the great group of PhD-fellows and research assistants working towards our shared goal. This would not have gone nearly as smoothly and painlessly as it did were it not for the quarterbacking of Geneviève, the enduring and positive spirits of Anne-Marthe and Kristine, and the calming and singing presence of Knut. Thanks for keeping the spirits up! I'd also like to extend my gratitude to the postdocs at NORMENT for helping a lowly PhD candidate along the way. Particularly the brilliant minds of Dag and Tobias for your invaluable contributions to the analyses and figures presented in this thesis. Thanks to Jarek, Dennis and Trung for always keeping your doors open and for sharing your insights and expertise with me. It has truly been a pleasure to get to know you and to have worked with you all!

Superlatives are insufficient to describe my supervisor Lars T. Westlye, towering at the helm of the StrokeMRI project. Your work ethic, proficiency and patience has been awe-inspiring and at times intimidating. Thank you for giving me this opportunity in the first place, and for not giving up on me even at times where I imagine that must have been tempting. At times where motivation and direction were lacking, I could always count on my co-supervisor Jan Egil Nordvik to guide me through. Thanks for that and all the spirited discussions along the way.

Last but surely not least, I would like to thank my family and friends for being there and offering welcome distractions throughout the course. Biological truisms aside, I would not be here without my mother's unconditional and all-encompassing support. Marthe my dear, I'm so fortunate that you took a liking to this ole chunk of coal and I will strive to reciprocate all you have given me, including your (hitherto) uncredited proof-reading and editing. Catch you all at O'Reilly's, next round is on me.

## **2. GENERAL SUMMARY**

The present thesis investigates age-related and stroke-induced differences in brain activation and neural network configuration, during states of rest and states of attentional demand. To this end, we employed a multiple object tracking (MOT) task at two load levels and compared functional magnetic resonance imaging between a group of younger and a group of older healthy participants (papers I and II), and between a group of sub-acute stroke patients and healthy controls (paper III).

In paper I, we probe the age-related differential network response during rest and attentional demand. Task-positive (TPN) and task-negative networks (TNN) represent functionally connected brain regions that reliably activate and deactivate, respectively, when performing attention-demanding tasks. The antagonistic relationship between these networks has been hypothesized to reflect ongoing regulation of cognitive control and task-related effort, and as such a prerequisite for efficient visuospatial attention. In the field of cognitive aging, attentional impairment is widely reported, but it has not been known to which degree these behavioral differences can be attributed to network-specific neuronal alterations in the TPN and

task-negative networks TNN, respectively. Therefore, by employing independent component analysis (ICA) to derive brain networks from fMRI data recorded during a blocked MOT task, which requires sustained multifocal attention, we sought to characterize age-related alterations in TPN and TNN during sustained visuospatial attention. The results demonstrated age-related differences in network response during MOT. We found for the old compared to the young group diminished activations and deactivations in the task-positive and task-negative network, respectively. Moreover, increasing task difficulty resulted in a diminished network response in the old compared to the young group. Performance level, as indicated by target detection accuracy, was higher in the young compared to the old group. Assessment of network co-activation showed for the younger group stronger correlations within networks that were designated as TPN and TNN, compared to the older group. Summarily, the findings supported the notion of neural dedifferentiation with increasing age.

In paper II, we again studied age-related differences during MOT using roughly the same study sample as in paper I (based on task performance, a small subset of participants in paper I were excluded in paper II and vice versa). Whereas in paper I we investigated task-related network activation and co-activation, in paper II we probed age-related differences in functional connectivity (FC) across rest and task. We utilized a machine learning classifier to investigate whether age-related connectivity changes become more apparent during cognitive engagement. Variability in brain activity reflects optimal brain function. To investigate age related differences in signal variability, we computed the standard deviation of signal amplitude (SDSA) across network nodes and performed groupwise comparisons within each cognitive condition. Results from the study revealed robust discrimination between cognitive states across age groups. Further, there was a load dependent increase in classification accuracy between age groups when the participants were task-engaged compared to the resting state condition. Thus, confirming that the MOT task-paradigm increases sensitivity to age-related differences in functional connectivity compared to an unconstrained resting state. Network nodes within the dorsal attention network (DAN) and the default mode network (DMN) – representing the main task-positive and task-negative networks, respectively – were shown to be the nodes most sensitive to age effects. These networks have an anti-correlated relationship which were found reduced in the older group comparative to the younger group, corroborating the neural dedifferentiation theory and

converging with the findings in paper I. Overall, signal variability was higher for the younger group, and nodes within the DAN and DMN showed strongest the effects of task.

In paper III, we used the same methodological framework as in paper II, this time to investigate functional connectivity differences between a group of healthy controls and a group of sub-acute ischemic stroke patients. We again showed high classification accuracy between resting state and the two load levels of the MOT task. However, machine learning classification did not discriminate stroke patients from healthy controls beyond chance-level accuracy. The inherent demands of the study selected for a patient group with clinically mild strokes, and fMRI findings together with behavioral data converged to suggest that mild strokes might impart sparse effects on cognitive function and neural networks beyond the lesion proper.

### 3. LIST OF PAPERS

1. Dørum, E.S., Alnæs, D., Kaufmann, T., Richard, G., Lund, M.J, Tønnesen, S., Sneve, M.H., Mathiesen, N.C., Rustan, Ø.G., Gjertsen, Ø., Vatn, S., Fure, B., Andreassen, O.A., Nordvik, J.E., Westlye, L.T. (2016). Age-related differences in brain network activation and co-activation during multiple object tracking. *Brain and Behavior* 6: 1- 15. e00533, <https://doi.org/10.1002/brb3.533>
2. Dørum, E. S., Kaufmann, T., Alnæs, D., Andreassen, O. A., Richard, G., Kolskår, K. K., Nordvik, J.E., Westlye, L. T. (2017). Increased sensitivity to age-related differences in brain functional connectivity during continuous multiple object tracking compared to resting-state. *NeuroImage*, 148, 364-372. <https://doi.org/10.1016/j.neuroimage.2017.01.048>
3. Dørum, E. S., Kaufmann, T., Alnæs, D., Richard, G., Kolskår, K. K., Engvig, A.M., Sanders, Ulrichsen, K., Ihle-Hansen, H., Nordvik, J. E., Westlye, L.T. (2020). Functional brain network modeling in sub-acute stroke patients and healthy controls during rest and continuous attentive tracking. *Heliyon* 6(9), e04854. <https://doi.org/10.1016/j.heliyon.2020.e04854>

#### 4. INTRODUCTION

Although wisdom accrues throughout a lifetime of amassed knowledge, lived experiences and life-lessons gathered - the inevitable course of senescence is that of diminishing acuity across the span of cognitive faculties. Behind the slow and often imperceptible cognitive decline that comes with advancing age is an accumulation of widespread change in the cerebral architecture. These changes are often found accelerated in neurodegenerative pathologies; meaning to better understand aging is to better understand, and hopefully ameliorate a range of brain disorders like Alzheimer's and Parkinson's disease. Sudden damage to brain tissue, by contrast, such as occurring in a cerebral stroke may result in immediate and irreversible behavioral changes depending on the extent and location of the damage. Regardless of the underlying mechanisms or speed of onset, loss of cognitive capabilities can be a devastating encounter, not only experienced by the effected individual, but with extensive ramifications for the next of kin, local communities and health services at large.

The complexity of human brain is formidable, and accordingly, the neurobiological basis underlying cerebral processes including age-related decline and disease states remains elusive. However, the scientific and technological developments of the last half century have ushered in paradigmatic advancements in the field of neuroscience to allow for *in vivo* investigation and visualization of the structural and functional human brain. Arguably, the most powerful tool for assessing brain organization, fMRI utilizes the disparate magnetic properties of the hemoglobin molecule in states of oxygenation and deoxygenation to infer neural activity. At rest, fMRI studies have revealed synchronous activity between spatially dispersed brain regions, giving rise to the concept of functional connectivity and revealing a network organization structure of the human brain. Considering that neural activity in part reflects cognitive context, task-based fMRI paradigms allow us to assess spatial and temporal changes in neural activity during various cognitive states.

The present thesis is structured around three original research articles. All three papers are cross-sectional cohort studies using task-based fMRI to compare neuroimaging data obtained from older and younger healthy adults (papers I and II), and sub-acute stroke patients and healthy controls (paper III). The thesis comprises three main sections: (1) an introduction which provides a general framework of key concepts and the current state of knowledge, on which the three

papers are built. Herein, the biological basis underlying functional brain networks and the fMRI signal from which the networks are derived, is reviewed. Emphasis is put on networks subserving visual attention processing, and the network-level effects of stroke and cognitive aging. Part (2) presents a summary of the three papers, which includes the specific research questions that were asked and the methods that were employed. The final section (3) discusses the findings in this thesis context of the current state of knowledge, and how this thesis might serve to contribute to the field. This section includes methodological consideration, concluding remarks and future directions.

#### **4.1 Functional magnetic resonance imaging**

By utilizing the properties of Hydrogen atoms to form images, MRI technology allows for detailed *in vivo* visualization of biological tissue. The technique is non-invasive and does not emit ionizing radiation, in contrast to x-rays and CT-scans. While structural MRI allows for detailed three-dimensional images of neuroanatomy with a high degree of spatial resolution, fMRI is applied to acquire information regarding brain activity. fMRI does not measure brain activity directly. The physiologic basis of the fMRI signal is the blood-oxygen level dependent (BOLD) response, which simply put, is the relative concentration difference between the deoxygenated and the oxygenated configurations of the hemoglobin molecule within the red blood cells, as it binds to and transports oxygen throughout the cerebral vascular system. Neural activity causes a multicellular response that alters local perfusion - also known as neurovascular coupling - producing a local surge in blood flow (Goense et al., 2012; Leniger-Follert & Hossmann, 1979), which changes the ratio of the oxygenated/deoxygenated state of the hemoglobin molecule in the microvasculature surrounding the activated neural regions. This change in oxygenation status leads to an increased BOLD signal that is recorded in an MRI scanner by virtue of the different magnetic properties of the hemoglobin molecule when it's bound to oxygen (non-paramagnetic) and when it's not (paramagnetic) (Logothetis et al., 2001). Thus, the BOLD signal is an indirect measure of brain activity, inferred through alterations in hemodynamic parameters such as cerebral blood flow, cerebral blood volume and cerebral metabolic rate of oxygen consumption (Buxton et al., 2004). The BOLD response evoked by neural activity follows a specific time course known as the hemodynamic response function (HRF) which is used to model the neural event to fMRI data (Lindquist & Wager, 2007).

Functional neuroimaging has provided invaluable insight into neural mechanisms and core organizational principles of the cerebral cortex. fMRI, in conjunction with graph theoretical analyses has revealed a network level topology that shares properties with other complex systems such as social- and information technological networks (Bullmore & Sporns, 2009).

#### 4.1.1 Resting-state fMRI and brain networks

The brain – even at rest – exhibits a continuous activity of low frequency BOLD signal fluctuations (Biswal et al., 1995). By investigating whole-brain correlations in signal activity, studies have identified spatially dispersed brain regions that fluctuate synchronously in the absence of stimuli (De Luca et al., 2006; van den Heuvel & Hulshoff Pol, 2010). This temporal dependence of neuronal activity defines the concept of functional connectivity (Friston, 1994), and studies have shown reproducible connectivity patterns to identify canonical resting-state networks that are consistent across healthy subjects (Damoiseaux et al., 2006; Seitzman et al., 2019). Networks such as sensorimotor, frontal, visual, dorsal attention and default mode networks (Fox & Raichle, 2007) constitute examples of commonly described large-scale resting-state networks (figure 1).

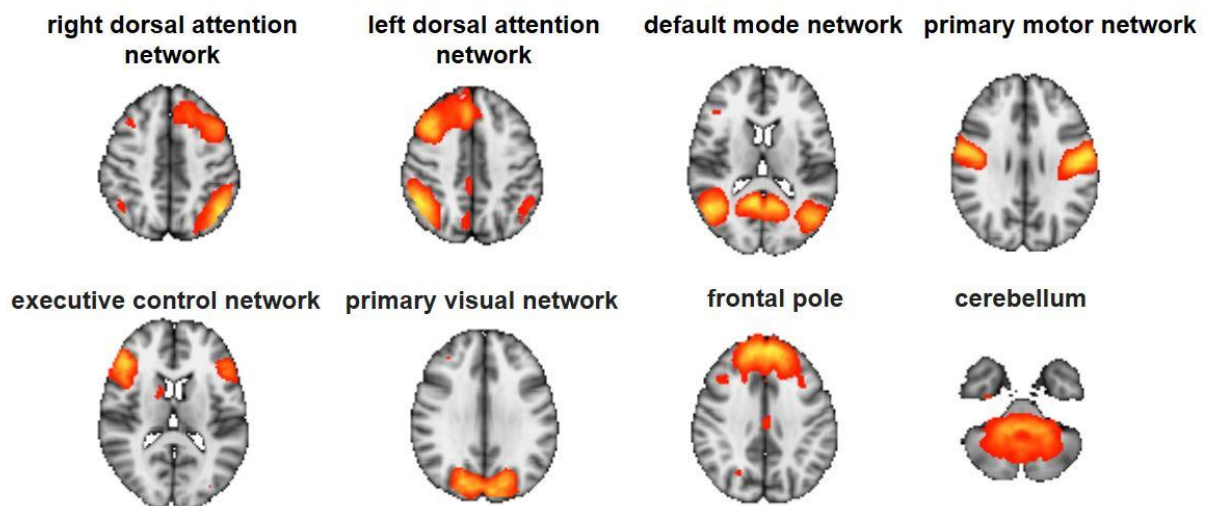


Figure 1. Adapted from paper III. Visual depiction of 8 commonly reported resting-state networks.

Resting-state fMRI studies have emerged the view of the brain as a complex integrative network, and thus provided a unique insight into the functional architecture and organizational principles of the human brain. Clinical applicability is still at a nascent stage, but resting-state fMRI has shown useful in diagnosing and monitoring disease progression in neurodegenerative (Cordova-Palomera et al., 2017; Kivistö et al., 2014) and neuropsychiatric disorders (Kaufmann et al., 2015), as well as guiding neurosurgery to minimize functional loss in tumor resection and epilepsy surgery (Lee et al., 2013).

The main approaches to investigate functional connectivity between brain regions are 1) local seed-based analyses, where regions of interest (ROIs) are selected *a priori* and the corresponding time-series (the signal measured at each voxel throughout a run) are correlated with the time-series of other brain regions (Reid et al., 2017; Smitha et al., 2017), and 2) whole-brain connectivity analyses which rely on model-free, data-driven methods to estimate connectivity patterns in the entire brain from the statistical properties of the source data (Smith et al., 2011). The former relies on selecting predefined brain ROIs to be investigated, and thus the information provided is locally limited while interpreting the results is relatively straightforward. The latter offers the advantage of being applicable to experimental paradigms without an *a priori* model and enables whole-brain connectivity assessment. However, given the higher data complexity, interpretations of between-group differences has shown more complicated (Fox et al., 2007). Although seed-based and data-driven methods differ conceptually and methodologically, they yield results with a high degree of convergence (Joel et al., 2011).

Model-free whole-brain analyses include decomposition techniques such as principal component analyses (PCA) (Viviani et al., 2005) and independent component analyses (ICA) (Abou Elseoud et al., 2011; Beckmann et al., 2005), as well as various clustering procedures (Cordes et al., 2002; Golland et al., 2008; Thirion et al., 2006; van den Heuvel & Hulshoff Pol, 2010). PCA reduces the dimensionality of the fMRI data by parsing the set of variables into a smaller set of uncorrelated variables that captures most of the variance. For this purpose, it is a particularly useful analysis tool prior to ICA and machine learning algorithms, as the uncorrelated variables are more computationally efficient for downstream analyses. ICA is perhaps the most used tool for data-driven connectivity analyses. ICA separates the fMRI signal into independent spatial components and corresponding time-series, yielding signal sources that

are spatially maximal independent from each other. These signal sources, or independent components represent nodes in the brain network, that are functionally interconnected through network edges. Although in fMRI research, network edges are inferred through synchronous activity; structural imaging studies have shown functional brain networks to be dependent on the underlying anatomy (Tewarie et al., 2014; van den Heuvel et al., 2009). Graph theory, a mathematical branch, serves as the operating framework for investigating network properties of the human brain (Bullmore & Sporns, 2009). The arrangement of nodes and edges (network topology) is optimized for a high degree of local and global information exchange with low wiring cost (Fornito et al., 2010). This is particularly evident in networks that exhibit ‘small-world topology’ where nodes are locally clustered sharing short range interconnections (Sporns et al., 2005). Perturbations in network topology during disease states causes brain networks to organize less efficiently and clinical deficits can in part be explained by system level alterations.

fMRI research comparing brain activation and network characteristics typically rely on mean BOLD signal activity. Considering that the brain is constantly in flux, signal variability – once attributed to mere noise in the data – has been shown to serve a functional role for neural systems to adapt to the changing environment and respond to a greater range of stimuli (Garrett et al., 2010). The natural state of the brain is inherently variable (Pinneo, 1966), and increased signal variability has been linked to better performance in cognitive tasks (Garrett et al., 2011), and in younger compared to older populations (Grady & Garrett, 2014). In neurodegenerative and psychiatric disorders, both increased as well as decreased variability across a range of brain regions has been linked to disease state and severity (Han et al., 2011; Millar et al., 2020; Yang et al., 2014; Zhao et al., 2018), suggesting that an optimal degree of variability is requisite for healthy brain function.

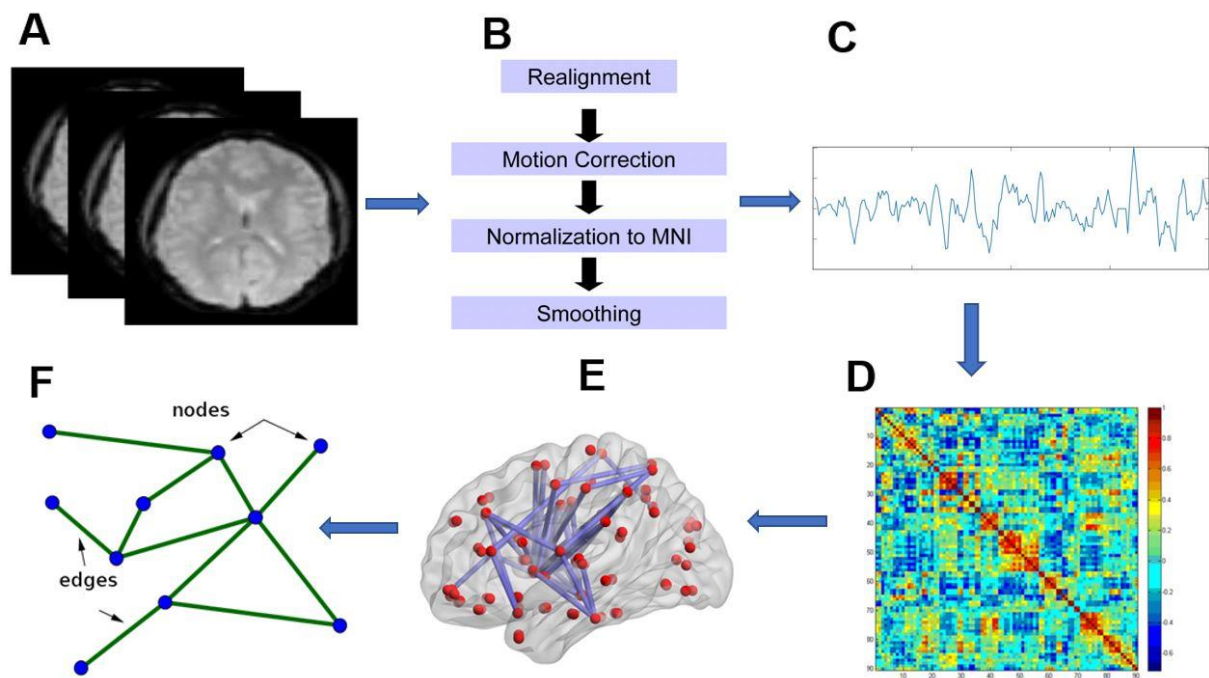


Figure 2. Flow chart of data processing and network estimation for fMRI. A) Acquisition of individual fMRI images; and B) preprocessing; with C) corresponding time series; used to estimate D) a functional connectivity matrix based on correlated activity between nodes; E) the generated whole brain functional network in anatomic space; F) simple model diagram for graph theory analysis.

#### 4.1.2 Task-based fMRI

Functional imaging captures brain activity in the subject being investigated during his or her given cognitive state. In resting-state studies, participants are instructed to lie as still as possible while letting their mind wander without falling asleep. In task-based paradigms, participants perform various tasks depending on the phenomena being investigated. By mapping brain areas that show increased activation in response to task, these tools have allowed for *in vivo* assessing neural correlates subserving motor (Turesky et al., 2018), language (Pillai et al., 2003), visual (DeYoe et al., 1996), attention (Culham et al., 2001) and memory processing (Osaka et al., 2003), as well as a multitude of other sensory, motor and cognitive operations (Drobyshevsky et al., 2006; Schwartz et al., 2005).

Interestingly, bilateral brain regions in the medial prefrontal cortices, precuneus and angular gyri show consistent deactivation during task and activation at rest (Mevel et al., 2011;

Raichle et al., 2001). These distributed regions comprise the brain's default mode network and divides the brain into two opposing systems; the task-negative DMN and task-positive networks such as attention-, visual-, sensorimotor-, salience and executive control networks (Chai et al., 2012; Greicius et al., 2003; Power et al., 2011). The DMN is generally thought to support internal mentation. The role of the DMN in internally oriented cognition is evidenced by increased network activity when subjects are mind wandering, monitoring their internal states and processing autobiographical memory (Buckner et al., 2008; Mason et al., 2007; Raichle et al., 2001). The opposing dynamics between task-negative and task-positive brain systems suggests an antagonistic relationship competing for limited processing resources and serving conflicting operations. Externally oriented task paradigms invoke an allocation of resources from the DMN to task-positive networks, with increasing task demand yielding greater contrast in activation/deactivation responses (Buckner et al., 2008; McKiernan et al., 2006).

Whilst brain activity in specific cerebral regions becomes markedly altered between rest and task, FC (temporal synchronicity of low-frequency signal fluctuations) show a high degree of correspondence across condition (Cole et al., 2014; Fox et al., 2007; Smith et al., 2009). This suggests an intrinsic functional network architecture that is stable across mental states, accounting for most of the variation in behavior considering that this intrinsic network configuration determines FC both at rest and during task. Although functional network alterations between conditions are small, task-evoked FC changes do exist. Networks that weakly activate or show deactivation, also show decreased FC during task, suggesting a decoupling of task-irrelevant networks (Tomasi et al., 2014). More surprisingly, several studies have also shown decreased FC in neural networks that activate during task (Cohen & Maunsell, 2009; Cole et al., 2021; Ito et al., 2020). A somewhat counterintuitive finding as one would expect that task-evoked network activity would be observed along with stronger network connections. This task-related activity/connectivity relationship can be accounted for by considering that overall activity flow is the product of activations times FC, which would accommodate for finding FC decreases and still have overall increased neural interactions (Cole et al., 2021). Nevertheless, the relationship between different measures of brain function is convoluted, highlighting the complexity of cerebral dynamics.

## 4.2 Visual attention and multiple object tracking

Perhaps the most oft-quoted definition of attention begins with stating the intuitive nature and collective familiarity we have with the phenomenon: “*Everyone knows what attention is*” declared the influential psychologist William James writing in the late 19<sup>th</sup> century (James, 2007). Attentional control is such an indispensable constituent piece in higher level cognition and goal-directed behavior, so as to seem second nature in everyday life (Hasher & Zacks, 1988; Petersen & Posner, 2012). It allows us to navigate through the endless amount of information that the environment presents us with, by purposefully prioritizing and ignoring information based on what is deemed relevant for behavior – akin to a highlighter rendering sections of text more salient to the reader. James’ quote goes on to further describe key features of attention: “*It is taking possession of the mind, in clear and vivid form, of one out of what seems several simultaneously possible objects or trains of thought. Focalization, concentration of consciousness is of its essence. It implies a withdrawal from some things in order to deal effectively with others.*”

Facilitated by the tremendous technological and methodological advances within neurophysiological and neuroimaging techniques, *in vivo* research studies offer insight into the biological underpinnings of the working brain, now well over a century following James’ life and work. Early neuroscientific research on visual attention was somewhat impeded by the rather nebulous and vague ontology of attention as a unitary concept without described neural correlates that could be investigated empirically. In their seminal paper at the infancy of neuroimaging research, Peterson and Posner conceptualized three different, but interrelated subsystems with distinct neuroanatomy that constitute attention: alerting, orienting and detection (1990). Alerting, or arousal prepares the brain for signal detection and helps maintain vigilance, involving the ascending reticular activating system in the brain stem and midbrain with projections to the cortex (Yeo et al., 2013). Orientation involves the ability to prioritize the sensory inputs. Selective orientation of attention can further be sub-categorized according to the nature of the stimuli being attended to. Thus, we distinguish between attention driven by goal-oriented behavior such as the act of dutifully writing or reading text, and stimulus-oriented behavior such as the reflexive reaction evoked by loud noises or bright flickering lights. The former being an example of attention driven by endogenous or top-down processes, whilst the

latter is conceptualized as attention that is exogenously driven or under bottom-up control. Neuroimaging research has revealed distinct cerebral anatomy and neural networks subserving these attentional systems (Corbetta & Shulman, 2002). Endogenous attention is mediated by a dorsal frontoparietal network comprising the intraparietal sulcus (IPS), and frontal eye fields (FEF), whilst the exogenous attention system comprises hubs in the ventral frontal cortex and the temporoparietal junction (Vossel et al., 2014). Thus, these attention systems are also referred to according to their neuroanatomical distributions as the dorsal and ventral attention networks, acronymized as DAN and VAN, respectively. In their 1990 paper Peterson and Posner identified target detection as the third major attentional subsystem, with neural correlates in frontal, parietal, and cingular regions (Gratton et al., 2018). Target detection meaning the capture of awareness that occurs once a target is detected, at the cost of being attentive to other targets. This process involves the focalization of attention and relates to the limited capacity of the attention system. Activity in these frontoparietal or cingular areas has since been shown to correlate with a number of diverse operations involving top-down control, such as self-regulation (Posner et al., 2007) and action selection (Shenhav et al., 2013). Thus, this system is now considered a part of an executive control network, reflecting its more extensive role in the execution of cognitive operations (Petersen & Posner, 2012).

Visual attention functions effectively through a set of mechanisms that limits the processing to a subset of visual stimuli from all other stimuli that is presented through the visual stream. These mechanisms serve varied functions in visual processing including selecting and enhancing relevant stimuli whilst suppressing irrelevant stimuli, decomposition of the stimulus into constituent dimensions (color, shape, orientation etc.) and visual recognition where the signal is identified (Evans et al., 2011). For all three papers included in the present thesis, visual attention is probed using a multiple object tracking task (Pylyshyn & Storm, 1988). MOT involves the tracking of multiple target objects amongst identical distractor objects, and as such requires goal-oriented selective and sustained visual attention (Luo et al., 2021). Since objects are moving randomly, successful tracking relies on constructing mental representations that maintain the integrity for the objects despite positional change (Pylyshyn, 2001). In addition to visual attention, the task relies on coordinated visuomotor processes and working memory. When task-engagement is combined with neuroimaging data, multiple object tracking is seen to reliably activate core regions of the DAN (Alnæs et al., 2014; Culham et al., 2001), in a load-dependent

manner (Jovicich et al., 2001), thus making the paradigm ideally suited for investigating neural mechanisms subserving sustained visual attention.

### **4.3. Brain networks in aging**

Cognitive aging refers to the decline in cognitive performance and accompanying neurobiological alterations observed with advancing age. The most prevalent neurodegenerative diseases such as Alzheimer's, Parkinson's disease and cerebrovascular disease are inextricably linked to advancing age. In fact, given the prevalence of neurodegenerative findings in otherwise healthy elderly individuals, brain aging has been proposed to form a continuum with neurodegeneration (Hou et al., 2019; Hung et al., 2010). Accordingly, understanding the processes underlying cognitive aging is paramount in developing preventive and ameliorative interventions aiming to lessen a substantial disease burden.

The age of onset and trajectory of age-related cognitive decline is highly variable between individuals and across cognitive domains. Crystallized cognitive abilities involving knowledge acquisition and the ability to recall information remain preserved until approximately the age of 60 (Cattell, 1963; Wang & Kaufman, 1993), while fluid abilities that require the ability to manipulate and process new information (Bugg et al., 2006), begin to decline as early as the mid-20' (Harada et al., 2013). The human brain, being an exceedingly complex multi-level system, exhibits widespread age-related alterations at all levels of resolution ranging from molecular changes in calcium homeostasis, mitochondrial dysfunction and neurotransmitter pathways (Tripathi, 2012; Zia et al., 2021); cellular loss and dysregulation affecting neurons and glial cells (Baker & Petersen, 2018; von Bernhardi et al., 2015); and morphological changes, most notably gray matter volumetric reduction and loss of white matter integrity (Ge et al., 2002; Inano et al., 2011).

In the field of brain imaging, early studies showed overactivation for senior adults compared to younger adults performing the same cognitive task (Cabeza et al., 1997; Grady et al., 1994). This relative activity increase seen with advancing age was frequently observed in the prefrontal cortex, an anatomical region particularly vulnerable to age-related atrophy (Tisserand & Jolles, 2003). Further, frontal regions that showed a preferred hemispherical lateralization for younger subject, showed bilateral recruitment in older subjects (Cabeza et al., 1997). Models

such as the posterior to anterior shift in aging (PASA; Davis et al., 2008), and Hemispheric Asymmetry Reduction in OLDER adults (HAROLD; Cabeza, 2002) were devised to interpret these commonly encountered patterns of age-related increased frontal recruitment and bilaterality, respectively. Age-related increases in frontal recruitment is thought to reflect compensation for neuronal tissue loss when overactivation positively correlates with successful task performance (Rossi et al., 2004). Conversely, when overactivation is negatively correlated with performance, this pattern is deemed to represent maladaptive neuromodulation inducing unwanted noise into the system (Nashiro et al., 2018). While overactivation is frequently seen for older subjects at low and moderate task difficulty (when differences in performance compared to younger participants is minimal), at higher cognitive loads, the same brain regions show under-recruitment for the older participants along with detrimental effects on performance (Cappell et al., 2010; Mattay et al., 2006). This pattern of activity has been proposed to reflect effective compensatory mechanisms where older adults – due to processing inefficiencies – recruit more neural circuitry at lower task demands, which eventually reaches a resource ceiling due to insufficient reserve capacity. A tradeoff that has been termed compensation-related utilization of neural circuitry or CRUNCH (Reuter-Lorenz & Cappell, 2008). Of particular interest in cognitive aging and imaging studies, is the task-negative default mode network. The DMN is suppressed during cognitive demanding tasks, but less so with advancing age (Grady et al., 2006), and the relative failure to deactivate the DMN is related to reduced cognitive task performance for older adults (Damoiseaux et al., 2008).

From behavioral studies, Lindenberger (1994) and Baltes (1997) demonstrated that visual and auditory acuity were strong predictors of successful task performance in a range of cognitive tasks for older adults, but not for younger ones. Indicating that sensory functions evolve from being independent features in early adulthood to become interrelated with various other cognitive operations with advancing age. The ability of younger adults to engage selective neural pathways in response to different tasks seemingly declines with age, a term the authors coined neural dedifferentiation. Commonly reported findings of older adults activating both cerebral hemispheres in tasks that elicit unilateral activations for younger subjects (Cabeza, 2002; Reuter-Lorenz et al., 1999), along with network-level studies showing an age-related decreased ratio of within-network to between-network connectivity (Damoiseaux, 2017; Ferreira et al., 2016; Goh,

2011) further the notion of neural dedifferentiation, and form a key link between behavioral- and brain-based approaches to cognitive aging.

Importantly, overcompensation, CRUNCH and dedifferentiation hypotheses aren't mutually exclusive theories of cognitive aging. In the rapidly developing field of behavioral and neuroimaging research, these theories have rather been developed as explanatory models attempting to encompass emerging research findings within a general framework. To account for a more dynamic and adaptive view of the human brain, the scaffolding theory of aging and cognition or STAC was proposed in 2010 (Reuter-Lorenz & Park). The STAC model has since been revised (STAC-r) to account for the lifetime effect of factors (exercise, lifestyle, behavioral interventions, deleterious events etc.) that influence aging trajectories (Reuter-Lorenz & Park, 2014).

The STAC-r model (fig. 3) explains the brain's response to cognitive challenges, which are not unique to, albeit more frequently encountered in advancing age. Scaffolding refers to the development of alternate neural circuits to achieve cognitive goals and has a protective function in cognitive aging. In childhood and youth, capacity for neural plasticity and skill acquisition is high, explained neurobiologically by the honing of efficient and modular neural circuitry. With advancing age and the accumulation of neural challenges, efficiency of the modular networks decreases and there's a compensatory reliance on scaffolding networks to achieve the similar cognitive performance. However, eventually progressive neural pathology exhaust neural capacity to reorganize, the scaffold collapses and cognitive impairment ensues.

The STAC-r model explains age-related frontal overactivation by proposing the frontal cortex as a locus for scaffolding, owing to its high flexibility and versatility in cognitive operations (Miller & Cohen, 2001). In the STAC-r framework, network dedifferentiation is an expression of progressive loss of efficiency in the honed and modular neural networks, with the need for additional neural recruitment for older adults. Similarly, decreased suppression of the DMN is reflective of compensatory utilization of scaffolded networks which are less efficient and selective.

### A Life Course Model of The Scaffolding Theory of Aging and Cognition (STAC-R)

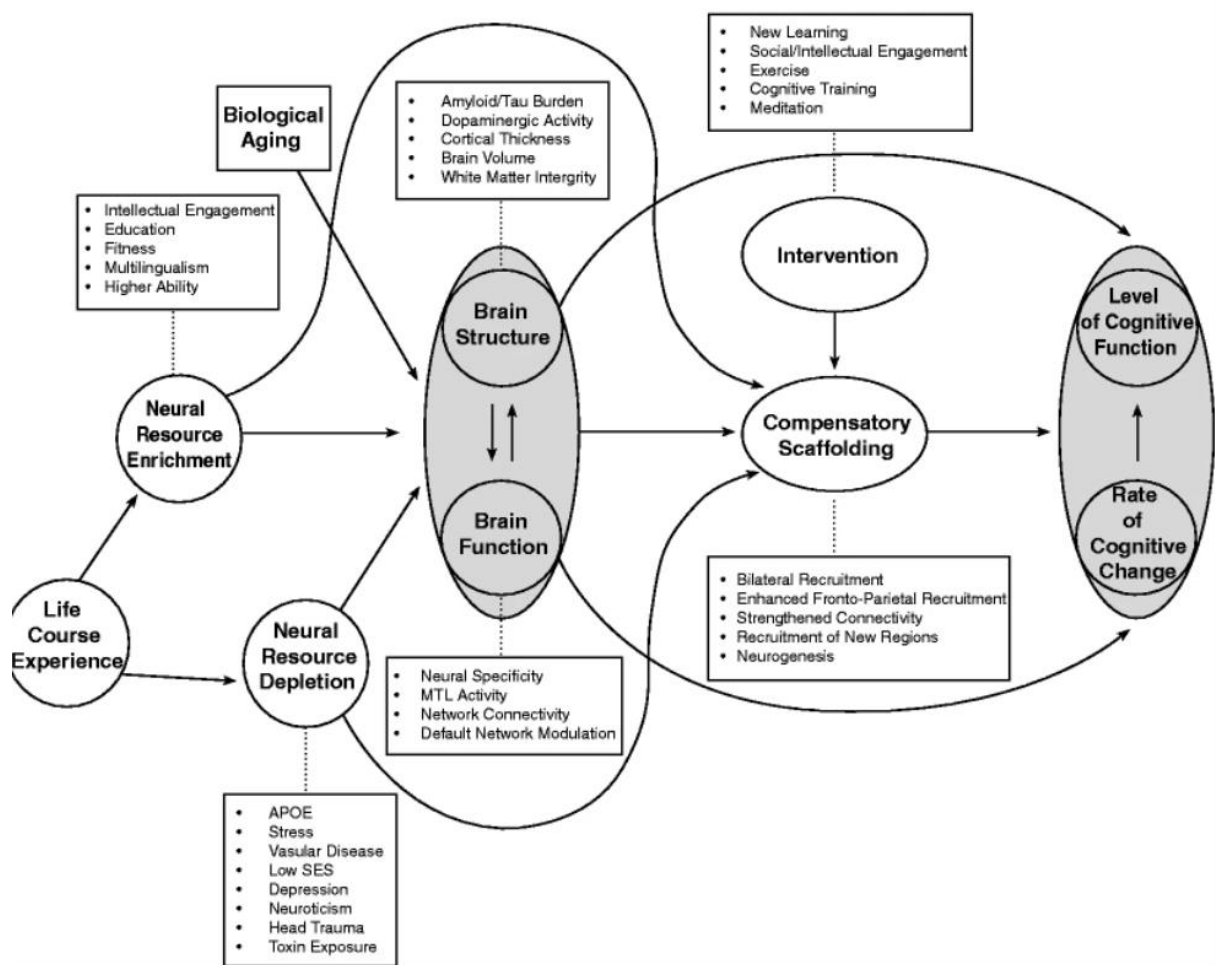


Figure 3. Conceptual model of the scaffolding theory of aging and cognition revised (STAC-r; Reuter-Lorenz & Park, 2014)

#### 4.4. Brain networks in cerebral stroke

A cerebral stroke occurs when blood flow to a brain area is impeded. The tissue supplied by the compromised vasculature becomes oxygen deprived and cells undergo ischemic cell death within minutes of onset. Cerebrovascular disease contributes significantly to the global health burden as it ranks the second most common cause of death and disability adjusted life years (DALY's), with an estimated lifetime risk of almost 25% for those aged 25 and older (Gorelick, 2019). And whilst rates of stroke mortality has decreased the last two decades, the absolute

number of yearly strokes, stroke survivors and DALY's lost is increasing (Feigin et al., 2014). Stroke survivors endure a prolonged period of rehabilitation with the aim of regaining as much function as possible. A wide variety of factors influence stroke prognosis including age, stroke severity, mechanism and location, the presence of comorbidities and level of stroke unit and rehabilitation care and treatment.

Brain strokes, also known as cerebrovascular accidents (CVAs), are broadly categorized as ischemic (vascular blockage) and hemorrhagic (vascular rupture) according to the mechanism of injury (Grysiewicz et al., 2008). Hemorrhagic strokes are further subdivided into intracranial hemorrhage (ICH) and subarachnoid hemorrhage (Feigin et al.) according to the location of the rupture, the former occurring within the brain parenchyma and the latter occurring in the subarachnoid space between the arachnoid and pia mater. Ischemic strokes account for approximately 87% of all CVAs. While hemorrhagic strokes are less prevalent (ICH make up 10% and SAH 3%), they are more likely to be fatal (Benjamin et al., 2019). Regardless of the underlying etiology, once a stroke incident occurs, a complex cascade of interrelated and coordinated processes takes place including loss of cell ion homeostasis, immune system activation, glial cell response and blood-brain barrier disruption leading to necrotic cell death in the compromised brain tissue (Woodruff et al., 2011). In non-lethal cases, clinical recovery ensues the following days, weeks, months and even years after the stroke incident. Multiple factors influence recovery and can predict favorable outcomes, including a reorganization of neural networks (Carter et al., 2012; Diao et al., 2020).

The notion that a focal brain lesion exerts neurophysiological effects in distant areas was most notably proposed by the neuropathologist Constantin von Monakow, who coined the term diaschisis as it relates to brain function in 1914 (Carrera & Tononi, 2014). Diaschisis from Greek meaning severe or split through (*dia* – through or across, and *schizein* – to split), was a novel heuristic breaking with the prevailing localist viewpoint that brain function was localized to specific areas in the cerebral cortex. Advances in neuroimaging and statistical modeling have since provided empirical evidence for lesion effects on whole-brain network properties, to the extent that stroke can be considered a network disease.

Early fMRI studies in stroke-induced motor deficits have shown decreased activity in the ipsilesional hemisphere with increased recruitment of homologous areas in the unaffected

contralesional hemisphere (Johansen-Berg et al., 2002; Ward et al., 2003), giving rise to the notion that stroke recovery induces cortical reorganization. A commonly reported network-level finding is decreased connectivity within the lesioned hemisphere in the first days and weeks following a stroke (Carter et al., 2010; Golestani et al., 2013). Clinical recovery is predicted by connectivity normalization in the nodes that showed alterations in the acute phase (Golestani et al., 2013; Rehme, Fink, et al., 2011). Studies investigating longitudinal changes in the functional organization of brain networks, suggests a shift towards increased functional segregation of affected networks underlies successful recovery (Duncan & Small, 2016; Wang et al., 2010). Decreased connectivity in homotopic regions between hemispheres, along with increased intrahemispheric connectivity between normally disconnected networks are robust network findings that can predict behavioral deficits in the subacute phase (Baldassarre et al., 2014; He et al., 2007). A plurality of connectivity studies in stroke research have focused on resting state rather than task connectivity due to feasibility reasons. The task data that do exist show similar patterns to resting state with decreased connectivity as the dominant trend, with normalization to healthy control level with time (Rehme, Eickhoff, et al., 2011; Rosso et al., 2013),

## **5. METHODS AND MATERIALS**

The PhD-project presented in this thesis is part of a larger StrokeMRI project conducted at the Norwegian Centre for Mental Disorders Research (NORMENT) and Oslo University Hospital (OUS). StrokeMRI is a collaborative effort focused on studying cognitive aging, brain health, stroke rehabilitation and recovery (Beck et al., 2022; Kolskår et al., 2021; Richard et al., 2020; Richard et al., 2018; Sanders et al., 2021; Ulrichsen et al., 2020). To this end, stroke patients in both subacute and chronic phases of recovery were included, in addition to healthy controls. Stroke patients that were recruited in the study for paper III in the present thesis, were also invited to participate in an intervention study investigating the effects of computerized cognitive training (CCT) and transcranial direct current stimulation (tDCS) on cognitive improvement (Kolskår et al., 2019). Written and informed consent was obtained from each participant prior to inclusion. All facets of the project were performed in accordance with the Helsinki declaration, and the project has been approved by the Regional Committee for Medical and Health Research Ethics (South-East Norway, 2014/694; 2015/1282).

## 5.1. Study samples

Healthy controls were included in the analyses for all three papers. They were recruited through newspaper ads, social media and word of mouth. Inclusion criteria were age above 18 and normal or corrected-to-normal vision. Intelligence quotient (IQ) was obtained using the vocabulary and matrix reasoning subtests from the Wechsler Abbreviated Scale of Intelligence (WASI; Wechsler, 1999). Subtest scores were converted to Full Scale IQ (FSIQ) estimates. Exclusion criteria were reported history of neurological or psychiatric condition (including substance- and alcohol abuse), FSIQ below 70, concurrent use of medication significantly affecting the nervous system (e.g., antidepressants, opioid analgesics, anticonvulsive- or mood stabilizing drugs) and any contraindication for MRI.

A total of 52 participants were recruited in the sample pool for both papers I and II. These papers thus have a high degree of overlapping participants. After the scanner session, two participants were excluded due to excess in-scanner motion. Further exclusions were then made based on performance on the MOT task. For both paper I and II, participants that performed at chance or below chance-level during the low load condition were excluded. Additionally, for paper I, two participants had accuracy scores that exceeded 2.5 standard deviations below the mean and were thus subject to further exclusion. Thus, the final sample sizes consisted of 45 and 47 participants in papers I and II, respectively. The participants were then grouped into an older and a younger age group according to the median split.

For paper III, the patient cohort was recruited from the stroke units at Ullevål, Oslo University hospital (OUS), Diakonhjemmet hospital and Bærum hospital. Inclusion criteria were age above 18, clinically and radiologically documented stroke and enrolment within 14 days of hospital admittance. Exclusion criteria were clinical condition leading to inability to actively participate in the fMRI session, and MOT performance below chance level on the low condition. From the 54 patients initially enrolled in the study, 10 were excluded (3 were diagnosed with diseases other than stroke, 3 had stroke-related visual and/or motor impairments rendering them incapable of performing the MOT task, 4 were unable to complete the MRI protocol and/or the neuropsychological tests) yielding a final sample of 44 stroke patients. A total of 100 age and sex-matched healthy controls were recruited using the same selection criteria as for papers I and II. Table 1 gives the general overview of sample characteristics for each paper.

Group	Paper I		Paper II		Paper III	
	Young	Old	Young	Old	HC	Pat
N (%females)	24 (66.7)	21 (53.4)	25 (68.0)	22 (54.55)	100 (40.0)	44 (25.0)
Age (mean [SD])	24.4 (5.1)	64.7 (7.4)	24.2 (5.1)	65.1 (7.5)	63.1 (11.2)	63.1 (14.8)
Age range	20-43	47-78	18-43	47-79	35-81	34-87
Years of education (mean [SD])	15.5 (1.4)	15.1 (3.1)	15.4 (1.5)	15.1 (3.0)	15.82 (2.9)	15.18 (2.0)
MOT accuracy L1 (mean [SD])	97.9 (7.5)	94.4 (10.9)	90.0 (13.5)	82.3 (16.9)	84.0 (24.0)	77.7 (24.9)
MOT accuracy L2 (mean [SD])	88.9 (14.5)	77.8 (20.6)	80.4 (18.8)	69.6 (22.6)	71.7 (23.5)	66.5 (23.9)

**Table 1.** General overview of the sample characteristics included in each study. HC: Healthy controls, Pat: patients.

## 5.2. MRI acquisition

Imaging data was obtained from a General Electric (Signa HDxt) 3.0T scanner with an 8-channel head coil (papers I and II), and a General Electric (Discovery MR750) 3.0T scanner with a 32-channel head coil (paper III), at the Section of Radiology and Nuclear Medicine, Oslo University Hospital (OUS). For all three papers, functional data were acquired with a T2\*-weighted 2D gradient echo planar imaging sequence (EPI), the first five volumes were discarded. Additionally, a T1-weighted structural scan was obtained for all three papers.

Papers I and II: 200 volumes were collected from the resting state condition and 217 (paper I) and 140 (paper II) volumes from the MOT conditions (TR: 2,400 ms; TE: 30 ms; FA: 90; voxel size: 3.75x3.75x3.2 mm; slices: 48; FOV: 240x240 mm; duration: 533 s). The structural scan was acquired using a sagittal T1-weighted fast spoiled gradient echo (FSPGR) (TR: 7.8 s; TE: 2.956 ms; TI: 450 ms; FA: 12°; voxel size: 1.0×1.0×1.2 mm; slices: 170; FOV: 256 mm<sup>2</sup>; duration: 428 s).

Paper III: 200 volumes collected for the resting-state condition and 152 volumes for the two MOT load conditions (TR: 2250 ms; TE: 30 ms; FA: 79°; voxel size: 2.67 x 2.67 x 3.0 mm; slices: 43; FOV: 96x96 x129 mm. The sagittal T1-weighted FSPGR sequence (TR: 8.16 ms; TE: 3.18 ms; TI: 450 ms; FA: 12°; voxel size: 1.0x1.0x1.0 mm; slices: 188; FOV: 256 x 256 x 188 mm; duration: 288 s), and a T2-FLAIR (TR: 8000 ms; TE: 127 ms, TI: 2240; voxel size: 1.0 x 1.0 x 1.0 mm; duration 443 s) for lesion demarcation.

### **5.3. fMRI paradigms**

In the three papers, functional imaging was obtained during a multiple object tracking (MOT) task (Pylyshyn & Storm, 1988). Participants underwent one resting state run and three versions of MOT, including one blocked and two continuous tracking runs, performed in the MRI scanner during the same session. Paper I reports data obtained during the blocked run, while papers II and III report the continuous runs. MOT explores sustained goal-driven attention as it requires attention to dynamically moving objects, and by modifying the number of target objects, the task allows for manipulation of attentional load. The task matches attentional processes that the environment exposes us to everyday. Whether it be navigating through traffic, participating in sports, supervising children or wild game hunting - continuous deployment of attention to moving objects are paramount. At task onset, 10 identical blue objects are presented on the in-scanner screen, shortly thereafter one or two objects change color to red, signifying their designation as target objects before changing back to blue, thus rendering them again indistinguishable from the distractor object. After a 12 second interval of Brownian motion, one of the 10 objects are highlighted by changing color to green. Participants are then prompted to mark (by a button push) whether the highlighted object was one of the target objects or not. Along with sustained visual attention, the MOT task requires visual selection at the beginning of each trial as well as working memory throughout the task.

From electrophysiological and neuroimaging studies, several brain regions have shown to preferentially activate during task engagement, such as the intraparietal sulcus (IPS), the superior parietal lobule (SPL), frontal eye fields (FEF), human motion area (MT+) and the precentral sulcus (PreCS).

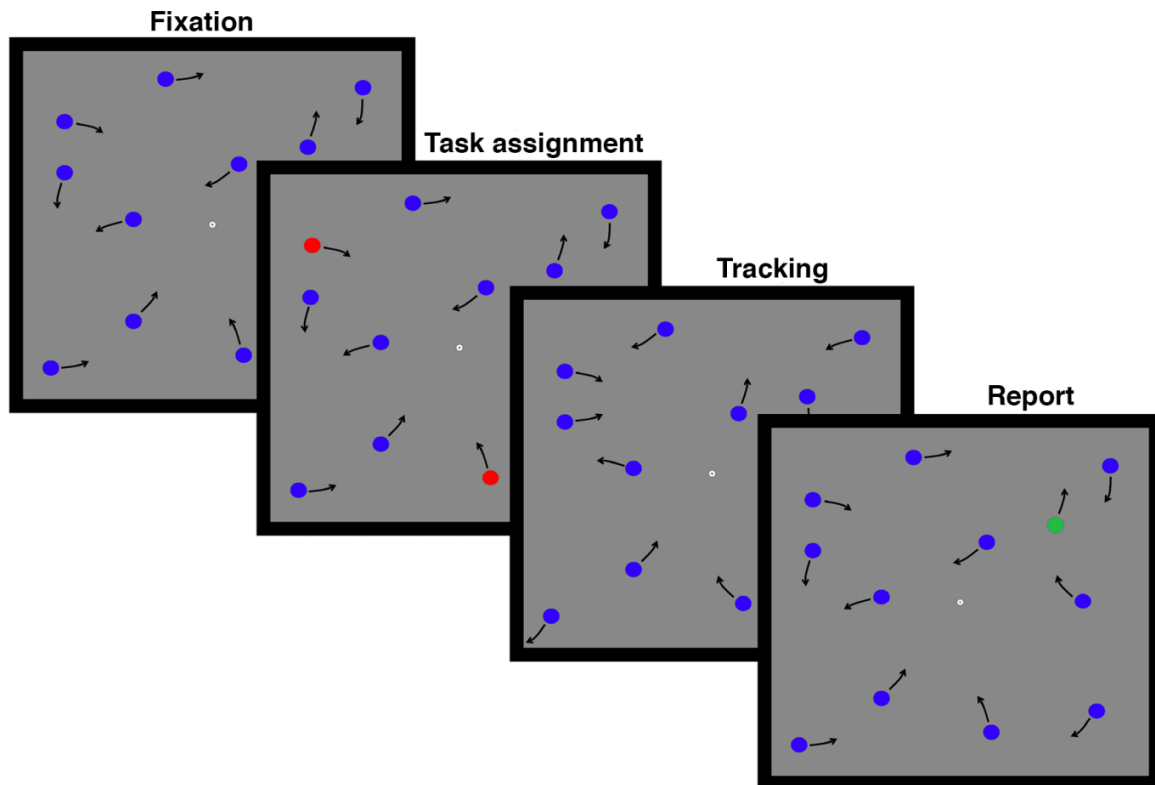


Figure 4. MOT task

#### 5.4. fMRI processing and analysis

On a single-subject level, we processed functional MRI data using the FMRI Expert Analysis Tool (FEAT) from the FMRIB Software Library (FSL; Smith et al., 2004). The preprocessing steps included spatial smoothing (FWHM = 6 mm), high-pass filtering (sigma = 64 s), motion correction (MCFLIRT), and single-session ICA using MELODIC (Beckmann & Smith, 2004). In-scanner subject motion was calculated as the average root mean square of the displacement from one frame to its previous frame for each dataset. Independent samples t-tests revealed significant more in-scanner movement for the older compared to the younger group in papers I and II, whilst no significant motion differences between stroke patients and healthy controls in paper III. Steps were taken to ensure that group differences were not introduced by motion effects or data cleaning in papers I and II. For paper I, the estimated network responses were also run on the uncleaned dataset yielding largely unchanged effects. In paper II, mean estimated motion was added as an additional covariate in the functional connectivity estimations for both

groups, yielding also here largely unchanged effects. To identify and remove noise components, we used FMRIB's ICA-based Xnoiseifier (FIX; Salimi-Khorshidi et al., 2014) with a standard training set and threshold of 20, yielding a cleaned dataset for each subject. Instead of regressing out the global signal (GSR), white matter, or CSF, we regressed out noise components using an ICA-based approach (FIX) which has been shown superior in denoising fMRI data compared to conventional techniques (Pruim et al., 2015). Automated brain segmentation of the T1-weighted data was performed using FreeSurfer (Fischl et al., 2002) to obtain brain masks used for co-registration to a standard coordinate system using FLIRT (Jenkinson & Smith, 2001), optimized by boundary-based registration (BBR; Greve & Fischl, 2009) and FNIRT (Andersson et al., 2007a, 2007b).

### **5.5. Voxel-wise general linear model (GLM) – Paper I**

Voxel-wise analyses were employed in paper I to investigate BOLD signal changes over experimental conditions, with the aim of replicating activation patterns seen in previous MOT studies, thus confirming the paradigm as a powerful tool for investigating sustained visual attention. The experimental design included blocks of fixation, passive viewing, MOT load 1, MOT load 2 and a tracking condition (averaging L1 and L2). The contrasts explored were tracking vs. passive viewing, and L1 vs. L2. GLM analyzes each voxel's timeseries independently, with the onset and duration of the tracking and passive viewing blocks modeled with the fixation blocks as implicit baseline. The timing of the HRF is subject to regional differences that was accounted for by adding a temporal derivative to the model, after the design matrix was filtered and convolved with the HRF. We tested for the difference between young and old over the given contrasts, after subjecting individual contrast parameter maps to whole-brain group analysis based on a random effect model. To correct for multiple comparisons, we performed cluster-level correction with voxel-wise Z-score > 2,3 and a corrected cluster significance of  $p < 0,05$ .

### **5.6. Group Independent component analysis (ICA) and network estimation - Papers I, II and III**

All three papers use ICA analyses where individually processed, cleaned, filtered and normalized datasets were submitted to a temporal concatenation group spatial ICA using MELODIC in FSL (Jenkinson et al., 2012). Components were classified as noise and non-noise

components based on the spatial distribution of the component maps and/or the frequency distribution of the components time series (Kelly et al., 2010), yielding 28, 32 and 30 non-noise components in the three papers, respectively. Next, subject-specific individual time series and component spatial maps were estimated using dual regression (Filippini et al., 2009). For paper I, the generated time series were further submitted to time-series regression using the individual GLM design matrices for the voxel-wise analyses. Regression coefficients for the two tracking conditions (L2-L1) were subtracted for each subject and submitted to group-level analyses, to assess associations between component activation in the old and young group for the L2 > L1 contrast. For papers II and III, the individual time-series of the noise components were regressed out of the time-series of the non-noise components to estimate functional connectivity matrices using FSLNets (Smith et al., 2011). Here, for paper III, to remove the common variance from the stroke lesions, a segmented lesion mask was added as an additional component in the individual dual regression. The estimated time-series of the lesion mask was then removed from the time-series of the components prior to network modeling. In a graph theoretical framework, components represent nodes in an extended brain network, connected by edges defined as temporal correlations between node pairs. Temporal correlations were estimated using regularized partial correlations with a data driven automated estimation of the regularization parameter lambda (Brier et al., 2015; Ledoit & Wolf, 2003) to yield networks that do not depend on a preselected, global lambda value (Deligianni et al., 2014; Kaufmann et al., 2016).

### **5.7. Edgewise univariate analysis – Papers II and III**

Network estimation yielded functional connectivity matrices comprising 32 nodes and 496 unique edges in paper II, and 30 nodes with 435 edges in paper III. Edgewise associations were further explored using repeated measures analysis of variance (ANOVA), testing for effects of group, condition (resting state and two load level continuous runs and interaction). To control for family wise error rate, we used a false discovery rate (FDR) level  $q=0.05$  to adjust the alpha level for each test, assuming independence or positive dependence (Nichols & Hayasaka, 2003).

## **5.8. Multivariate machine learning analysis - Papers II and III**

Regularized partial correlations between components represent the edges between nodes in the functional connectivity network. For papers II and III, we then employed multivariate machine learning to assess the predictive value of the FC measures across condition (rest, MOT L1 and MOT L2), and group (old vs. young in paper I and stroke vs. healthy controls in paper II). Using a regularized linear discriminant analysis classifier (linkage LDA) (Friedman, 1989; Schafer & Strimmer, 2005), the estimated network edges were used in classification tasks to classify between young and old participants (paper II) and stroke patients and healthy controls (paper III), within resting state and load conditions. Further, classification between resting state and load conditions within and across groups were done in both papers II and III. The robustness of the model was assessed using leave-one-out (LOO) cross-validation procedures, and reliability was assessed across 10000 permutations. For paper III, where the healthy control group comprised over twice as many subjects as the stroke group, we performed the group classification within a nested loop of 100 iterations, in which we each time randomly picked healthy control to correct for uneven sample sizes.

## **5.9. Eigenvector centrality – Paper II**

Eigenvector centrality is a measure of the relative importance of individual nodes in the functional connectivity network. In paper II we sought to investigate which nodes were more influential in discriminating between the old and the young group. Eigenvector centrality mapping (ECM) provides an index of weighted nodal centrality and reflects the number of edges to a node, while giving more weight to connections to nodes having a high degree of centrality (i.e., more connections). Preprocessed cleaned and normalized continuous tracking and resting state runs were processed in LIPSIA (Lohmann et al., 2001), and submitted to nodewise ECM estimation (Lohmann et al., 2010), using edgewise partial eta-squared effect sizes, testing for main effect of group, condition (resting state and two load level continuous runs) and interaction.

### **5.10. Standard deviation of signal amplitude (SDSA) – Paper II and III**

Variability in BOLD signal activity reflects healthy brain function. Studies have shown that the natural state of the brain is inherently variable, reflecting optimization of responsiveness to the changing environment and the ability to flexibly transition between cognitive states (Grady & Garrett, 2014). In papers II and III we investigate variability on node level by computing the standard deviation of BOLD signal amplitude for each component's time series, using FSLNets (Smith et al., 2011). Group differences were tested using an analysis of covariance (ANCOVA), covarying for sex (paper II), and sex as well as age (paper III).

### **5.11. Lesion mask – Paper III**

To be eligible for study inclusion, patients had to have a radiologically confirmed stroke. Stroke lesions were first identified by neuroradiologists at the respective Stroke units during standard clinical investigation upon hospital admittance. Patients that were enrolled in the study then underwent structural imaging including T1, FLAIR and DWI as part of the MRI protocol, which were used by the neuroradiologist at Oslo University Hospital to describe lesion characteristics. Informed by radiological descriptions, the lesions were semi-automatically delineated in native space, using the Clusterize-Toolbox (de Haan et al., 2015) based on visible structural damage and hyperintensity changes on FLAIR images. These images registered with the high-resolution T1 using linear transformation with 6 degrees of freedom. T1 images were further registered to MNI152 standard space by linear affine transformations (with 12 degrees of freedom). Native-to-standard transformation matrices (nearest neighbor interpolation) were applied to register the binarized lesion masks to standard space. In subsequent group ICA and network estimation, individual lesion masks were included as an additional component in individual dual regression runs to estimate time series for each component. The estimated time series from the lesion component was discarded from the component's time series that were used for network modeling.

### **5.12. Clinical assessment – Paper III**

All patients enrolled in the study were clinically evaluated and treated at the respective Stroke units in which they were admitted. Treatment was in line with the national guidelines (Helsedirektoratet, 2017). Stroke severity was assessed according to the National Institute of Health Stroke Scale (NIHSS; Lyden et al., 2009) by an attending physician specialized in either internal medicine, neurology or geriatric medicine. Individual NIHSS scores at the time of discharge were reported in Paper III. Stroke subtypes were classified by the specialized physicians, using the Trial of Org 10 172 in Acute Stroke Treatment (TOAST) classification system to subtype stroke lesions based on etiology. The Montreal Cognitive Assessment (MoCA) tool (Nasreddine et al., 2005) was used to assess general cognitive performance in both the patient and the control group. For the patients, the test was administered during hospital admittance, after the patients were clinically stable to optimize test validity.

### **5.13. Non-imaging statistical analyses – Papers I, II and III**

Non-imaging statistical data was analyzed in SPSS (IBM\_Corp, 2015). Demographic group differences were assessed using Chi square (handedness, sex distribution) and t-tests (education, neuropsychological tests). Group differences in MOT performance were evaluated with a two-by-two repeated measures ANOVA using load demand (L1 and L2) as within subject factor and group (young and old for papers I and II, patients and controls for paper III). For paper I, parameter estimates (beta values) were derived from the GLM analysis for each network during each condition. Group difference in network activation as well as load dependent activations (L2-L1) were explored using paired samples t-test and an ANCOVA with the beta values as the dependent variable, including sex and group as fixed factors. The association between beta values and MOT task performance during L2 as well as other neuropsychological estimates were tested with an ANCOVA, with performance scores as the dependent variable and sex and group as fixed factors. To test for load dependent between-network correlations in activation, we computed Pearson's correlation between the beta values in each network, yielding a 28 by 28 correlation matrix. We then tested for group differences by comparing the correlation

coefficients between the groups using Fisher's r-to-z transformation.

## **6. RESEARCH QUESTIONS**

### **PAPER I**

How are age-differential responses to attentional demand reflected in task-positive and task-negative network modulation. To what degree does network activations correlate with task performance? What are the age-related effects on brain network co-activations?

### **PAPER II**

Are age-related differences in brain networks more pronounced during an attentional task compared to rest? What brain nodes and connections are most discriminant in classifying younger and older participants? What are the effects of age and task on brain signal variability?

### **PAPER III**

How does stroke affect cognitive behavior and brain network characteristics? Are the stroke-induced effects more pronounced during an attentional task compared to rest?

## **7. SUMMARY OF PAPERS**

### **Paper I**

The brain is highly organized in a network fashion comprising sub-networks with regional hubs dispersed throughout the cortex. Task-based fMRI studies have shown differential patterns of brain activity when participants are engaged in cognitive demanding tasks as compared to rest, revealing task-positive networks (TPN) that activate and task-negative networks (TNN) that deactivate during task.

In this paper we investigate age-related differences in brain network activity during a multiple object tracking (MOT) task, in a group of younger ( $n = 25$ , mean age =  $24.4 \pm 5.1$  years)

and older ( $n = 21$ , mean age =  $64.7 \pm 7.4$  years) healthy participants. We utilized voxel-level general linear model (GLM) analysis and independent component analysis (ICA) to compare brain network activation and co-activation during two load levels of attentional demand.

Results indicated better task performance in the younger compared to the older group. Assessing the association between performance accuracy and network activity revealed no significant correlations in the old group, for the young group there was a positive correlation between performance and TPN activations. fMRI data revealed diminished activations in TPN, as well as diminished deactivations in TNN for the older comparative to the younger group. Further, the increase in task difficulty from 1 load to 2 load demand, resulted in greater relative network responses in the younger group, although no strong relationship between network activation and task performance was found. Sub-networks within the TPN and TNN showed stronger co-activations in the younger group, suggesting age-related neural dedifferentiation. The level of activation and deactivation of the task-positive and task-negative networks, respectively, was only weakly correlated; indicating that the two measures of task-related neuronal recruitment may reflect partly independent neuronal mechanisms of cognitive aging.

## **Paper II**

Whereas some cognitive functions decline even in healthy aging, others show only minor changes and may even improve during the course of life. The heterogeneity across cognitive domains is mirrored in a differential network vulnerability of brain connectivity, which has been proposed as a candidate imaging biomarker for age-related cognitive decline, and risk and progression of dementia. This domain-selective cognitive vulnerability suggests that a constrained cognitive paradigm may comprise a more sensitive context for the study of age-related brain network alterations compared to an unconstrained resting state paradigm.

We compared fMRI functional connectivity indices obtained from a group of younger ( $n=25$ , mean age  $24.16 \pm 5.11$ ) and a group of older ( $n=22$ , mean age  $65.09 \pm 7.53$ ) adults during rest and two load levels of a MOT task. We applied multivariate machine learning based on a cross-validated regularized linear discriminant analysis technique to discriminate cognitive load and age groups using the full set of brain connectivity features, which were estimated using independent component analysis, dual regression, and regularized partial correlations.

Compared to resting-state, functional connectivity estimated during continuous tracking strongly increased group classification accuracy. Further, connectivity patterns during rest and task were more distinguishable in young compared to older individuals. Nodes within the default mode and the dorsal attention networks were most discriminative when comparing the two age groups, and we found age-related reductions in the anti-correlation between attention-and default mode networks, corroborating the notion of cognitive and neuronal dedifferentiation in aging. Our findings suggest that cognitive tasks provide a more sensitive framework for studying age-related network differences, a finding that has implications in the ongoing search for imaging biomarkers across the clinical neurosciences.

### **Paper III**

The complex constellation of symptoms following a stroke is not fully explained by the loss of function caused by the localized cerebral tissue damage, but better understood as the result of disruptions to the functional network architecture of distributed brain systems.

In paper II, we demonstrated differential connectivity patterns between a group of younger and a group of older healthy adults, and we found that a constrained cognitive paradigm comprises a more sensitive context for the study of age-related brain network alterations. In paper III - using the same methodology - we sought to explore the network alterations associated with cerebral strokes, and whether data obtained during an attentive tracking task was more sensitive to diagnosis compared to an unconstrained resting state paradigm.

Multivariate machine learning yielded high accuracy when classifying between resting-state and two load levels of attentional demand, for both groups, indicating high sensitivity to cognitive context. However, discrimination between stroke patients and healthy controls was not found to be beyond chance-level, and task-data did not increase sensitivity to diagnosis compared to resting state. Supported by statistically insignificant group differences in MOT-performance and cognitive assessment, results suggest that clinically mild ischemic strokes yield minimal behavioral and whole-brain neuronal effects.

## **8. ETHICAL CONSIDERATIONS**

All research performed in this thesis and in the larger StrokeMRI project were conducted in accordance with the Helsinki declaration. Each facet has been subject to review and approval by the Regional Committee for Medical and Health Research Ethics (South-East Norway, 2014/694; 2015/1282), and by the data protection regulation (personvernombudet) at Oslo University Hospital.

Stroke research is fraught with ethical issues that were carefully considered upon project inception and during data collection. Particularly, stroke patients are vulnerable individuals who may be compromised in information processing and decision-making. To ensure ethical inclusion standards, each patient was first assessed and deemed cognitively, physically and emotionally eligible for enrolment by a physician working at the respective stroke unit. Patients were then approached by a StrokeMRI researcher and reassessed before final inclusion. Patients were thoroughly assured that the decision to participate or not would not affect treatment or level of care. We obtained verbal and written informed consent from both stroke patients and healthy controls prior to data collection.

MRI images acquired from both stroke patients and healthy controls were individually reviewed by a neuroradiologist. Incidental findings that required further follow-up were reported to each participant and – upon request – a radiological description was sent to their primary physician. Although not reported in the present thesis, blood samples and blood pressure measurements were obtained in each study participant. Clinically relevant information from these assessments were handled similarly to the incidental MRI findings.

## **9. DISCUSSION**

The overarching aim of this thesis was to investigate the neural network correlates in cognitive aging and cerebral stroke, and how the networks are modulated by attentional demand. To this end, fMRI data was collected from a group of older and younger healthy participants (papers I and II), and a group of subacute stroke patients and matched controls (paper III) during

an unconstrained resting state and two load levels of a multiple object tracking task. Additionally, data was gathered from neuropsychological testing, MoCA, a cognitive screening tool particularly devised for stroke patients (Nasreddine et al., 2005) and a stroke severity scale.

Findings in papers I and II demonstrated robust effects of age on neural networks. Results in paper I provide evidence for attenuated brain activity modulations in task-positive and task negative networks for older subjects during attentional demand. Moreover, we observed alterations in the system-level coordinated patterns of network activity, with less within-network specificity for older subjects. In paper II, the system-level approach was explored further by estimating whole-brain functional connectivity features. Here, a machine learning classifier successfully discriminated between older and younger participants, with group differences becoming more pronounced during task compared to rest. Encouraged by the findings in paper II; we applied the same techniques to investigate connectivity alterations between a group of sub-acute mild stroke patients and healthy controls in paper III. However, after regressing out individual lesion effects on whole-brain networks, the results yielded no significant group differences. Additionally, we investigated differences in brain signal variability in papers II and III. Again, we observed effects of age with overall greater variability for the younger compared to the older group, but no significant variability differences between stroke patients and controls. In the following section, these findings and their implications will be discussed in light of relevant theories and current state of knowledge.

### **9.1 Stroke in the context of age**

Cognitive aging “describes the process of gradual, longitudinal changes in cognitive functions that accompany the aging process” (Blazer et al., 2015). Although technically not a disease; aging is the accumulation of deleterious processes that contribute to biological system failure. In the context of reliability theory where diseases are specific cases of system failure, aging does not interact on the system itself, but rather causes these failures to increase in intensity with age (Gavrilov & Gavrilova, 2001). Neural alterations observed in cognitive aging are often seen accelerated in neurodegenerative and psychiatric disorders. Studying the biological underpinnings of the aging brain, therefore, may not only advance approaches to the debilitating consequences of senescence, but also elucidate common mechanisms involved in a range of conditions affecting the human brain. Advancing age is a particularly pertinent topic in

the context of stroke research. Aging in itself is a risk factor for stroke, in that stroke occurs more frequently – approximately 75% of all strokes occur in people aged 65 years and above (Yousufuddin & Young, 2019) – and engenders more severe outcomes in the older population (Sohrabji et al., 2013). To evaluate the neuroimaging effects of stroke (and any other age-associated neurodegenerative disorder for that matter), it is important to have knowledge about aging physiology to better identify the sources of observed effects and how they interact.

## **9.2 Over- or underactivation with advancing age?**

Findings in both papers I and II demonstrate overall decreased attentional task performance for older compared to younger participants, with fMRI data showing age-related differential network modulations in response to task demands. In paper I, looking at brain network activations during task; DAN activations and DMN deactivations were diminished for the older relative to the younger participants. The commonly reported finding of age-related overactivation in task-positive networks at low load levels was not encountered, as DAN activation was stronger for the younger group during both load levels of task demand. Overactivation with advancing age, in the presence of positive behavioral correlates, has been interpreted as a compensatory feature as auxiliary neural recruitment is needed to make up for a supply-demand gap caused by depleted neural resources to meet the same task requirements (Cabeza et al., 2018). In paper I, there was no evidence of such compensation taking place. No significant association between task-related network modulation and task accuracies was encountered in either group, thus limiting any strong inferences to be made regarding the specific contributions of DAN and DMN modulation on the ability to successfully perform the MOT task. The older group did perform significantly worse than the younger group at the load 2 task demand, concomitantly with diminished DAN activation and DMN deactivation. This finding could reflect reduced task-positive neural resources and a relative failure to suppress task-irrelevant brain regions, as a feature of the detrimental effects of advancing age on attention. Both the CRUNCH and STAC-r models of cognitive aging accommodate for finding underactivation in attentional networks for older adults once task difficulty exceeds a certain threshold and neural resources become exhausted. However, this theoretical limit was not encountered in the study, given the low load demand set on the MOT task and the high response accuracy (the older group had an approximated average response accuracy of 94% during load 1

and 78% during load 2). Indeed, mean performance accuracies during the load 1 level of task demand were statistically insignificant between the groups, yet DAN modulation was also here comparatively diminished in the older group. Further, the relative increase in DAN activation when increasing task difficulty (from 1 to 2 load levels) was significantly reduced for the older group, representing a lower capacity for additional DAN recruitment upon higher demand. Prevailing compensation models of cognitive aging suggest that - when performance is equal between older and young groups - there is a need for increased neural recruitment to compensate for the gross and microscopic cerebral aging effects.

While task-positive overactivation for older participants is the most reported finding in cross-sectional studies, underactivation in task-positive regions has also been reported (Dulas & Duarte, 2011; Maillet & Rajah, 2013). The papers that have reported age-related frontal overactivations have primarily been cross-sectional studies utilizing large age-spans when comparing younger and older groups (for review, see Grady, 2012). In a study by Nyberg and colleagues (2010) cross-sectional results indicated frontal overrecruitment for older subjects during a cognitive task, longitudinal estimates, however, revealed activity reductions in the same frontal areas. Further, studies using life-span samples and continuous age-increments have reported diminished age-related frontoparietal BOLD modulations during visuospatial (Rieck et al., 2017) and working memory (Archer et al., 2018) tasks, suggesting that differential network modulation findings are in part design dependent. A general overview of the extant literature thus shows no consistent direction of task-related DAN modulation in the context of aging, nor a consistent coupling between activity and behavioral effects. The CRUNCH and STAC-r models are arguably the most influential compensation models of cognitive aging at present. They do, however, axiomatically derive from the premise of frontal over-recruitment as a ubiquitous feature of cognitive aging. Frontal underactivations with preserved behavioral correlates as found in paper I is not encountered for in either model. A challenge in aging research and neuroscience in general is the emergence of ill-defined concepts that suffer from being poorly operational and difficult to falsify (Nilsson & Lovden, 2018). Added to this, the reproducibility-crisis in the field of neuroimaging calls for greater transparency in methods and reporting, and strict delineation between hypothesis-driven and exploratory research (Poldrack et al., 2017). The CRUNCH model sought to address some of these problems by introducing a clear and testable CRUNCH-point. Regrettably, very few studies to date have tested the hypothesis, and results have been

conflicting (for review, see Jamadar, 2020). The present thesis did not seek to test the CRUNCH model, or other specific cognitive aging theory. And although the results do not align with models based on compensation, the results in this study certainly do not invalidate any of the proposed aging models. Findings reported here, in the context of the broad literature, support the future need for the development of models that are empirically approachable, and a general emphasis on rigorous testing of aging models, replication checks and meta-research (Ioannidis et al., 2015).

### **9.3 Effects of age on DAN and DMN dynamics**

In paper I, results showed a positive association between DAN and DMN activations when increasing load demand for the older group, while no significant correlations between activation patterns between these two networks were found for the younger group. This illustrates that, when task difficulty increases, the anticorrelated relationship between the DMN and DAN becomes attenuated for older adults. The ICA-approach used in paper I yielded in total 28 non-noise components corresponding to brain networks, where the DAN and the DMN were each parsed into five separate subnetworks. Task related co-activation in components within these networks were significantly stronger for the younger participants. These findings affirm decreased within-network co-activity and a relative loss of maintaining anticorrelation between task positive and task negative networks for older adults. Loss of network specificity with an increased reliance on between-network recruitment and a diminished contrast between task-positive and task-negative networks underlies network dedifferentiation are well established findings in aging research (Li et al., 2015; Tomasi & Volkow, 2012). It is important here to make a distinction between network co-activations and functional connectivity. BOLD activation differences during blocks of rest and trials, as implemented in paper I, is a measure of differential neurovascular coupling (neuronal activity) evoked by different mind states. Networks that activate during trial blocks are thought to represent the underlying biological response necessary to perform the task at hand. The co-activation patterns observed in paper I thus reflect general age-related feature differences in within-and between network configurations. Care should be taken when interpreting co-activity between networks that are spatially dispersed and subserve specialized functions. Brain regions that perform independent operations may activate jointly during any compound task without being part of a common network. A task with both auditory

and visual stimuli would indeed activate auditory- and visual networks simultaneously, without necessarily implying that these networks are functionally linked.

Whereas BOLD signal changes answer questions pertaining to which brain regions activate and deactivate across conditions – in paper II we studied age group differences in functional connectivity, that is, the synchronicity of signal fluctuations between brain regions. Here, we used a continuous version of the MOT task to investigate age differences in functional network configurations, and how networks are modulated by task. The dynamics of FC reflect evolving patterns of neural communication and FC indices serve as an interlinked and complementary approach to BOLD activation studies in understanding brain function. The interdependence between FC and BOLD activation has been demonstrated in studies where resting state connectivity is shown to predict activation during cognitive tasks (Grigg & Grady, 2010; Mennes et al., 2010), and disconnection of task-irrelevant brain regions is correlated with enhanced task performance (Tomasi et al., 2014). Additionally, FC measures are altered both during and following task engagement (Wang et al., 2012) reflecting adaptive network properties serving to balance functional segregation and integration with the objective of optimizing cost efficiency (Fu et al., 2017)

Brain signal synchronicity is facilitated by anatomical interconnectedness according to the Hebbian maxim of “*neurons that fire together, wire together*” (Greicius et al., 2009; Honey et al., 2009). The functional connectivity network comprises nodes (brain regions) connected through edges (signal time correlates between nodes). Task evoked connectivity changes reflects network modulation to optimize (increase connectivity) or deprioritize (decreased connectivity) anatomical pathways. In paper II, eigenvector centrality indices implicated the DAN and DMN as central network hubs. Briefly, eigenvector centrality is a graph theoretical measure that assigns value to a network node based on the number and relative influence of the nodes that it connects to. The higher the value of the node, the more influential it is in the network. The DAN was shown particularly relevant in attentional task processing, and the DMN particularly susceptible to aging effect. Unsurprisingly, task engagement yielded the strongest connectivity increases between DAN and visual networks, while connectivity decreases were seen between the DAN and task-negative sensorimotor nodes. Group effects were primarily seen in DMN-connected edges. Notably, paper II showed aging-associated positive DAN-DMN connectivity

which compliments findings in paper I and supports the concept that DAN-DMN coupling and loss of anticorrelation is hallmark feature in cognitive aging.

The DMN is known to play a role in internal mentation and is seen to preferentially deactivate when subjects are engaged in behavioral tasks (Fox et al., 2005; Raichle et al., 2001), thus forming an antagonistic system to task-positive networks, most notably the DAN. Activation in the DAN during attentional demand reflects coordinated neural recruitment in response to stimuli, as DAN subregions have specific functions each contributing to efficient visual attentional processing. For example, the frontal eye fields (FEF) provide a mental spotlight for the objects to be tracked, and guides eye movement (Thompson et al., 2005); the interparietal sulcus (IPS) is involved in selection among competing stimuli (Mevorach et al., 2009); and the superior parietal lobule functions in spatial attentional shifts (Corbetta et al., 1995). While the interpretation of task-positive activations is more intuitive, the significance of DMN suppression in response to externally oriented cognition has garnered a lot of interest in cognitive research and has been widely studied in the context of aging and disease.

From its significance in self-referential thought processes, the DMN is proposed to enable construction of mental models that support internally oriented computations (Anticevic et al., 2012). By this nature, when cognitive goals are externally directed, DMN disengagement serves to filter out distractive internal thoughts such as mind-wandering, that otherwise would interfere with optimal cognitive behavior (McKiernan et al., 2003). The functional importance of DAN and DMN antagonism is also evident in its coordination with other large-scale brain network. Sensory networks are coupled with the DMN when task goals are internally focused (such as the retrieval of autobiographical memory), but not in externally demanding task (such as visual attention tasks) where sensory networks are coupled with the DAN (Chadick & Gazzaley, 2011; Turkheimer et al., 2015). An anatomically interposed executive control network is thought to function as a mediator to flexibly facilitate the dynamic network coupling based on goal orientation (Spreng et al., 2010). Hierarchical clustering has revealed this frontoparietal control network (FPN) to be organized into two separate subsystems where subsystem A exhibit stronger connectivity with the DAN than the DMN and an opposite relationship for subsystem B (Dixon et al., 2018). The existence of multiple control networks has been evidenced from resting-state (Dosenbach et al., 2006) and lesion studies (Nomura et al., 2010). In large-scale network

estimations the frontoparietal control network and the DAN are highly adjacent or intermixed and are thus often grouped together (Gordon et al., 2017). However, network estimation analyses used in the present thesis managed to successfully identify components representing the frontoparietal control network in both papers I and II. In paper I, one (IC8) component extracted from the ICA was designated a right-lateralized frontoparietal node, discernable from the canonical DAN. In paper II, the same ICA approach yielded one right-oriented (IC1) and one left-oriented (IC2) component corresponding to the FPN. The FPN showed strong load-dependent activity during MOT for both age groups, confirming its relevance during attentive tracking. Whilst there were no significant group differences in magnitude of activity (paper I), there was however, a strong age group difference in connectivity between the FPN and DMN (paper II). Whereas the FPN and the DMN were decoupled for younger participants, these edges were functionally connected for the older group at rest, with task condition yielding a load-dependent increase in connectivity strength. Generally, this affirms the trend of more between-network dependencies and loss of network segregation with advancing age. It is well established that the FPN and DMN couple during tasks that require top-down control to guide attention to internally oriented cognitive goals (Gao & Lin, 2012; Gerlach et al., 2011; Spreng et al., 2010). Here, the FPN-DMN connection has a functional relevance, considering the role of the FPN as a mediator of attentional control that shifts from coupling with the DAN upon external task demands, to couple with the DMN when task goals are directed internally. Thus, the finding of a preferential FPN-DMN coupling for older adults during an externally oriented task might represent a common network configuration in cognitive aging. No study to date has used the MOT paradigm to elucidate these specific network modulations in the context of aging research. However, these findings have been encountered in studies involving working memory (Sambataro et al., 2010) and planning (Turner & Spreng, 2015). The latter paper prompted the authors to promote the concept of a default-executive coupling hypothesis of aging (DECHA). This hypothesis posits that the age-related changes in the functional architecture of the brain are reflective of changing modes of cognition. Broadly, age-related changes in cognitive abilities divide cognition into crystallized and fluid abilities (Cattell, 1963; Wang & Kaufman, 1993). Crystallized abilities involve knowledge acquisition and the ability to recall information reflected in general knowledge and vocabulary tests. These skills show an improvement until approximately the age of 60 before a plateau into the 80's followed by decline (Salthouse, 2010). Fluid abilities require

the ability to manipulate and process new information, placing high demand on processing speed and reaction time while relying less upon prior knowledge (Bugg et al., 2006). Age-related decline in fluid abilities appears as early as the mid-20s (Harada et al., 2013). These two facets of cognitive capabilities thus show inverted trajectories in adulthood. Accrual of semantic knowledge during the lifespan along with declines in fluid capabilities leads to a shift in cognitive modes, where goal-directed cognition becomes increasingly reliant on past knowledge and experiences (Spreng & Turner, 2019). When task goals are congruent with the knowledge expanse, this shift is beneficial to performance (Spreng & Schacter, 2012). When prior knowledge is task-irrelevant, it becomes a distracting intrusion. The DECHA model speculates that the FNP-DMN coupling is the neural conduit through which knowledge enters the focus of attention (Spreng & Turner, 2019). When taken together, findings in paper I and II are congruent with the DECHA-model, although no *a priori* hypotheses were proposed with this theory in mind. Again, the vast complexity of the working mind has yielded partly conflicting research findings and heralded a myriad of explanatory models that, to date, have yet to meet sufficient standards of reproducibility and predictive power. The future bodes well for further technological advancements to improve quality and quantity of data, which will only stress the importance of scientific rigor when interpreting the data and developing new models.

#### **9.4 BOLD variability: signal disguised as noise**

The exceedingly the most common and straightforward way researchers have investigated the BOLD signal is by looking at mean values. More recently, temporal variability of the BOLD signal has garnered attention as a proxy measure of neural network health, where greater variability reflects greater dynamic range and the ability to explore various functional states (Garrett et al., 2010; Wang et al., 2020). By computing the standard deviation of signal amplitude (SDSA) in paper II, findings were in alignment with previous research (Grady & Garrett, 2014) demonstrating overall less signal variation for the older cohort. Previous studies have also reported less variability in chronic stroke patients (Kielar et al., 2016), however, just as paper III did not find significant group differences between stroke patients and controls in functional connectivity, nor did we find significant differences in signal variability. The SDSA analyses did however provide some interesting results to consider. The greatest age group differences in signal variability were found in cerebellar nodes, and contrary to the general trend,

greater variability was encountered for the older compared to the younger group. Similar findings have previously been reported (Garrett et al., 2010, 2011) without an accompanying proposed hypothesis of underlying mechanisms. At face value, this might suggest inverted aging trajectories for cerebral and cerebellar nodes. Possibly, a compensatory feature where cerebellar networks increase dynamic range in response to less efficient cerebral networks, assuming that cerebellar neurons are more resilient to aging affects. There are, however, also particular confounds of note when interpreting cerebellum-specific findings in whole-brain analyses (for review, see Diedrichsen et al., 2010); 1) The BOLD signal is an admixture of neural and vascular effects. The relatively small spatial extent of the cerebellum, and its proximity to dense vasculature and the respiratory tract, renders it particularly susceptible to physiological noise which effects variability analyses more than mean based ones (Schlerf et al., 2012); 2) The architecture of the cerebellum is quite distinct from the neocortex, so the source of the neural signal, neurovascular coupling and blood flow do not necessarily conform to the same ratios. Although methods to correct for some of these problems have been established (Schlerf et al., 2014; van der Zwaag et al., 2015), the distinctiveness of the cerebellum poses a challenge for whole-brain level analyses where underlying assumptions do not tailor to separate brain regions. Future research should be mindful of regional differences in anatomy and physiology when interpreting regional effects in whole-brain studies.

### **9.5 On the search for imaging biomarkers: machine learning and the value of task**

Cerebral stroke is a leading cause of death and disability worldwide, and with improved primary hospital care, population growth and a burgeoning elderly population, the amount of stroke survivors are projected to increase dramatically over the next couple of years (Béjot et al., 2019). A stroke incident is an exceedingly individually variable diagnosis in terms of etiology, pathomechanism, location and extent of lesion, corresponding symptomatology and clinical outcomes. Henceforth, there's a growing demand for identifying reliable biomarkers (objectively measured features of normal biological processes, disease states or pharmacologic responses) to predict outcomes, monitor progression, and individualize prevention, treatment and rehabilitation strategies. In clinical trials, stratifying and subgrouping patients according to appropriate biomarkers reduces variance which permits smaller sample sizes to be used whilst maintaining power (Cramer, 2010). Presently, to extract clinical utility from neuroimaging data, radiologists

examine individual brain scans emphasizing the anatomical characteristics of a lesion (e.g., size, location, adjoining tissue reaction), or perform analyses of clinically relevant features such as cortical thickness. Considering the complexity and interconnectedness of the human brain, a holistic approach may offer a superior avenue in which to explore relevant biomarkers and explain the final clinical phenotype following a stroke incident.

The resting-state fMRI paradigm requires participants to lie still while looking at an empty screen within the scanner room. Due to its simplicity and relatively low individual demand, this paradigm accommodates for studying patients with functional deficits that would otherwise interfere with the ability to perform task-based paradigms. However, as behavioral deficits become more pronounced when behavior is challenged, it's reasonable to assume that neural patterns subserving behavior become more distinct in a cognitively demanding context. This hypothesis was tested and confirmed in paper II, where machine learning classification based on FC indices yielded load-dependent increased classification accuracies in distinguishing between older and younger participants during MOT compared to rest. By showing that a task setting provides a more sensitive framework to explore age group FC differences, this finding has implications in the ongoing search for potential neuroimaging biomarkers in a range of brain disorders.

Machine learning classification on fMRI data has been explored in disorders such as schizophrenia (Arbabshirani et al., 2013; Calhoun et al., 2008), autism (Sadeghi et al., 2017; Uddin et al., 2013), attention deficit hyperactivity disorder (ADHD; Qureshi et al., 2017; Zhu et al., 2008) and mild cognitive impairment (MCI)/Alzheimer's disease (Challis et al., 2015; Onoda et al., 2017; Zhang et al., 2021). A majority of the studies are binary classification between patients and controls on resting state data, with average classification accuracy around 80% (for review, see Du et al., 2018). Few, but some machine learning classification studies have also explored the impact of task data. Network activation differences distinguished schizophrenia patients from healthy controls with 93% accuracy at rest, increasing to 98% accuracy during an auditory oddball task in a study by Du and colleagues (2012). Park et al. probed a range of task paradigms and showed that gambling punishment and emotion tasks distinguished ADHD subtypes based on connectivity features with over 90% accuracy (Park et al., 2016). In a recent paper, Lee and colleagues (2021) used differential activation patterns to distinguish insomniacs

from healthy controls, and found that multi-task data outperformed single-task data analyzed separately. This finding further reflects the usefulness of extracting relevant features during different cognitive processes to get a more complete neural representation of various clinical phenotypes. In aging studies, machine learning classification based on whole-brain FC has been successfully applied to resting state fMRI (Meier et al., 2012; Vergun et al., 2013; Wen et al., 2019), however, no such study to date has also included the implementation of task data. Hence, the methodological approach and subsequent findings in paper II has shown the benefits of investigating age-group differences in FC in a cognitively demanding setting, and that parametrically increasing task demand, might increase sensitivity to capture neuroimaging biomarkers that would otherwise elude resting state data.

Machine learning techniques in stroke research have primarily been applied to structural imaging, with automated algorithms showing great effectiveness and utility in determining diagnosis (Takahashi et al., 2014), time of stroke onset (Lee et al., 2020), and in predicting functional outcomes (Forkert et al., 2015; Rondina et al., 2016). Connectivity-based classification approaches in stroke research have identified potential biomarkers using ROIs pre-selected on basis of the functional deficits under investigation. For instance, post-stroke hand motor impairment was accurately classified from patients without such deficits driven by reduced interhemispheric connectivity between primary motor areas, and increased connectivity between primary and premotor areas (Rehme et al., 2015). To date, no study has probed stroke-induced connectivity changes on whole-brain level using machine learning classification. In paper III, we used the same methodological approach as in paper II to investigate differences in whole-brain connectivity features during rest and MOT, between a group of sub-acute stroke patients and healthy controls. However, whereas paper II revealed significant group differences between older and younger healthy subjects, group differences between stroke patients and controls did not reach statistical significance. The demands of the study selected for minimally severe stroke patients, reflected in low NIHSS scores and behavioral results at par with the healthy controls. Thus, our findings demonstrated that minimally severe strokes need not produce significant alterations in whole-brain network configuration concomitant with minimal behavioral deficits. Although we did not find any significant difference between patients and controls in the metrics that we probed, this is not to say that the stroke subjects were without clinical sequelae. Hidden deficits such as fatigue, depression and memory changes etc. are well

known to affect stroke-survivors and may have a large impact in quality of life (Lapadatu & Morris, 2019; Schöttke et al., 2020; Ulrichsen et al., 2020). Other important outcome measures such as return to work and social reintegration were not included in our study, but is of great importance on individual and societal levels. With increasing numbers of stroke survivors and increasing age of retirement, research, particularly within neurorehabilitation, can benefit from including such variables in future studies.

## **9.6 Methodologic considerations**

Research presented in this thesis come with several limitations which affects the generalizability of findings. These include factors related to the sampling, study design and methodology, as well as inherent challenges in the field of neuroimaging, aging and stroke research. This chapter is by no means an exhaustive list, but rather a selection of principal limitations worth consideration when interpreting study findings. Certain limitations that are not expounded upon here, may be visited elsewhere in the discussion section where appropriate.

### **9.6.1 Study sample and selection bias**

The healthy controls enrolled in all three papers were recruited through newspaper ads and social media. In papers I and II, participants' Full Scale Intelligence Quotient (FSIQ) was estimated using the Wechsler Abbreviated Scale of Intelligence (WASI) test yielding average IQ scores of around 120, which is substantially higher than the national average. The recruitment strategy as well as the geographic location in which the study was performed – urban dwellers are known to outperform rural dwellers in standardized cognitive tests (Cassarino & Setti, 2015) – biased the final sample towards higher performing participants. The stroke sample in paper III comprised patients with mild clinical severity (average NIHSS below 1). This was partly due to the extensive MRI protocol which protracted the assessment to exceed an hour total scanning time, which is a substantial amount for health individuals, let alone individuals who recently suffered a cerebral stroke (average time between scanning and stroke symptom onset was approximately 8 days). As there were no apparent clinical or diagnostic benefits of study enrolment, one might speculate that the stroke patients that agreed to participate were partly incentivized by the desire to contribute to science and the novelty of task-based fMRI, which suggests a selection bias towards high cognitive function. Each cohort in all three papers,

including the stroke patient group had on average more years of education than the general population, further substantiating the fact that the convenience samples gathered were cognitively more proficient than the general patient- and overall population.

### **9.6.2 Study design**

There is tremendous inter-individual variability in cognitive aging. Research on episodic memory – an area particularly susceptible to age-related decline – has shown certain octogenarians to perform as well as, or even superior to 40-year-old individuals (Habib et al., 2007). Aging exerts effects on multiple levels of microscopic and macroscopic neurobiology that also interacts with the environmental factors throughout the lifespan. As such, group-level effects for an older cohort draws the risk of containing individual outliers that skew group averages. A cross-sectional, compared to longitudinal design does not account for effects of birth cohort, such as the increase in IQ test scores for successive generations (Trahan et al., 2014), or the effects of age variant and invariant cognitive differences, as a large proportion of variance in cognitive performance for older adults were present in childhood (Deary et al., 2004). The age group cohorts in papers I and II were matched in terms of average years of education. In both papers, both the younger and older groups had over 15 years of education, commensurate with a completed bachelor's degree. It is worth to note that the proportion of population that enter and achieve academic degrees has steadily increased in Norway since the second world war (Vabø, 2003). This trend is not particular to Norway, but is encountered across industrialized nations worldwide, in part due to changes in societal class structures, technological development and increased competence requirements in the labor market. For a birth cohort born in the sixties, 15 years of education represents a considerably lower proportion of the population compared to birth cohorts born in the subsequent decades. Consequently, it is reasonable to assume that cross-sectional studies with age group cohorts that are matched in education and IQ will select for cognitively higher functioning individuals in the upper age range.

It follows from the cross-sectional design that the stroke patients were assessed following the stroke event. The absence of baseline patient data makes it difficult to establish a causal link between stroke-induced alterations and pre-existing group differences. Further, the patients enrolled in the study were not expressly incentivized to participate in any other way than to contribute to scientific endeavor. This suggests a selection towards a higher functioning patient

sample compared to the general stroke population. A longitudinal study with data before and after the stroke incident would be an optimal design to investigate stroke effects on group and individual levels. No such study to date has been published on human participants and the feasibility to conduct such a study would be greatly limited by the cost of time and resources.

The practice of pre-registering hypotheses and analyses in scientific research has gained prominence over the recent years. Widespread pre-registration on open platforms increases transparency, mitigates the risk of publication bias and enhances the overall quality and credibility of scientific findings. Regrettably, the research presented in this thesis was not submitted to a pre-registry. This is not to say that the science was conducted without proper rigor, but rather due to it not being standard practice at the time. Considering the reproducibility crisis in experimental research (Baer & Gilmore, 2018; Ioannidis, 2005; Johnson et al., 2017), there is a growing need to implement practices aimed at enhancing the dependability and resilience of scientific investigations. Pre-registration is an unequivocal mean to this objective, complemented by an emphasis on collaboration, data sharing and the cultivation of a milieu fostering ethical research practices.

### **9.6.3 BOLD signal alterations in aging and stroke.**

The BOLD signal is dependent on local concentration of deoxygenated hemoglobin produced by the interactions between neural activity and vascular response. This neurovascular coupling is influenced by several physiological factors such as cerebral blood flow, volume and oxygen consumption that are impacted by age and disease (for review, see D'Esposito et al., 2003). To properly interpret fMRI findings, especially in group comparison studies, it is paramount to be cognizant of the underlying sources of the observed signal. Aging and stroke confers altered vascular and hemodynamic properties that attenuates the neurovascular response and influences the relationship between neuronal and non-neuronal contributors to the BOLD signal (Kumral et al., 2020). Further, individuals of advancing age are more likely to use regular medication. This is certainly the case following a cerebral stroke, where secondary prophylactic drugs such as platelet inhibitors and lipid-lowering compounds are often necessitated. Due to the nature of the BOLD signal, pharmacological effects are not limited to psychoactive drugs, but is also seen in vasoactive compounds as well as in medication, where at face value, one would not expect a direct effect on neurovascular coupling (Williams et al., 2019; Xu et al., 2008). Possible

interaction effects between drugs, age and disease states further complicates the picture. The common method of minimizing unwanted drug effects (as was done in all three papers) is to exclude participants on psychoactive medication and with a history of drug abuse. However, as shown, this does not exclude possible pharmacological confounds in its entirety.

## **10. CONCLUDING REMARKS AND FUTURE DIRECTIONS**

Inherent to human nature is a tremendous interest in understanding the inner workings of the human brain. Neuroimaging is still a relatively recent discipline that hinges on technology which is ever improving. These factors considered, the future of the field is bright with promises of further advancements, yet also vulnerable to existing and emerging challenges. The complexity of cerebral neurobiology and the nature of the BOLD signal requires careful and deferential consideration when interpreting fMRI finding. Future studies using longitudinal designs and rigorous confound correction with an emphasis on developing models that are testable and reproducible, will further this field of research. Meta-research and large, multi-center datasets can offer an avenue to resolve contradictory findings and help introduce replicable brain models.

## 11. REFERENCES

- Abou Elseoud, A., Littow, H., Remes, J., Starck, T., Nikkinen, J., Nissila, J., Timonen, M., Tervonen, O., & Kiviniemi, V. (2011). Group-ICA Model Order Highlights Patterns of Functional Brain Connectivity. *Front Syst Neurosci*, 5, 37. <https://doi.org/10.3389/fnsys.2011.00037>
- Alnæs, D., Sneve, M. H., Espeseth, T., Endestad, T., van de Pavert, S. H., & Laeng, B. (2014). Pupil size signals mental effort deployed during multiple object tracking and predicts brain activity in the dorsal attention network and the locus coeruleus. *J Vis*, 14(4). <https://doi.org/10.1167/14.4.1>
- Andersson, J. L. R., Jenkinson, M., & Smith, S. (2007a). *Non-linear optimisation. FMRIB technical report TR07JA1* (FMRIB Analysis Group of the University of Oxford, Issue).
- Andersson, J. L. R., Jenkinson, M., & Smith, S. (2007b). *Non-linear registration, aka Spatial normalisation FMRIB technical report TR07JA2* (FMRIB Analysis Group of the University of Oxford, Issue).
- Anticevic, A., Cole, M. W., Murray, J. D., Corlett, P. R., Wang, X. J., & Krystal, J. H. (2012). The role of default network deactivation in cognition and disease. *Trends Cogn Sci*, 16(12), 584-592. <https://doi.org/10.1016/j.tics.2012.10.008>
- Arbabshirani, M. R., Kiehl, K. A., Pearlson, G. D., & Calhoun, V. D. (2013). Classification of schizophrenia patients based on resting-state functional network connectivity. *Front Neurosci*, 7, 133. <https://doi.org/10.3389/fnins.2013.00133>
- Archer, J. A., Lee, A., Qiu, A., & Chen, S. A. (2018). Working memory, age and education: A lifespan fMRI study. *PLoS One*, 13(3), e0194878. <https://doi.org/10.1371/journal.pone.0194878>
- Baer, D. R., & Gilmore, I. S. (2018). Responding to the growing issue of research reproducibility. *Journal of Vacuum Science & Technology A*, 36(6).
- Baker, D. J., & Petersen, R. C. (2018). Cellular senescence in brain aging and neurodegenerative diseases: evidence and perspectives. *J Clin Invest*, 128(4), 1208-1216. <https://doi.org/10.1172/JCI95145>
- Baldassarre, A., Ramsey, L., Hacker, C. L., Callejas, A., Astafiev, S. V., Metcalf, N. V., Zinn, K., Rengachary, J., Snyder, A. Z., Carter, A. R., Shulman, G. L., & Corbetta, M. (2014). Large-scale changes in network interactions as a physiological signature of spatial neglect. *Brain*, 137(Pt 12), 3267-3283. <https://doi.org/10.1093/brain/awu297>
- Baltes, P. B., & Lindenberger, U. (1997). Emergence of a powerful connection between sensory and cognitive functions across the adult life span: a new window to the study of cognitive aging? *Psychol Aging*, 12(1), 12-21. <https://doi.org/10.1037//0882-7974.12.1.12>
- Beck, D., de Lange, A. G., Pedersen, M. L., Alnaes, D., Maximov, II, Voldsbekk, I., Richard, G., Sanders, A. M., Ulrichsen, K. M., Dorum, E. S., Kolskar, K. K., Hogestol, E. A., Steen, N. E., Djurovic, S., Andreassen, O. A., Nordvik, J. E., Kaufmann, T., & Westlye, L. T. (2022). Cardiometabolic risk factors associated with brain age and accelerate brain ageing. *Hum Brain Mapp*, 43(2), 700-720. <https://doi.org/10.1002/hbm.25680>
- Beckmann, C. F., DeLuca, M., Devlin, J. T., & Smith, S. M. (2005). Investigations into resting-state connectivity using independent component analysis. *Philos Trans R Soc Lond B Biol Sci*, 360(1457), 1001-1013. <https://doi.org/10.1098/rstb.2005.1634>

- Beckmann, C. F., & Smith, S. M. (2004). Probabilistic independent component analysis for functional magnetic resonance imaging. *IEEE Trans Med Imaging*, 23(2), 137-152. <https://doi.org/10.1109/TMI.2003.822821>
- Béjot, Y., Bailly, H., Graber, M., Garnier, L., Laville, A., Dubourget, L., Mielle, N., Chevalier, C., Durier, J., & Giroud, M. (2019). Impact of the Ageing Population on the Burden of Stroke: The Dijon Stroke Registry. *Neuroepidemiology*, 52(1-2), 78-85. <https://doi.org/10.1159/000492820>
- Benjamin, E. J., Muntner, P., Alonso, A., Bittencourt, M. S., Callaway, C. W., Carson, A. P., Chamberlain, A. M., Chang, A. R., Cheng, S., Das, S. R., Delling, F. N., Djousse, L., Elkind, M. S. V., Ferguson, J. F., Fornage, M., Jordan, L. C., Khan, S. S., Kissela, B. M., Knutson, K. L., Kwan, T. W., Lackland, D. T., Lewis, T. T., Lichtman, J. H., Longenecker, C. T., Loop, M. S., Lutsey, P. L., Martin, S. S., Matsushita, K., Moran, A. E., Mussolino, M. E., O'Flaherty, M., Pandey, A., Perak, A. M., Rosamond, W. D., Roth, G. A., Sampson, U. K. A., Satou, G. M., Schroeder, E. B., Shah, S. H., Spartano, N. L., Stokes, A., Tirschwell, D. L., Tsao, C. W., Turakhia, M. P., VanWagner, L. B., Wilkins, J. T., Wong, S. S., Virani, S. S., American Heart Association Council on, E., Prevention Statistics, C., & Stroke Statistics, S. (2019). Heart Disease and Stroke Statistics-2019 Update: A Report From the American Heart Association. *Circulation*, 139(10), e56-e528. <https://doi.org/10.1161/CIR.0000000000000659>
- Biswal, B., Yetkin, F. Z., Haughton, V. M., & Hyde, J. S. (1995). Functional connectivity in the motor cortex of resting human brain using echo-planar MRI. *Magn Reson Med*, 34(4), 537-541. <https://doi.org/10.1002/mrm.1910340409>
- Blazer, D. G., Yaffe, K., & Karlawish, J. (2015). Cognitive aging: a report from the Institute of Medicine. *JAMA*, 313(21), 2121-2122. <https://doi.org/10.1001/jama.2015.4380>
- Brier, M. R., Mitra, A., McCarthy, J. E., Ances, B. M., & Snyder, A. Z. (2015). Partial covariance based functional connectivity computation using Ledoit-Wolf covariance regularization. *Neuroimage*, 121, 29-38. <https://doi.org/10.1016/j.neuroimage.2015.07.039>
- Buckner, R. L., Andrews-Hanna, J. R., & Schacter, D. L. (2008). The brain's default network: anatomy, function, and relevance to disease. *Ann N Y Acad Sci*, 1124, 1-38. <https://doi.org/10.1196/annals.1440.011>
- Bugg, J. M., Zook, N. A., DeLosh, E. L., Davalos, D. B., & Davis, H. P. (2006). Age differences in fluid intelligence: contributions of general slowing and frontal decline. *Brain Cogn*, 62(1), 9-16. <https://doi.org/10.1016/j.bandc.2006.02.006>
- Bullmore, E., & Sporns, O. (2009). Complex brain networks: graph theoretical analysis of structural and functional systems. *Nat Rev Neurosci*, 10(3), 186-198. <https://doi.org/10.1038/nrn2575>
- Buxton, R. B., Uludag, K., Dubowitz, D. J., & Liu, T. T. (2004). Modeling the hemodynamic response to brain activation. *Neuroimage*, 23 Suppl 1, S220-233. <https://doi.org/10.1016/j.neuroimage.2004.07.013>
- Cabeza, R. (2002). Hemispheric asymmetry reduction in older adults: the HAROLD model. *Psychol Aging*, 17(1), 85-100. <https://doi.org/10.1037//0882-7974.17.1.85>
- Cabeza, R., Albert, M., Belleville, S., Craik, F. I. M., Duarte, A., Grady, C. L., Lindenberger, U., Nyberg, L., Park, D. C., Reuter-Lorenz, P. A., Rugg, M. D., Steffener, J., & Rajah, M. N. (2018). Maintenance, reserve and compensation: the cognitive neuroscience of healthy ageing. *Nat Rev Neurosci*, 19(11), 701-710. <https://doi.org/10.1038/s41583-018-0068-2>

- Cabeza, R., Grady, C. L., Nyberg, L., McIntosh, A. R., Tulving, E., Kapur, S., Jennings, J. M., Houle, S., & Craik, F. I. (1997). Age-related differences in neural activity during memory encoding and retrieval: a positron emission tomography study. *J Neurosci*, *17*(1), 391-400. <https://doi.org/10.1523/JNEUROSCI.17-01-00391.1997>
- Calhoun, V. D., Maciejewski, P. K., Pearlson, G. D., & Kiehl, K. A. (2008). Temporal lobe and "default" hemodynamic brain modes discriminate between schizophrenia and bipolar disorder. *Hum Brain Mapp*, *29*(11), 1265-1275. <https://doi.org/10.1002/hbm.20463>
- Cappell, K. A., Gmeindl, L., & Reuter-Lorenz, P. A. (2010). Age differences in prefrontal recruitment during verbal working memory maintenance depend on memory load. *Cortex*, *46*(4), 462-473. <https://doi.org/10.1016/j.cortex.2009.11.009>
- Carrera, E., & Tononi, G. (2014). Diaschisis: past, present, future. *Brain*, *137*(Pt 9), 2408-2422. <https://doi.org/10.1093/brain/awu101>
- Carter, A. R., Astafiev, S. V., Lang, C. E., Connor, L. T., Rengachary, J., Strube, M. J., Pope, D. L., Shulman, G. L., & Corbetta, M. (2010). Resting interhemispheric functional magnetic resonance imaging connectivity predicts performance after stroke. *Ann Neurol*, *67*(3), 365-375. <https://doi.org/10.1002/ana.21905>
- Carter, A. R., Shulman, G. L., & Corbetta, M. (2012). Why use a connectivity-based approach to study stroke and recovery of function? *Neuroimage*, *62*(4), 2271-2280. <https://doi.org/10.1016/j.neuroimage.2012.02.070>
- Cassarino, M., & Setti, A. (2015). Environment as 'Brain Training': A review of geographical and physical environmental influences on cognitive ageing. *Ageing Res Rev*, *23*(Pt B), 167-182. <https://doi.org/10.1016/j.arr.2015.06.003>
- Cattell, R. B. (1963). Theory of fluid and crystallized intelligence: A critical experiment. *Journal of educational psychology*, *54*(1), 1.
- Chadick, J. Z., & Gazzaley, A. (2011). Differential coupling of visual cortex with default or frontal-parietal network based on goals. *Nat Neurosci*, *14*(7), 830-832. <https://doi.org/10.1038/nn.2823>
- Chai, X. J., Castanon, A. N., Ongur, D., & Whitfield-Gabrieli, S. (2012). Anticorrelations in resting state networks without global signal regression. *Neuroimage*, *59*(2), 1420-1428. <https://doi.org/10.1016/j.neuroimage.2011.08.048>
- Challis, E., Hurley, P., Serra, L., Bozzali, M., Oliver, S., & Cercignani, M. (2015). Gaussian process classification of Alzheimer's disease and mild cognitive impairment from resting-state fMRI. *Neuroimage*, *112*, 232-243. <https://doi.org/10.1016/j.neuroimage.2015.02.037>
- Cohen, M. R., & Maunsell, J. H. (2009). Attention improves performance primarily by reducing interneuronal correlations. *Nat Neurosci*, *12*(12), 1594-1600. <https://doi.org/10.1038/nn.2439>
- Cole, M. W., Bassett, D. S., Power, J. D., Braver, T. S., & Petersen, S. E. (2014). Intrinsic and task-evoked network architectures of the human brain. *Neuron*, *83*(1), 238-251. <https://doi.org/10.1016/j.neuron.2014.05.014>
- Cole, M. W., Ito, T., Cocuzza, C., & Sanchez-Romero, R. (2021). The Functional Relevance of Task-State Functional Connectivity. *J Neurosci*, *41*(12), 2684-2702. <https://doi.org/10.1523/JNEUROSCI.1713-20.2021>
- Corbetta, M., & Shulman, G. L. (2002). Control of goal-directed and stimulus-driven attention in the brain. *Nat Rev Neurosci*, *3*(3), 201-215. <https://doi.org/10.1038/nrn755>

- Corbetta, M., Shulman, G. L., Miezin, F. M., & Petersen, S. E. (1995). Superior parietal cortex activation during spatial attention shifts and visual feature conjunction. *Science*, 270(5237), 802-805. <https://doi.org/10.1126/science.270.5237.802>
- Cordes, D., Haughton, V., Carew, J. D., Arfanakis, K., & Maravilla, K. (2002). Hierarchical clustering to measure connectivity in fMRI resting-state data. *Magn Reson Imaging*, 20(4), 305-317. [https://doi.org/10.1016/s0730-725x\(02\)00503-9](https://doi.org/10.1016/s0730-725x(02)00503-9)
- Cordova-Palomera, A., Kaufmann, T., Persson, K., Alnæs, D., Doan, N. T., Moberget, T., Lund, M. J., Barca, M. L., Engvig, A., Brækhus, A., Engedal, K., Andreassen, O. A., Selbaek, G., & Westlye, L. T. (2017). Disrupted global metastability and static and dynamic brain connectivity across individuals in the Alzheimer's disease continuum. *Sci Rep*, 7, 40268. <https://doi.org/10.1038/srep40268>
- Cramer, S. C. (2010). Stratifying patients with stroke in trials that target brain repair. *Stroke*, 41(10 Suppl), S114-116. <https://doi.org/10.1161/STROKEAHA.110.595165>
- Culham, J. C., Cavanagh, P., & Kanwisher, N. G. (2001). Attention response functions: characterizing brain areas using fMRI activation during parametric variations of attentional load. *Neuron*, 32(4), 737-745. [https://doi.org/10.1016/s0896-6273\(01\)00499-8](https://doi.org/10.1016/s0896-6273(01)00499-8)
- D'Esposito, M., Deouell, L. Y., & Gazzaley, A. (2003). Alterations in the BOLD fMRI signal with ageing and disease: a challenge for neuroimaging. *Nat Rev Neurosci*, 4(11), 863-872. <https://doi.org/10.1038/nrn1246>
- Damoiseaux, J. S. (2017). Effects of aging on functional and structural brain connectivity. *Neuroimage*, 160, 32-40. <https://doi.org/10.1016/j.neuroimage.2017.01.077>
- Damoiseaux, J. S., Beckmann, C. F., Arigita, E. J., Barkhof, F., Scheltens, P., Stam, C. J., Smith, S. M., & Rombouts, S. A. (2008). Reduced resting-state brain activity in the "default network" in normal aging. *Cereb Cortex*, 18(8), 1856-1864. <https://doi.org/10.1093/cercor/bhm207>
- Damoiseaux, J. S., Rombouts, S. A., Barkhof, F., Scheltens, P., Stam, C. J., Smith, S. M., & Beckmann, C. F. (2006). Consistent resting-state networks across healthy subjects. *Proc Natl Acad Sci U S A*, 103(37), 13848-13853. <https://doi.org/10.1073/pnas.0601417103>
- Davis, S. W., Dennis, N. A., Daselaar, S. M., Fleck, M. S., & Cabeza, R. (2008). Que PASA? The posterior-anterior shift in aging. *Cereb Cortex*, 18(5), 1201-1209. <https://doi.org/10.1093/cercor/bhm155>
- de Haan, B., Clas, P., Juenger, H., Wilke, M., & Karnath, H. O. (2015). Fast semi-automated lesion demarcation in stroke. *Neuroimage Clin*, 9, 69-74. <https://doi.org/10.1016/j.nicl.2015.06.013>
- De Luca, M., Beckmann, C. F., De Stefano, N., Matthews, P. M., & Smith, S. M. (2006). fMRI resting state networks define distinct modes of long-distance interactions in the human brain. *Neuroimage*, 29(4), 1359-1367. <https://doi.org/10.1016/j.neuroimage.2005.08.035>
- Deary, I. J., Whiteman, M. C., Starr, J. M., Whalley, L. J., & Fox, H. C. (2004). The impact of childhood intelligence on later life: following up the Scottish mental surveys of 1932 and 1947. *J Pers Soc Psychol*, 86(1), 130-147. <https://doi.org/10.1037/0022-3514.86.1.130>
- Deligianni, F., Centeno, M., Carmichael, D. W., & Clayden, J. D. (2014). Relating resting-state fMRI and EEG whole-brain connectomes across frequency bands. *Front Neurosci*, 8, 258. <https://doi.org/10.3389/fnins.2014.00258>
- DeYoe, E. A., Carman, G. J., Bandettini, P., Glickman, S., Wieser, J., Cox, R., Miller, D., & Neitz, J. (1996). Mapping striate and extrastriate visual areas in human cerebral cortex. *Proc Natl Acad Sci U S A*, 93(6), 2382-2386. <https://doi.org/10.1073/pnas.93.6.2382>

- Diao, Q., Liu, J., & Zhang, X. (2020). Enhanced positive functional connectivity strength in left-sided chronic subcortical stroke. *Brain Res*, 1733, 146727. <https://doi.org/10.1016/j.brainres.2020.146727>
- Diedrichsen, J., Verstynen, T., Schlerf, J., & Wiestler, T. (2010). Advances in functional imaging of the human cerebellum. *Curr Opin Neurol*, 23(4), 382-387. <https://doi.org/10.1097/WCO.0b013e32833be837>
- Dixon, M. L., De La Vega, A., Mills, C., Andrews-Hanna, J., Spreng, R. N., Cole, M. W., & Christoff, K. (2018). Heterogeneity within the frontoparietal control network and its relationship to the default and dorsal attention networks. *Proc Natl Acad Sci U S A*, 115(7), E1598-E1607. <https://doi.org/10.1073/pnas.1715766115>
- Dosenbach, N. U., Visscher, K. M., Palmer, E. D., Miezin, F. M., Wenger, K. K., Kang, H. C., Burgund, E. D., Grimes, A. L., Schlaggar, B. L., & Petersen, S. E. (2006). A core system for the implementation of task sets. *Neuron*, 50(5), 799-812. <https://doi.org/10.1016/j.neuron.2006.04.031>
- Drobyshevsky, A., Baumann, S. B., & Schneider, W. (2006). A rapid fMRI task battery for mapping of visual, motor, cognitive, and emotional function. *Neuroimage*, 31(2), 732-744. <https://doi.org/10.1016/j.neuroimage.2005.12.016>
- Du, W., Calhoun, V. D., Li, H., Ma, S., Eichele, T., Kiehl, K. A., Pearlson, G. D., & Adali, T. (2012). High classification accuracy for schizophrenia with rest and task FMRI data. *Front Hum Neurosci*, 6, 145. <https://doi.org/10.3389/fnhum.2012.00145>
- Du, Y., Fu, Z., & Calhoun, V. D. (2018). Classification and Prediction of Brain Disorders Using Functional Connectivity: Promising but Challenging. *Front Neurosci*, 12, 525. <https://doi.org/10.3389/fnins.2018.00525>
- Dulas, M. R., & Duarte, A. (2011). The effects of aging on material-independent and material-dependent neural correlates of contextual binding. *Neuroimage*, 57(3), 1192-1204. <https://doi.org/10.1016/j.neuroimage.2011.05.036>
- Duncan, E. S., & Small, S. L. (2016). Increased Modularity of Resting State Networks Supports Improved Narrative Production in Aphasia Recovery. *Brain Connect*, 6(7), 524-529. <https://doi.org/10.1089/brain.2016.0437>
- Evans, K. K., Horowitz, T. S., Howe, P., Pedersini, R., Reijnen, E., Pinto, Y., Kuzmova, Y., & Wolfe, J. M. (2011). Visual attention. *Wiley Interdiscip Rev Cogn Sci*, 2(5), 503-514. <https://doi.org/10.1002/wcs.127>
- Feigin, V. L., Forouzanfar, M. H., Krishnamurthi, R., Mensah, G. A., Connor, M., Bennett, D. A., Moran, A. E., Sacco, R. L., Anderson, L., Truelsen, T., O'Donnell, M., Venketasubramanian, N., Barker-Collo, S., Lawes, C. M., Wang, W., Shinohara, Y., Witt, E., Ezzati, M., Naghavi, M., Murray, C., Global Burden of Diseases, I., Risk Factors, S., & the, G. B. D. S. E. G. (2014). Global and regional burden of stroke during 1990-2010: findings from the Global Burden of Disease Study 2010. *Lancet*, 383(9913), 245-254. [https://doi.org/10.1016/s0140-6736\(13\)61953-4](https://doi.org/10.1016/s0140-6736(13)61953-4)
- Ferreira, L. K., Regina, A. C., Kovacevic, N., Martin Mda, G., Santos, P. P., Carneiro Cde, G., Kerr, D. S., Amaro, E., Jr., McIntosh, A. R., & Busatto, G. F. (2016). Aging Effects on Whole-Brain Functional Connectivity in Adults Free of Cognitive and Psychiatric Disorders. *Cereb Cortex*, 26(9), 3851-3865. <https://doi.org/10.1093/cercor/bhv190>
- Filippini, N., MacIntosh, B. J., Hough, M. G., Goodwin, G. M., Frisoni, G. B., Smith, S. M., Matthews, P. M., Beckmann, C. F., & Mackay, C. E. (2009). Distinct patterns of brain

- activity in young carriers of the APOE-epsilon4 allele. *Proc Natl Acad Sci U S A*, 106(17), 7209-7214. <https://doi.org/10.1073/pnas.0811879106>
- Fischl, B., Salat, D. H., Busa, E., Albert, M., Dieterich, M., Haselgrove, C., van der Kouwe, A., Killiany, R., Kennedy, D., Klaveness, S., Montillo, A., Makris, N., Rosen, B., & Dale, A. M. (2002). Whole brain segmentation: automated labeling of neuroanatomical structures in the human brain. *Neuron*, 33(3), 341-355. [https://doi.org/10.1016/s0896-6273\(02\)00569-x](https://doi.org/10.1016/s0896-6273(02)00569-x)
- Forkert, N. D., Verleger, T., Cheng, B., Thomalla, G., Hilgetag, C. C., & Fiehler, J. (2015). Multiclass Support Vector Machine-Based Lesion Mapping Predicts Functional Outcome in Ischemic Stroke Patients. *PLoS One*, 10(6), e0129569. <https://doi.org/10.1371/journal.pone.0129569>
- Fornito, A., Zalesky, A., & Bullmore, E. T. (2010). Network scaling effects in graph analytic studies of human resting-state FMRI data. *Front Syst Neurosci*, 4, 22. <https://doi.org/10.3389/fnsys.2010.00022>
- Fox, M. D., & Raichle, M. E. (2007). Spontaneous fluctuations in brain activity observed with functional magnetic resonance imaging. *Nat Rev Neurosci*, 8(9), 700-711. <https://doi.org/10.1038/nrn2201>
- Fox, M. D., Snyder, A. Z., Vincent, J. L., Corbetta, M., Van Essen, D. C., & Raichle, M. E. (2005). The human brain is intrinsically organized into dynamic, anticorrelated functional networks. *Proc Natl Acad Sci U S A*, 102(27), 9673-9678. <https://doi.org/10.1073/pnas.0504136102>
- Fox, M. D., Snyder, A. Z., Vincent, J. L., & Raichle, M. E. (2007). Intrinsic fluctuations within cortical systems account for intertrial variability in human behavior. *Neuron*, 56(1), 171-184. <https://doi.org/10.1016/j.neuron.2007.08.023>
- Friedman, J. H. (1989). Regularized discriminant analysis. *Journal of the American statistical association*, 84(405), 165-175.
- Friston, K. J. (1994). Functional and effective connectivity in neuroimaging: a synthesis. *Human brain mapping*, 2(1-2), 56-78.
- Fu, Z., Tu, Y., Di, X., Biswal, B. B., Calhoun, V. D., & Zhang, Z. (2017). Associations between Functional Connectivity Dynamics and BOLD Dynamics Are Heterogeneous Across Brain Networks. *Front Hum Neurosci*, 11, 593. <https://doi.org/10.3389/fnhum.2017.00593>
- Gao, W., & Lin, W. (2012). Frontal parietal control network regulates the anti-correlated default and dorsal attention networks. *Hum Brain Mapp*, 33(1), 192-202. <https://doi.org/10.1002/hbm.21204>
- Garrett, D. D., Kovacevic, N., McIntosh, A. R., & Grady, C. L. (2010). Blood oxygen level-dependent signal variability is more than just noise. *J Neurosci*, 30(14), 4914-4921. <https://doi.org/10.1523/JNEUROSCI.5166-09.2010>
- Garrett, D. D., Kovacevic, N., McIntosh, A. R., & Grady, C. L. (2011). The importance of being variable. *J Neurosci*, 31(12), 4496-4503. <https://doi.org/10.1523/JNEUROSCI.5641-10.2011>
- Gavrilov, L. A., & Gavrilova, N. S. (2001). The reliability theory of aging and longevity. *J Theor Biol*, 213(4), 527-545. <https://doi.org/10.1006/jtbi.2001.2430>
- Ge, Y., Grossman, R. I., Babb, J. S., Rabin, M. L., Mannon, L. J., & Kolson, D. L. (2002). Age-related total gray matter and white matter changes in normal adult brain. Part I:

- volumetric MR imaging analysis. *AJNR Am J Neuroradiol*, 23(8), 1327-1333. <https://www.ncbi.nlm.nih.gov/pubmed/12223373>
- Gerlach, K. D., Spreng, R. N., Gilmore, A. W., & Schacter, D. L. (2011). Solving future problems: default network and executive activity associated with goal-directed mental simulations. *Neuroimage*, 55(4), 1816-1824. <https://doi.org/10.1016/j.neuroimage.2011.01.030>
- Goense, J., Merkle, H., & Logothetis, N. K. (2012). High-resolution fMRI reveals laminar differences in neurovascular coupling between positive and negative BOLD responses. *Neuron*, 76(3), 629-639. <https://doi.org/10.1016/j.neuron.2012.09.019>
- Goh, J. O. (2011). Functional Dedifferentiation and Altered Connectivity in Older Adults: Neural Accounts of Cognitive Aging. *Aging Dis*, 2(1), 30-48. <https://www.ncbi.nlm.nih.gov/pubmed/21461180>
- Golestani, A. M., Tymchuk, S., Demchuk, A., Goodyear, B. G., & Group, V.-S. (2013). Longitudinal evaluation of resting-state FMRI after acute stroke with hemiparesis. *Neurorehabil Neural Repair*, 27(2), 153-163. <https://doi.org/10.1177/1545968312457827>
- Golland, Y., Golland, P., Bentin, S., & Malach, R. (2008). Data-driven clustering reveals a fundamental subdivision of the human cortex into two global systems. *Neuropsychologia*, 46(2), 540-553. <https://doi.org/10.1016/j.neuropsychologia.2007.10.003>
- Gordon, E. M., Laumann, T. O., Gilmore, A. W., Newbold, D. J., Greene, D. J., Berg, J. J., Ortega, M., Hoyt-Drazen, C., Gratton, C., Sun, H., Hampton, J. M., Coalson, R. S., Nguyen, A. L., McDermott, K. B., Shimony, J. S., Snyder, A. Z., Schlaggar, B. L., Petersen, S. E., Nelson, S. M., & Dosenbach, N. U. (2017). Precision Functional Mapping of Individual Human Brains. *Neuron*, 95(4), 791-807 e797. <https://doi.org/10.1016/j.neuron.2017.07.011>
- Gorelick, P. B. (2019). The global burden of stroke: persistent and disabling. *Lancet Neurol*, 18(5), 417-418. [https://doi.org/10.1016/S1474-4422\(19\)30030-4](https://doi.org/10.1016/S1474-4422(19)30030-4)
- Grady, C. L. (2012). The cognitive neuroscience of ageing. *Nat Rev Neurosci*, 13(7), 491-505. <https://doi.org/10.1038/nrn3256>
- Grady, C. L., & Garrett, D. D. (2014). Understanding variability in the BOLD signal and why it matters for aging. *Brain Imaging Behav*, 8(2), 274-283. <https://doi.org/10.1007/s11682-013-9253-0>
- Grady, C. L., Maisog, J. M., Horwitz, B., Ungerleider, L. G., Mentis, M. J., Salerno, J. A., Pietrini, P., Wagner, E., & Haxby, J. V. (1994). Age-related changes in cortical blood flow activation during visual processing of faces and location. *J Neurosci*, 14(3 Pt 2), 1450-1462. <https://doi.org/10.1523/JNEUROSCI.14-03-01450.1994>
- Grady, C. L., Springer, M. V., Hongwanishkul, D., McIntosh, A. R., & Winocur, G. (2006). Age-related changes in brain activity across the adult lifespan. *Journal of cognitive neuroscience*, 18(2), 227-241.
- Gratton, C., Sun, H., & Petersen, S. E. (2018). Control networks and hubs. *Psychophysiology*, 55(3). <https://doi.org/10.1111/psyp.13032>
- Greicius, M. D., Krasnow, B., Reiss, A. L., & Menon, V. (2003). Functional connectivity in the resting brain: a network analysis of the default mode hypothesis. *Proc Natl Acad Sci U S A*, 100(1), 253-258. <https://doi.org/10.1073/pnas.0135058100>
- Greicius, M. D., Supekar, K., Menon, V., & Dougherty, R. F. (2009). Resting-state functional connectivity reflects structural connectivity in the default mode network. *Cereb Cortex*, 19(1), 72-78. <https://doi.org/10.1093/cercor/bhn059>

- Greve, D. N., & Fischl, B. (2009). Accurate and robust brain image alignment using boundary-based registration. *Neuroimage*, 48(1), 63-72.  
<https://doi.org/10.1016/j.neuroimage.2009.06.060>
- Grigg, O., & Grady, C. L. (2010). Task-related effects on the temporal and spatial dynamics of resting-state functional connectivity in the default network. *PLoS One*, 5(10), e13311.  
<https://doi.org/10.1371/journal.pone.0013311>
- Grysiewicz, R. A., Thomas, K., & Pandey, D. K. (2008). Epidemiology of ischemic and hemorrhagic stroke: incidence, prevalence, mortality, and risk factors. *Neurol Clin*, 26(4), 871-895, vii. <https://doi.org/10.1016/j.ncl.2008.07.003>
- Habib, R., Nyberg, L., & Nilsson, L. G. (2007). Cognitive and non-cognitive factors contributing to the longitudinal identification of successful older adults in the betula study. *Neuropsychol Dev Cogn B Aging Neuropsychol Cogn*, 14(3), 257-273.  
<https://doi.org/10.1080/13825580600582412>
- Han, Y., Wang, J., Zhao, Z., Min, B., Lu, J., Li, K., He, Y., & Jia, J. (2011). Frequency-dependent changes in the amplitude of low-frequency fluctuations in amnesic mild cognitive impairment: a resting-state fMRI study. *Neuroimage*, 55(1), 287-295.  
<https://doi.org/10.1016/j.neuroimage.2010.11.059>
- Harada, C. N., Natelson Love, M. C., & Triebel, K. L. (2013). Normal cognitive aging. *Clin Geriatr Med*, 29(4), 737-752. <https://doi.org/10.1016/j.cger.2013.07.002>
- Hasher, L., & Zacks, R. T. (1988). Working memory, comprehension, and aging: A review and a new view. *Psychology of learning and motivation*, 22, 193-225.
- He, B. J., Snyder, A. Z., Vincent, J. L., Epstein, A., Shulman, G. L., & Corbetta, M. (2007). Breakdown of functional connectivity in frontoparietal networks underlies behavioral deficits in spatial neglect. *Neuron*, 53(6), 905-918.  
<https://doi.org/10.1016/j.neuron.2007.02.013>
- Helsedirektoratet. (2017). *Nasjonal faglig retningslinjer*. Retrieved 14 May from <https://www.helsedirektoratet.no/retningslinjer/hjerneslag>
- Honey, C. J., Sporns, O., Cammoun, L., Gigandet, X., Thiran, J. P., Meuli, R., & Hagmann, P. (2009). Predicting human resting-state functional connectivity from structural connectivity. *Proc Natl Acad Sci U S A*, 106(6), 2035-2040.  
<https://doi.org/10.1073/pnas.0811168106>
- Hou, Y., Dan, X., Babbar, M., Wei, Y., Hasselbalch, S. G., Croteau, D. L., & Bohr, V. A. (2019). Ageing as a risk factor for neurodegenerative disease. *Nat Rev Neurol*, 15(10), 565-581.  
<https://doi.org/10.1038/s41582-019-0244-7>
- Hung, C. W., Chen, Y. C., Hsieh, W. L., Chiou, S. H., & Kao, C. L. (2010). Ageing and neurodegenerative diseases. *Ageing Res Rev*, 9 Suppl 1, S36-46.  
<https://doi.org/10.1016/j.arr.2010.08.006>
- IBM\_Corp. (2015). *IBM SPSS Statistics for Windows*. In IBM Corp, Armonk, NY (Version 23.0)
- Inano, S., Takao, H., Hayashi, N., Abe, O., & Ohtomo, K. (2011). Effects of age and gender on white matter integrity. *AJNR Am J Neuroradiol*, 32(11), 2103-2109.  
<https://doi.org/10.3174/ajnr.A2785>
- Ioannidis, J. P. (2005). Why most published research findings are false. *PLoS Med*, 2(8), e124.  
<https://doi.org/10.1371/journal.pmed.0020124>
- Ioannidis, J. P., Fanelli, D., Dunne, D. D., & Goodman, S. N. (2015). Meta-research: Evaluation and Improvement of Research Methods and Practices. *PLoS Biol*, 13(10), e1002264.  
<https://doi.org/10.1371/journal.pbio.1002264>

- Ito, T., Brincat, S. L., Siegel, M., Mill, R. D., He, B. J., Miller, E. K., Rotstein, H. G., & Cole, M. W. (2020). Task-evoked activity quenches neural correlations and variability across cortical areas. *PLoS Comput Biol*, *16*(8), e1007983. <https://doi.org/10.1371/journal.pcbi.1007983>
- Jamadar, S. D. (2020). The CRUNCH model does not account for load-dependent changes in visuospatial working memory in older adults. *Neuropsychologia*, *142*, 107446. <https://doi.org/10.1016/j.neuropsychologia.2020.107446>
- James, W. (2007). *The principles of psychology* (Vol. 1). Cosimo, Inc.
- Jenkinson, M., Beckmann, C. F., Behrens, T. E., Woolrich, M. W., & Smith, S. M. (2012). Fsl. *Neuroimage*, *62*(2), 782-790. <https://doi.org/10.1016/j.neuroimage.2011.09.015>
- Jenkinson, M., & Smith, S. (2001). A global optimisation method for robust affine registration of brain images. *Med Image Anal*, *5*(2), 143-156. [https://doi.org/10.1016/s1361-8415\(01\)00036-6](https://doi.org/10.1016/s1361-8415(01)00036-6)
- Joel, S. E., Caffo, B. S., van Zijl, P. C., & Pekar, J. J. (2011). On the relationship between seed-based and ICA-based measures of functional connectivity. *Magn Reson Med*, *66*(3), 644-657. <https://doi.org/10.1002/mrm.22818>
- Johansen-Berg, H., Rushworth, M. F., Bogdanovic, M. D., Kischka, U., Wimalaratna, S., & Matthews, P. M. (2002). The role of ipsilateral premotor cortex in hand movement after stroke. *Proc Natl Acad Sci U S A*, *99*(22), 14518-14523. <https://doi.org/10.1073/pnas.222536799>
- Johnson, V. E., Payne, R. D., Wang, T., Asher, A., & Mandal, S. (2017). On the Reproducibility of Psychological Science. *J Am Stat Assoc*, *112*(517), 1-10. <https://doi.org/10.1080/01621459.2016.1240079>
- Jovicich, J., Peters, R. J., Koch, C., Braun, J., Chang, L., & Ernst, T. (2001). Brain areas specific for attentional load in a motion-tracking task. *J Cogn Neurosci*, *13*(8), 1048-1058. <https://doi.org/10.1162/089892901753294347>
- Kaufmann, T., Elvsåshagen, T., Alnæs, D., Zak, N., Pedersen, P. O., Norbom, L. B., Quraishi, S. H., Tagliazucchi, E., Laufs, H., Bjørnerud, A., Malt, U. F., Andreassen, O. A., Roussos, E., Duff, E. P., Smith, S. M., Groote, I. R., & Westlye, L. T. (2016). The brain functional connectome is robustly altered by lack of sleep. *Neuroimage*, *127*, 324-332. <https://doi.org/10.1016/j.neuroimage.2015.12.028>
- Kaufmann, T., Skåtun, K. C., Alnæs, D., Doan, N. T., Duff, E. P., Tønnesen, S., Roussos, E., Ueland, T., Aminoff, S. R., Lagerberg, T. V., Agartz, I., Melle, I. S., Smith, S. M., Andreassen, O. A., & Westlye, L. T. (2015). Disintegration of Sensorimotor Brain Networks in Schizophrenia. *Schizophr Bull*, *41*(6), 1326-1335. <https://doi.org/10.1093/schbul/sbv060>
- Kelly, R. E., Jr., Alexopoulos, G. S., Wang, Z., Gunning, F. M., Murphy, C. F., Morimoto, S. S., Kanellopoulos, D., Jia, Z., Lim, K. O., & Hoptman, M. J. (2010). Visual inspection of independent components: defining a procedure for artifact removal from fMRI data. *J Neurosci Methods*, *189*(2), 233-245. <https://doi.org/10.1016/j.jneumeth.2010.03.028>
- Kielar, A., Deschamps, T., Chu, R. K., Jokel, R., Khatamian, Y. B., Chen, J. J., & Meltzer, J. A. (2016). Identifying Dysfunctional Cortex: Dissociable Effects of Stroke and Aging on Resting State Dynamics in MEG and fMRI. *Front Aging Neurosci*, *8*, 40. <https://doi.org/10.3389/fnagi.2016.00040>

- Kivistö, J., Soininen, H., & Pihlajamäki, M. (2014). Functional MRI in Alzheimer's disease. In *Advanced brain neuroimaging topics in health and disease-methods and applications* (pp. 499-509). IntechOpen. <https://doi.org/10.5772/58256>
- Kolskår, K. K., Richard, G., Alnæs, D., Dørum, E. S., Sanders, A.-M., Ulrichsen, K. M., Sánchez, J. M., Ihle-Hansen, H., Nordvik, J. E., & Westlye, L. T. (2019). A randomized, double blind study of computerized cognitive training in combination with transcranial direct current stimulation (tDCS) in stroke patients—utility of fMRI as marker for training outcome. *bioRxiv*, 603985.
- Kolskår, K. K., Richard, G., Alnæs, D., Dørum, E. S., Sanders, A.-M., Ulrichsen, K. M., Sánchez, J. M., Ihle-Hansen, H., Nordvik, J. E., & Westlye, L. T. (2021). Reliability, sensitivity, and predictive value of fMRI during multiple object tracking as a marker of cognitive training gain in combination with tDCS in stroke survivors. *Hum Brain Mapp*, 42(4), 1167-1181. <https://doi.org/10.1002/hbm.25284>
- Kumral, D., Sansal, F., Cesnaite, E., Mahjoory, K., Al, E., Gaebler, M., Nikulin, V. V., & Villringer, A. (2020). BOLD and EEG signal variability at rest differently relate to aging in the human brain. *Neuroimage*, 207, 116373. <https://doi.org/10.1016/j.neuroimage.2019.116373>
- Lapadatu, I., & Morris, R. (2019). The relationship between stroke survivors' perceived identity and mood, self-esteem and quality of life. *Neuropsychol Rehabil*, 29(2), 199-213. <https://doi.org/10.1080/09602011.2016.1272468>
- Ledoit, O., & Wolf, M. (2003). Improved estimation of the covariance matrix of stock returns with an application to portfolio selection. *Journal of empirical finance*, 10(5), 603-621.
- Lee, H., Lee, E. J., Ham, S., Lee, H. B., Lee, J. S., Kwon, S. U., Kim, J. S., Kim, N., & Kang, D. W. (2020). Machine Learning Approach to Identify Stroke Within 4.5 Hours. *Stroke*, 51(3), 860-866. <https://doi.org/10.1161/STROKEAHA.119.027611>
- Lee, M. H., Kim, N., Yoo, J., Kim, H. K., Son, Y. D., Kim, Y. B., Oh, S. M., Kim, S., Lee, H., Jeon, J. E., & Lee, Y. J. (2021). Multitask fMRI and machine learning approach improve prediction of differential brain activity pattern in patients with insomnia disorder. *Sci Rep*, 11(1), 9402. <https://doi.org/10.1038/s41598-021-88845-w>
- Lee, M. H., Smyser, C. D., & Shimony, J. S. (2013). Resting-state fMRI: a review of methods and clinical applications. *AJNR Am J Neuroradiol*, 34(10), 1866-1872. <https://doi.org/10.3174/ajnr.A3263>
- Leniger-Follert, E., & Hossmann, K. A. (1979). Simultaneous measurements of microflow and evoked potentials in the somatomotor cortex of the cat brain during specific sensory activation. *Pflugers Arch*, 380(1), 85-89. <https://doi.org/10.1007/BF00582617>
- Li, H. J., Hou, X. H., Liu, H. H., Yue, C. L., Lu, G. M., & Zuo, X. N. (2015). Putting age-related task activation into large-scale brain networks: A meta-analysis of 114 fMRI studies on healthy aging. *Neurosci Biobehav Rev*, 57, 156-174. <https://doi.org/10.1016/j.neubiorev.2015.08.013>
- Lindenberger, U., & Baltes, P. B. (1994). Sensory functioning and intelligence in old age: a strong connection. *Psychol Aging*, 9(3), 339-355. <https://doi.org/10.1037//0882-7974.9.3.339>
- Lindquist, M. A., & Wager, T. D. (2007). Validity and power in hemodynamic response modeling: a comparison study and a new approach. *Hum Brain Mapp*, 28(8), 764-784. <https://doi.org/10.1002/hbm.20310>

- Logothetis, N. K., Pauls, J., Augath, M., Trinath, T., & Oeltermann, A. (2001). Neurophysiological investigation of the basis of the fMRI signal. *Nature*, *412*(6843), 150-157. <https://doi.org/10.1038/35084005>
- Lohmann, G., Margulies, D. S., Horstmann, A., Pleger, B., Lepsien, J., Goldhahn, D., Schloegl, H., Stumvoll, M., Villringer, A., & Turner, R. (2010). Eigenvector centrality mapping for analyzing connectivity patterns in fMRI data of the human brain. *PLoS One*, *5*(4), e10232. <https://doi.org/10.1371/journal.pone.0010232>
- Lohmann, G., Muller, K., Bosch, V., Mentzel, H., Hessler, S., Chen, L., Zysset, S., & von Cramon, D. Y. (2001). LIPSIA--a new software system for the evaluation of functional magnetic resonance images of the human brain. *Comput Med Imaging Graph*, *25*(6), 449-457. [https://doi.org/10.1016/s0895-6111\(01\)00008-8](https://doi.org/10.1016/s0895-6111(01)00008-8)
- Luo, W., Xing, J., Milan, A., Zhang, X., Liu, W., & Kim, T.-K. (2021). Multiple object tracking: A literature review. *Artificial intelligence*, *293*, 103448.
- Lyden, P., Raman, R., Liu, L., Emr, M., Warren, M., & Marler, J. (2009). National Institutes of Health Stroke Scale certification is reliable across multiple venues. *Stroke*, *40*(7), 2507-2511. <https://doi.org/10.1161/STROKEAHA.108.532069>
- Maillet, D., & Rajah, M. N. (2013). Association between prefrontal activity and volume change in prefrontal and medial temporal lobes in aging and dementia: a review. *Ageing Res Rev*, *12*(2), 479-489. <https://doi.org/10.1016/j.arr.2012.11.001>
- Mason, M. F., Norton, M. I., Van Horn, J. D., Wegner, D. M., Grafton, S. T., & Macrae, C. N. (2007). Wandering minds: the default network and stimulus-independent thought. *Science*, *315*(5810), 393-395. <https://doi.org/10.1126/science.1131295>
- Mattay, V. S., Fera, F., Tessitore, A., Hariri, A. R., Berman, K. F., Das, S., Meyer-Lindenberg, A., Goldberg, T. E., Callicott, J. H., & Weinberger, D. R. (2006). Neurophysiological correlates of age-related changes in working memory capacity. *Neurosci Lett*, *392*(1-2), 32-37. <https://doi.org/10.1016/j.neulet.2005.09.025>
- McKiernan, K. A., D'Angelo, B. R., Kaufman, J. N., & Binder, J. R. (2006). Interrupting the "stream of consciousness": an fMRI investigation. *Neuroimage*, *29*(4), 1185-1191. <https://doi.org/10.1016/j.neuroimage.2005.09.030>
- McKiernan, K. A., Kaufman, J. N., Kucera-Thompson, J., & Binder, J. R. (2003). A parametric manipulation of factors affecting task-induced deactivation in functional neuroimaging. *J Cogn Neurosci*, *15*(3), 394-408. <https://doi.org/10.1162/089892903321593117>
- Meier, T. B., Desphande, A. S., Vergun, S., Nair, V. A., Song, J., Biswal, B. B., Meyerand, M. E., Birn, R. M., & Prabhakaran, V. (2012). Support vector machine classification and characterization of age-related reorganization of functional brain networks. *Neuroimage*, *60*(1), 601-613. <https://doi.org/10.1016/j.neuroimage.2011.12.052>
- Mennes, M., Kelly, C., Zuo, X. N., Di Martino, A., Biswal, B. B., Castellanos, F. X., & Milham, M. P. (2010). Inter-individual differences in resting-state functional connectivity predict task-induced BOLD activity. *Neuroimage*, *50*(4), 1690-1701. <https://doi.org/10.1016/j.neuroimage.2010.01.002>
- Mevel, K., Chetelat, G., Eustache, F., & Desgranges, B. (2011). The default mode network in healthy aging and Alzheimer's disease. *Int J Alzheimers Dis*, *2011*, 535816. <https://doi.org/10.4061/2011/535816>
- Mevorach, C., Shalev, L., Allen, H. A., & Humphreys, G. W. (2009). The left intraparietal sulcus modulates the selection of low salient stimuli. *J Cogn Neurosci*, *21*(2), 303-315. <https://doi.org/10.1162/jocn.2009.21044>

- Millar, P. R., Ances, B. M., Gordon, B. A., Benzinger, T. L. S., Fagan, A. M., Morris, J. C., & Balota, D. A. (2020). Evaluating resting-state BOLD variability in relation to biomarkers of preclinical Alzheimer's disease. *Neurobiol Aging*, 96, 233-245. <https://doi.org/10.1016/j.neurobiolaging.2020.08.007>
- Miller, E. K., & Cohen, J. D. (2001). An integrative theory of prefrontal cortex function. *Annu Rev Neurosci*, 24, 167-202. <https://doi.org/10.1146/annurev.neuro.24.1.167>
- Nashiro, K., Qin, S., O'Connell, M. A., & Basak, C. (2018). Age-related differences in BOLD modulation to cognitive control costs in a multitasking paradigm: global switch, local switch, and compatibility-switch costs. *Neuroimage*, 172, 146-161.
- Nasreddine, Z. S., Phillips, N. A., Bedirian, V., Charbonneau, S., Whitehead, V., Collin, I., Cummings, J. L., & Chertkow, H. (2005). The Montreal Cognitive Assessment, MoCA: a brief screening tool for mild cognitive impairment. *J Am Geriatr Soc*, 53(4), 695-699. <https://doi.org/10.1111/j.1532-5415.2005.53221.x>
- Nichols, T., & Hayasaka, S. (2003). Controlling the familywise error rate in functional neuroimaging: a comparative review. *Stat Methods Med Res*, 12(5), 419-446. <https://doi.org/10.1191/0962280203sm341ra>
- Nilsson, J., & Lovden, M. (2018). Naming is not explaining: future directions for the "cognitive reserve" and "brain maintenance" theories. *Alzheimers Res Ther*, 10(1), 34. <https://doi.org/10.1186/s13195-018-0365-z>
- Nomura, E. M., Gratton, C., Visser, R. M., Kayser, A., Perez, F., & D'Esposito, M. (2010). Double dissociation of two cognitive control networks in patients with focal brain lesions. *Proc Natl Acad Sci U S A*, 107(26), 12017-12022. <https://doi.org/10.1073/pnas.1002431107>
- Nyberg, L., Salami, A., Andersson, M., Eriksson, J., Kalpouzos, G., Kauppi, K., Lind, J., Pudas, S., Persson, J., & Nilsson, L. G. (2010). Longitudinal evidence for diminished frontal cortex function in aging. *Proc Natl Acad Sci U S A*, 107(52), 22682-22686. <https://doi.org/10.1073/pnas.1012651108>
- Onoda, K., Yada, N., Ozasa, K., Hara, S., Yamamoto, Y., Kitagaki, H., & Yamaguchi, S. (2017). Can a Resting-State Functional Connectivity Index Identify Patients with Alzheimer's Disease and Mild Cognitive Impairment Across Multiple Sites? *Brain Connect*, 7(7), 391-400. <https://doi.org/10.1089/brain.2017.0507>
- Osaka, M., Osaka, N., Kondo, H., Morishita, M., Fukuyama, H., Aso, T., & Shibasaki, H. (2003). The neural basis of individual differences in working memory capacity: an fMRI study. *Neuroimage*, 18(3), 789-797. [https://doi.org/10.1016/s1053-8119\(02\)00032-0](https://doi.org/10.1016/s1053-8119(02)00032-0)
- Park, B. Y., Kim, M., Seo, J., Lee, J. M., & Park, H. (2016). Connectivity Analysis and Feature Classification in Attention Deficit Hyperactivity Disorder Sub-Types: A Task Functional Magnetic Resonance Imaging Study. *Brain Topogr*, 29(3), 429-439. <https://doi.org/10.1007/s10548-015-0463-1>
- Petersen, S. E., & Posner, M. I. (2012). The attention system of the human brain: 20 years after. *Annu Rev Neurosci*, 35, 73-89. <https://doi.org/10.1146/annurev-neuro-062111-150525>
- Pillai, J. J., Araque, J. M., Allison, J. D., Sethuraman, S., Loring, D. W., Thiruvaiyaru, D., Ison, C. B., Balan, A., & Lavin, T. (2003). Functional MRI study of semantic and phonological language processing in bilingual subjects: preliminary findings. *Neuroimage*, 19(3), 565-576. [https://doi.org/10.1016/s1053-8119\(03\)00151-4](https://doi.org/10.1016/s1053-8119(03)00151-4)
- Pinneo, L. R. (1966). On noise in the nervous system. *Psychol Rev*, 73(3), 242-247. <https://doi.org/10.1037/h0023240>

- Poldrack, R. A., Baker, C. I., Durnez, J., Gorgolewski, K. J., Matthews, P. M., Munafò, M. R., Nichols, T. E., Poline, J. B., Vul, E., & Yarkoni, T. (2017). Scanning the horizon: towards transparent and reproducible neuroimaging research. *Nat Rev Neurosci*, *18*(2), 115-126. <https://doi.org/10.1038/nrn.2016.167>
- Posner, M. I., & Petersen, S. E. (1990). The attention system of the human brain. *Annu Rev Neurosci*, *13*, 25-42. <https://doi.org/10.1146/annurev.ne.13.030190.000325>
- Posner, M. I., Rothbart, M. K., Sheese, B. E., & Tang, Y. (2007). The anterior cingulate gyrus and the mechanism of self-regulation. *Cogn Affect Behav Neurosci*, *7*(4), 391-395. <https://doi.org/10.3758/cabn.7.4.391>
- Power, J. D., Cohen, A. L., Nelson, S. M., Wig, G. S., Barnes, K. A., Church, J. A., Vogel, A. C., Laumann, T. O., Miezin, F. M., Schlaggar, B. L., & Petersen, S. E. (2011). Functional network organization of the human brain. *Neuron*, *72*(4), 665-678. <https://doi.org/10.1016/j.neuron.2011.09.006>
- Pruim, R. H. R., Mennes, M., Buitelaar, J. K., & Beckmann, C. F. (2015). Evaluation of ICA-AROMA and alternative strategies for motion artifact removal in resting state fMRI. *Neuroimage*, *112*, 278-287. <https://doi.org/10.1016/j.neuroimage.2015.02.063>
- Pylyshyn, Z. W. (2001). Visual indexes, preconceptual objects, and situated vision. *Cognition*, *80*(1-2), 127-158. [https://doi.org/10.1016/s0010-0277\(00\)00156-6](https://doi.org/10.1016/s0010-0277(00)00156-6)
- Pylyshyn, Z. W., & Storm, R. W. (1988). Tracking multiple independent targets: evidence for a parallel tracking mechanism. *Spat Vis*, *3*(3), 179-197. <https://doi.org/10.1163/156856888x00122>
- Qureshi, M. N. I., Oh, J., Min, B., Jo, H. J., & Lee, B. (2017). Multi-modal, Multi-measure, and Multi-class Discrimination of ADHD with Hierarchical Feature Extraction and Extreme Learning Machine Using Structural and Functional Brain MRI. *Front Hum Neurosci*, *11*, 157. <https://doi.org/10.3389/fnhum.2017.00157>
- Raichle, M. E., MacLeod, A. M., Snyder, A. Z., Powers, W. J., Gusnard, D. A., & Shulman, G. L. (2001). A default mode of brain function. *Proc Natl Acad Sci U S A*, *98*(2), 676-682. <https://doi.org/10.1073/pnas.98.2.676>
- Rehme, A. K., Eickhoff, S. B., Wang, L. E., Fink, G. R., & Grefkes, C. (2011). Dynamic causal modeling of cortical activity from the acute to the chronic stage after stroke. *Neuroimage*, *55*(3), 1147-1158. <https://doi.org/10.1016/j.neuroimage.2011.01.014>
- Rehme, A. K., Fink, G. R., von Cramon, D. Y., & Grefkes, C. (2011). The role of the contralesional motor cortex for motor recovery in the early days after stroke assessed with longitudinal FMRI. *Cereb Cortex*, *21*(4), 756-768. <https://doi.org/10.1093/cercor/bhq140>
- Rehme, A. K., Volz, L. J., Feis, D. L., Bomilcar-Focke, I., Liebig, T., Eickhoff, S. B., Fink, G. R., & Grefkes, C. (2015). Identifying Neuroimaging Markers of Motor Disability in Acute Stroke by Machine Learning Techniques. *Cereb Cortex*, *25*(9), 3046-3056. <https://doi.org/10.1093/cercor/bhu100>
- Reid, A. T., Hoffstaedter, F., Gong, G., Laird, A. R., Fox, P., Evans, A. C., Amunts, K., & Eickhoff, S. B. (2017). A seed-based cross-modal comparison of brain connectivity measures. *Brain Struct Funct*, *222*(3), 1131-1151. <https://doi.org/10.1007/s00429-016-1264-3>
- Reuter-Lorenz, P. A., & Cappell, K. A. (2008). Neurocognitive aging and the compensation hypothesis. *Current directions in psychological science*, *17*(3), 177-182.

- Reuter-Lorenz, P. A., & Park, D. C. (2010). Human neuroscience and the aging mind: a new look at old problems. *J Gerontol B Psychol Sci Soc Sci*, 65(4), 405-415.  
<https://doi.org/10.1093/geronb/gbq035>
- Reuter-Lorenz, P. A., & Park, D. C. (2014). How does it STAC up? Revisiting the scaffolding theory of aging and cognition. *Neuropsychol Rev*, 24(3), 355-370.  
<https://doi.org/10.1007/s11065-014-9270-9>
- Reuter-Lorenz, P. A., Stanczak, L., & Miller, A. C. (1999). Neural recruitment and cognitive aging: Two hemispheres are better than one, especially as you age. *Psychological Science*, 10(6), 494-500.
- Richard, G., Kolskår, K., Ulrichsen, K. M., Kaufmann, T., Alnæs, D., Sanders, A.-M., Dørum, E. S., Sánchez, J. M., Petersen, A., Ihle-Hansen, H., Nordvik, J. E., & Westlye, L. T. (2020). Brain age prediction in stroke patients: Highly reliable but limited sensitivity to cognitive performance and response to cognitive training. *Neuroimage Clin*, 25, 102159.  
<https://doi.org/10.1016/j.nicl.2019.102159>
- Richard, G., Kolskår, K. K., Sanders, A.-M., Kaufmann, T., Petersen, A., Doan, N. T., Sánchez, J. M., Alnæs, D., Ulrichsen, K. M., Dørum, E. S., Andreassen, O. A., Nordvik, J. E., & Westlye, L. T. (2018). Assessing distinct patterns of cognitive aging using tissue-specific brain age prediction based on diffusion tensor imaging and brain morphometry. *PeerJ*, 6, e5908. <https://doi.org/10.7717/peerj.5908>
- Rieck, J. R., Rodrigue, K. M., Boylan, M. A., & Kennedy, K. M. (2017). Age-related reduction of BOLD modulation to cognitive difficulty predicts poorer task accuracy and poorer fluid reasoning ability. *Neuroimage*, 147, 262-271.  
<https://doi.org/10.1016/j.neuroimage.2016.12.022>
- Rondina, J. M., Filippone, M., Girolami, M., & Ward, N. S. (2016). Decoding post-stroke motor function from structural brain imaging. *Neuroimage Clin*, 12, 372-380.  
<https://doi.org/10.1016/j.nicl.2016.07.014>
- Rossi, S., Miniussi, C., Pasqualetti, P., Babiloni, C., Rossini, P. M., & Cappa, S. F. (2004). Age-related functional changes of prefrontal cortex in long-term memory: a repetitive transcranial magnetic stimulation study. *Journal of Neuroscience*, 24(36), 7939-7944.
- Rosso, C., Valabregue, R., Attal, Y., Vargas, P., Gaudron, M., Baronnet, F., Bertasi, E., Humbert, F., Peskine, A., Perlberg, V., Benali, H., Lehericy, S., & Samson, Y. (2013). Contribution of corticospinal tract and functional connectivity in hand motor impairment after stroke. *PLoS One*, 8(9), e73164. <https://doi.org/10.1371/journal.pone.0073164>
- Sadeghi, M., Khosrowabadi, R., Bakouie, F., Mahdavi, H., Eslahchi, C., & Pouretmad, H. (2017). Screening of autism based on task-free fMRI using graph theoretical approach. *Psychiatry Res Neuroimaging*, 263, 48-56.  
<https://doi.org/10.1016/j.psychresns.2017.02.004>
- Salimi-Khorshidi, G., Douaud, G., Beckmann, C. F., Glasser, M. F., Griffanti, L., & Smith, S. M. (2014). Automatic denoising of functional MRI data: combining independent component analysis and hierarchical fusion of classifiers. *Neuroimage*, 90, 449-468.  
<https://doi.org/10.1016/j.neuroimage.2013.11.046>
- Salthouse, T. A. (2010). Selective review of cognitive aging. *J Int Neuropsychol Soc*, 16(5), 754-760. <https://doi.org/10.1017/S1355617710000706>
- Sambataro, F., Murty, V. P., Callicott, J. H., Tan, H. Y., Das, S., Weinberger, D. R., & Mattay, V. S. (2010). Age-related alterations in default mode network: impact on working

- memory performance. *Neurobiol Aging*, 31(5), 839-852.  
<https://doi.org/10.1016/j.neurobiolaging.2008.05.022>
- Sanders, A.-M., Richard, G., Kolskår, K., Ulrichsen, K. M., Kaufmann, T., Alnæs, D., Beck, D., Dørum, E. S., de Lange, A. G., Egil Nordvik, J., & Westlye, L. T. (2021). Linking objective measures of physical activity and capability with brain structure in healthy community dwelling older adults. *Neuroimage Clin*, 31, 102767.  
<https://doi.org/10.1016/j.nicl.2021.102767>
- Schafer, J., & Strimmer, K. (2005). A shrinkage approach to large-scale covariance matrix estimation and implications for functional genomics. *Stat Appl Genet Mol Biol*, 4, Article32. <https://doi.org/10.2202/1544-6115.1175>
- Schlerf, J., Ivry, R. B., & Diedrichsen, J. (2012). Encoding of sensory prediction errors in the human cerebellum. *J Neurosci*, 32(14), 4913-4922.  
<https://doi.org/10.1523/JNEUROSCI.4504-11.2012>
- Schlerf, J., Wiestler, T., Verstynen, T., & Diedrichsen, J. (2014). Big challenges from the little brain—imaging the cerebellum. *Advanced brain neuroimaging topics in health and disease—methods and applications*, 191-215.
- Schöttke, H., Gerke, L., Dusing, R., & Mollmann, A. (2020). Post-stroke depression and functional impairments - A 3-year prospective study. *Compr Psychiatry*, 99, 152171.  
<https://doi.org/10.1016/j.comppsy.2020.152171>
- Schwartz, S., Vuilleumier, P., Hutton, C., Maravita, A., Dolan, R. J., & Driver, J. (2005). Attentional load and sensory competition in human vision: modulation of fMRI responses by load at fixation during task-irrelevant stimulation in the peripheral visual field. *Cereb Cortex*, 15(6), 770-786. <https://doi.org/10.1093/cercor/bhh178>
- Seitzman, B. A., Snyder, A. Z., Leuthardt, E. C., & Shimony, J. S. (2019). The State of Resting State Networks. *Top Magn Reson Imaging*, 28(4), 189-196.  
<https://doi.org/10.1097/RMR.0000000000000214>
- Shenhav, A., Botvinick, M. M., & Cohen, J. D. (2013). The expected value of control: an integrative theory of anterior cingulate cortex function. *Neuron*, 79(2), 217-240.  
<https://doi.org/10.1016/j.neuron.2013.07.007>
- Smith, S. M., Fox, P. T., Miller, K. L., Glahn, D. C., Fox, P. M., Mackay, C. E., Filippini, N., Watkins, K. E., Toro, R., Laird, A. R., & Beckmann, C. F. (2009). Correspondence of the brain's functional architecture during activation and rest. *Proc Natl Acad Sci U S A*, 106(31), 13040-13045. <https://doi.org/10.1073/pnas.0905267106>
- Smith, S. M., Jenkinson, M., Woolrich, M. W., Beckmann, C. F., Behrens, T. E., Johansen-Berg, H., Bannister, P. R., De Luca, M., Drobnjak, I., Flitney, D. E., Niazy, R. K., Saunders, J., Vickers, J., Zhang, Y., De Stefano, N., Brady, J. M., & Matthews, P. M. (2004). Advances in functional and structural MR image analysis and implementation as FSL. *Neuroimage*, 23 Suppl 1, S208-219. <https://doi.org/10.1016/j.neuroimage.2004.07.051>
- Smith, S. M., Miller, K. L., Salimi-Khorshidi, G., Webster, M., Beckmann, C. F., Nichols, T. E., Ramsey, J. D., & Woolrich, M. W. (2011). Network modelling methods for FMRI. *Neuroimage*, 54(2), 875-891. <https://doi.org/10.1016/j.neuroimage.2010.08.063>
- Smitha, K. A., Akhil Raja, K., Arun, K. M., Rajesh, P. G., Thomas, B., Kapilamoorthy, T. R., & Kesavadas, C. (2017). Resting state fMRI: A review on methods in resting state connectivity analysis and resting state networks. *Neuroradiol J*, 30(4), 305-317.  
<https://doi.org/10.1177/1971400917697342>

- Sohrabji, F., Bake, S., & Lewis, D. K. (2013). Age-related changes in brain support cells: Implications for stroke severity. *Neurochem Int*, 63(4), 291-301. <https://doi.org/10.1016/j.neuint.2013.06.013>
- Sporns, O., Tononi, G., & Kotter, R. (2005). The human connectome: A structural description of the human brain. *PLoS Comput Biol*, 1(4), e42. <https://doi.org/10.1371/journal.pcbi.0010042>
- Spreng, R. N., & Schacter, D. L. (2012). Default network modulation and large-scale network interactivity in healthy young and old adults. *Cereb Cortex*, 22(11), 2610-2621. <https://doi.org/10.1093/cercor/bhr339>
- Spreng, R. N., Stevens, W. D., Chamberlain, J. P., Gilmore, A. W., & Schacter, D. L. (2010). Default network activity, coupled with the frontoparietal control network, supports goal-directed cognition. *Neuroimage*, 53(1), 303-317. <https://doi.org/10.1016/j.neuroimage.2010.06.016>
- Spreng, R. N., & Turner, G. R. (2019). The Shifting Architecture of Cognition and Brain Function in Older Adulthood. *Perspect Psychol Sci*, 14(4), 523-542. <https://doi.org/10.1177/1745691619827511>
- Takahashi, N., Lee, Y., Tsai, D. Y., Matsuyama, E., Kinoshita, T., & Ishii, K. (2014). An automated detection method for the MCA dot sign of acute stroke in unenhanced CT. *Radiol Phys Technol*, 7(1), 79-88. <https://doi.org/10.1007/s12194-013-0234-1>
- Tewarie, P., Hillebrand, A., van Dellen, E., Schoonheim, M. M., Barkhof, F., Polman, C. H., Beaulieu, C., Gong, G., van Dijk, B. W., & Stam, C. J. (2014). Structural degree predicts functional network connectivity: a multimodal resting-state fMRI and MEG study. *Neuroimage*, 97, 296-307. <https://doi.org/10.1016/j.neuroimage.2014.04.038>
- Thirion, B., Dodel, S., & Poline, J. B. (2006). Detection of signal synchronizations in resting-state fMRI datasets. *Neuroimage*, 29(1), 321-327. <https://doi.org/10.1016/j.neuroimage.2005.06.054>
- Thompson, K. G., Biscoe, K. L., & Sato, T. R. (2005). Neuronal basis of covert spatial attention in the frontal eye field. *J Neurosci*, 25(41), 9479-9487. <https://doi.org/10.1523/JNEUROSCI.0741-05.2005>
- Tisserand, D. J., & Jolles, J. (2003). On the involvement of prefrontal networks in cognitive ageing. *Cortex*, 39(4-5), 1107-1128. [https://doi.org/10.1016/s0010-9452\(08\)70880-3](https://doi.org/10.1016/s0010-9452(08)70880-3)
- Tomasi, D., & Volkow, N. D. (2012). Aging and functional brain networks. *Mol Psychiatry*, 17(5), 471, 549-458. <https://doi.org/10.1038/mp.2011.81>
- Tomasi, D., Wang, R., Wang, G. J., & Volkow, N. D. (2014). Functional connectivity and brain activation: a synergistic approach. *Cereb Cortex*, 24(10), 2619-2629. <https://doi.org/10.1093/cercor/bht119>
- Trahan, L. H., Stuebing, K. K., Fletcher, J. M., & Hiscock, M. (2014). The Flynn effect: a meta-analysis. *Psychol Bull*, 140(5), 1332-1360. <https://doi.org/10.1037/a0037173>
- Tripathi, A. (2012). New cellular and molecular approaches to ageing brain. *Ann Neurosci*, 19(4), 177-182. <https://doi.org/10.5214/ans.0972.7531.190410>
- Turesky, T. K., Olulade, O. A., Luetje, M. M., & Eden, G. F. (2018). An fMRI study of finger tapping in children and adults. *Hum Brain Mapp*, 39(8), 3203-3215. <https://doi.org/10.1002/hbm.24070>
- Turkheimer, F. E., Leech, R., Expert, P., Lord, L. D., & Vernon, A. C. (2015). The brain's code and its canonical computational motifs. From sensory cortex to the default mode

- network: A multi-scale model of brain function in health and disease. *Neurosci Biobehav Rev*, 55, 211-222. <https://doi.org/10.1016/j.neubiorev.2015.04.014>
- Turner, G. R., & Spreng, R. N. (2015). Prefrontal Engagement and Reduced Default Network Suppression Co-occur and Are Dynamically Coupled in Older Adults: The Default-Executive Coupling Hypothesis of Aging. *J Cogn Neurosci*, 27(12), 2462-2476. [https://doi.org/10.1162/jocn\\_a\\_00869](https://doi.org/10.1162/jocn_a_00869)
- Uddin, L. Q., Supekar, K., Lynch, C. J., Khouzam, A., Phillips, J., Feinstein, C., Ryali, S., & Menon, V. (2013). Salience network-based classification and prediction of symptom severity in children with autism. *JAMA Psychiatry*, 70(8), 869-879. <https://doi.org/10.1001/jamapsychiatry.2013.104>
- Ulrichsen, K. M., Alnæs, D., Kolskår, K. K., Richard, G., Sanders, A.-M., Dørum, E. S., Ihle-Hansen, H., Pedersen, M. L., Tornås, S., Nordvik, J. E., & Westlye, L. T. (2020). Dissecting the cognitive phenotype of post-stroke fatigue using computerized assessment and computational modeling of sustained attention. *Eur J Neurosci*, 52(7), 3828-3845. <https://doi.org/10.1111/ejn.14861>
- Vabø, A. (2003). Universiteter under forandring—makt og motstand. *Sosiologisk tidsskrift*, 11(1), 75-85.
- van den Heuvel, M. P., & Hulshoff Pol, H. E. (2010). Exploring the brain network: a review on resting-state fMRI functional connectivity. *Eur Neuropsychopharmacol*, 20(8), 519-534. <https://doi.org/10.1016/j.euroneuro.2010.03.008>
- van den Heuvel, M. P., Mandl, R. C., Kahn, R. S., & Hulshoff Pol, H. E. (2009). Functionally linked resting-state networks reflect the underlying structural connectivity architecture of the human brain. *Hum Brain Mapp*, 30(10), 3127-3141. <https://doi.org/10.1002/hbm.20737>
- van der Zwaag, W., Jorge, J., Buttica, D., & Gruetter, R. (2015). Physiological noise in human cerebellar fMRI. *MAGMA*, 28(5), 485-492. <https://doi.org/10.1007/s10334-015-0483-6>
- Vergun, S., Deshpande, A. S., Meier, T. B., Song, J., Tudorascu, D. L., Nair, V. A., Singh, V., Biswal, B. B., Meyerand, M. E., Birn, R. M., & Prabhakaran, V. (2013). Characterizing Functional Connectivity Differences in Aging Adults using Machine Learning on Resting State fMRI Data. *Front Comput Neurosci*, 7, 38. <https://doi.org/10.3389/fncom.2013.00038>
- Viviani, R., Gron, G., & Spitzer, M. (2005). Functional principal component analysis of fMRI data. *Hum Brain Mapp*, 24(2), 109-129. <https://doi.org/10.1002/hbm.20074>
- von Bernhardi, R., Eugenin-von Bernhardi, L., & Eugenin, J. (2015). Microglial cell dysregulation in brain aging and neurodegeneration. *Front Aging Neurosci*, 7, 124. <https://doi.org/10.3389/fnagi.2015.00124>
- Vossel, S., Geng, J. J., & Fink, G. R. (2014). Dorsal and ventral attention systems: distinct neural circuits but collaborative roles. *Neuroscientist*, 20(2), 150-159. <https://doi.org/10.1177/1073858413494269>
- Wang, J.-J., & Kaufman, A. S. (1993). Changes in fluid and crystallized intelligence across the 20-to 90-year age range on the K-BIT. *Journal of Psychoeducational Assessment*, 11(1), 29-37.
- Wang, L., Yu, C., Chen, H., Qin, W., He, Y., Fan, F., Zhang, Y., Wang, M., Li, K., Zang, Y., Woodward, T. S., & Zhu, C. (2010). Dynamic functional reorganization of the motor execution network after stroke. *Brain*, 133(Pt 4), 1224-1238. <https://doi.org/10.1093/brain/awq043>

- Wang, Y., Ao, Y., Yang, Q., Liu, Y., Ouyang, Y., Jing, X., Pang, Y., Cui, Q., & Chen, H. (2020). Spatial variability of low frequency brain signal differentiates brain states. *PLoS One*, *15*(11), e0242330. <https://doi.org/10.1371/journal.pone.0242330>
- Wang, Z., Liu, J., Zhong, N., Qin, Y., Zhou, H., & Li, K. (2012). Changes in the brain intrinsic organization in both on-task state and post-task resting state. *Neuroimage*, *62*(1), 394-407. <https://doi.org/10.1016/j.neuroimage.2012.04.051>
- Ward, N. S., Brown, M. M., Thompson, A. J., & Frackowiak, R. S. (2003). Neural correlates of motor recovery after stroke: a longitudinal fMRI study. *Brain*, *126*(Pt 11), 2476-2496. <https://doi.org/10.1093/brain/awg245>
- Wechsler, D. (1999). The Wechsler Abbreviated Scale of Intelligence (WASI). 1999. USA, *Psychological Corporation*.
- Wen, X., Dong, L., Chen, J., Xiang, J., Yang, J., Li, H., Liu, X., Luo, C., & Yao, D. (2019). Detecting the Information of Functional Connectivity Networks in Normal Aging Using Deep Learning From a Big Data Perspective. *Front Neurosci*, *13*, 1435. <https://doi.org/10.3389/fnins.2019.01435>
- Williams, V. J., Trombetta, B. A., Jafri, R. Z., Koenig, A. M., Wennick, C. D., Carlyle, B. C., Ekhlaspour, L., Ahima, R. S., Russell, S. J., Salat, D. H., & Arnold, S. E. (2019). Task-related fMRI BOLD response to hyperinsulinemia in healthy older adults. *JCI Insight*, *5*(14). <https://doi.org/10.1172/jci.insight.129700>
- Woodruff, T. M., Thundyil, J., Tang, S. C., Sobey, C. G., Taylor, S. M., & Arumugam, T. V. (2011). Pathophysiology, treatment, and animal and cellular models of human ischemic stroke. *Mol Neurodegener*, *6*(1), 11. <https://doi.org/10.1186/1750-1326-6-11>
- Xu, G., Fitzgerald, M. E., Wen, Z., Fain, S. B., Alsop, D. C., Carroll, T., Ries, M. L., Rowley, H. A., Sager, M. A., Asthana, S., Johnson, S. C., & Carlsson, C. M. (2008). Atorvastatin therapy is associated with greater and faster cerebral hemodynamic response. *Brain Imaging Behav*, *2*(2), 94. <https://doi.org/10.1007/s11682-007-9019-7>
- Yang, G. J., Murray, J. D., Repovs, G., Cole, M. W., Savic, A., Glasser, M. F., Pittenger, C., Krystal, J. H., Wang, X. J., Pearlson, G. D., Glahn, D. C., & Anticevic, A. (2014). Altered global brain signal in schizophrenia. *Proc Natl Acad Sci U S A*, *111*(20), 7438-7443. <https://doi.org/10.1073/pnas.1405289111>
- Yeo, S. S., Chang, P. H., & Jang, S. H. (2013). The ascending reticular activating system from pontine reticular formation to the thalamus in the human brain. *Front Hum Neurosci*, *7*, 416. <https://doi.org/10.3389/fnhum.2013.00416>
- Yousufuddin, M., & Young, N. (2019). Aging and ischemic stroke. *Aging (Albany NY)*, *11*(9), 2542-2544. <https://doi.org/10.18632/aging.101931>
- Zhang, T., Liao, Q., Zhang, D., Zhang, C., Yan, J., Ngetich, R., Zhang, J., Jin, Z., & Li, L. (2021). Predicting MCI to AD Conversation Using Integrated sMRI and rs-fMRI: Machine Learning and Graph Theory Approach. *Front Aging Neurosci*, *13*, 688926. <https://doi.org/10.3389/fnagi.2021.688926>
- Zhao, Z., Wu, J., Fan, M., Yin, D., Tang, C., Gong, J., Xu, G., Gao, X., Yu, Q., Yang, H., Sun, L., & Jia, J. (2018). Altered intra- and inter-network functional coupling of resting-state networks associated with motor dysfunction in stroke. *Hum Brain Mapp*, *39*(8), 3388-3397. <https://doi.org/10.1002/hbm.24183>
- Zhu, C. Z., Zang, Y. F., Cao, Q. J., Yan, C. G., He, Y., Jiang, T. Z., Sui, M. Q., & Wang, Y. F. (2008). Fisher discriminative analysis of resting-state brain function for attention-

deficit/hyperactivity disorder. *Neuroimage*, 40(1), 110-120.

<https://doi.org/10.1016/j.neuroimage.2007.11.029>

Zia, A., Pourbagher-Shahri, A. M., Farkhondeh, T., & Samarghandian, S. (2021). Molecular and cellular pathways contributing to brain aging. *Behav Brain Funct*, 17(1), 6.

<https://doi.org/10.1186/s12993-021-00179-9>





# Age-related differences in brain network activation and co-activation during multiple object tracking

Erlend S. Dørum<sup>1,2,3</sup> | Dag Alnæs<sup>2</sup> | Tobias Kaufmann<sup>2</sup> | Geneviève Richard<sup>1,2,3</sup> |  
Martina J. Lund<sup>2</sup> | Siren Tønnesen<sup>2</sup> | Markus H. Sneve<sup>3</sup> | Nina C. Mathiesen<sup>2</sup> |  
Øyvind G. Rustan<sup>2</sup> | Øivind Gjertsen<sup>4</sup> | Sigurd Vatn<sup>5</sup> | Brynjar Fure<sup>5</sup> |  
Ole A. Andreassen<sup>2</sup> | Jan Egil Nordvik<sup>1</sup> | Lars T. Westlye<sup>2,3</sup>

<sup>1</sup>Sunnaas Rehabilitation Hospital HT, Nesodden, Norway

<sup>2</sup>NORMENT, KG Jebsen Centre for Psychosis Research, Division of Mental Health and Addiction, Oslo University Hospital & Institute of Clinical Medicine, University of Oslo, Oslo, Norway

<sup>3</sup>Department of Psychology, University of Oslo, Oslo, Norway

<sup>4</sup>Department of Radiology, Oslo University Hospital, Oslo, Norway

<sup>5</sup>Department of Geriatric Medicine, Oslo University Hospital, Oslo, Norway

## Correspondence

Erlend S. Dørum, Norwegian Centre for Mental Disorders Research (NORMENT), KG Jebsen Centre for Psychosis Research, Division of Mental Health and Addiction, Oslo University Hospital, Nydalen, Oslo, Norway.

Email: e.s.dorum@medisin.uio.no

## Abstract

**Introduction:** Multiple object tracking (MOT) is a powerful paradigm for measuring sustained attention. Although previous fMRI studies have delineated the brain activation patterns associated with tracking and documented reduced tracking performance in aging, age-related effects on brain activation during MOT have not been characterized. In particular, it is unclear if the task-related activation of different brain networks is correlated, and also if this coordination between activations within brain networks shows differential effects of age.

**Methods:** We obtained fMRI data during MOT at two load conditions from a group of younger ( $n = 25$ , mean age =  $24.4 \pm 5.1$  years) and older ( $n = 21$ , mean age =  $64.7 \pm 7.4$  years) healthy adults. Using a combination of voxel-wise and independent component analysis, we investigated age-related differences in the brain network activation. In order to explore to which degree activation of the various brain networks reflect unique and common mechanisms, we assessed the correlations between the brain networks' activations.

**Results:** Behavioral performance revealed an age-related reduction in MOT accuracy. Voxel and brain network level analyses converged on decreased load-dependent activations of the dorsal attention network (DAN) and decreased load-dependent deactivations of the default mode networks (DMN) in the old group. Lastly, we found stronger correlations in the task-related activations within DAN and within DMN components for younger adults, and stronger correlations between DAN and DMN components for older adults.

**Conclusion:** Using MOT as means for measuring attentional performance, we have demonstrated an age-related attentional decline. Network-level analysis revealed age-related alterations in network recruitment consisting of diminished activations of DAN and diminished deactivations of DMN in older relative to younger adults. We found stronger correlations within DMN and within DAN components for younger adults and stronger correlations between DAN and DMN components for older adults, indicating age-related alterations in the coordinated network-level activation during attentional processing.

## KEYWORDS

attention, cognitive aging, DAN, default mode network, DMN, dorsal attention network, MOT, multiple object tracking

This is an open access article under the terms of the Creative Commons Attribution License, which permits use, distribution and reproduction in any medium, provided the original work is properly cited.

## 1 | INTRODUCTION

Attention entails a differential allocation of cognitive resources toward task-relevant information at the expense of that deemed less relevant. It is a core property of perceptual and cognitive operations, and in common with a range of other cognitive domains, declines with age throughout the adult lifespan (McDowd & Shaw, 2000). Although the mechanisms and neural correlates of such age-related decline are not completely understood, the most consistent findings to date point toward disruptions in interconnected brain networks (Andrews-Hanna et al., 2007; Parks & Madden, 2013).

Studies in functional neuroimaging have identified neural networks with differential responses during task paradigms. Networks routinely exhibiting increased activity during tasks are described as task-positive networks (TPN) (Duncan, 2013; Hugdahl, Raichle, Mitra, & Specht, 2015), while another well-described network showing an opposite pattern of activation to that of TPN, is the default mode network (DMN). Typically, DMN exhibits higher activity during resting conditions and decreased activation during cognitively demanding tasks (Beckmann, DeLuca, Devlin, & Smith, 2005; Raichle et al., 2001). A dorsal frontoparietal TPN known as the dorsal attention network (DAN) has been proposed as the source of endogenous, top-down attention signals in the brain (Ruff et al., 2008). DAN is involved in mapping task-relevant sensory information to adequate behaviors, and supports sustained and selective visuospatial attention through biasing the competition for representational space in sensory cortices (Corbetta, Kincade, Ollinger, McAvoy, & Shulman, 2000; Corbetta, Patel, & Shulman, 2008; Corbetta & Shulman, 2002; Gitelman et al., 1999), and by increasing the baseline activity for an attended object, suppressing distractors and limiting the number of object representations (Bar, 2003; Pessoa, Kastner, & Ungerleider, 2003). Critical nodes include the superior parietal lobe (SPL), inferior parietal sulcus (IPS), posterior parietal cortex, and the frontal eye fields (FEF) (Fox et al., 2005; Szczepanski, Pinsk, Douglas, Kastner, & Saalman, 2013; Toro, Fox, & Paus, 2008). A recent meta-analysis by Li et al. (2015) reviewing age-related changes in activations during tasks encompassing multiple cognitive domains including attention, memory, and executive function, indicated a crucial role of increased DAN in successful compensation for older adults. Insight into the effects of aging on DAN modulation is therefore an attractive target for studies aiming to delineate the neural mechanisms of cognitive aging.

While the DAN and other TPNs display increased activation in response to demanding tasks, the DMN, including the medial prefrontal and medial parietal cortex, the posterior cingulate and precuneus, and the medial temporal lobe (Spreng, Mar, & Kim, 2009; Uddin, Clare Kelly, Biswal, Xavier Castellanos, & Milham, 2009), typically shows increasing activity during periods without specific task demands (Raichle et al., 2001). The dichotomous relationship between these networks generally becomes more pronounced as attentional demand increases, reflected both in increased activation in DAN (Wojciulik & Kanwisher, 1999) and increased deactivation in DMN (Mckiernan, Kaufman, Kucera-Thompson, & Binder, 2003).

Some studies suggest that the enhancement of relevant information largely remains intact, while efficient neural suppression of irrelevant information seems to be compromised in aging (Alain & Woods, 1999; Czigler, Csibra, & Ambró, 1996; Gazzaley, Cooney, Rissman, & D'Esposito, 2005). Other reported age-related decline both in task-related enhancement as well as inefficient suppression (Logan, Sanders, Snyder, Morris, & Buckner, 2002; Tomasi, Wang, Wang, & Volkow, 2014). Previous fMRI studies have shown less pronounced DMN deactivation during cognitive tasks (Damoiseaux et al., 2008; Grady, Springer, Hongwanishkul, McIntosh, & Winocur, 2006; Lustig et al., 2003; Miller et al., 2008; Persson, Lustig, Nelson, & Reuter-Lorenz, 2007) as well as reduced resting-state DMN connectivity (Esposito et al., 2008; Mowinckel, Espeseth, & Westlye, 2012) in older adults. Diminished DMN deactivations during task performance may indicate reduced network regulation and dynamic range of network modulation to altering task demands (Spreng & Schacter, 2012), supporting the view of the aging brain as more rigid and less cortically selective within the given cognitive states. In line with the hypothesis that disruptions of large-scale brain networks contribute to aging-related cognitive decline, Andrews-Hanna et al. (2007) observed age-related decreases in functional connectivity within both DMN and DAN, which were associated with poor cognitive performance.

In this study, we investigated age differences in the task-related activations across a range of brain networks during multiple object tracking (MOT) (Pylyshyn & Storm, 1988). MOT is a powerful paradigm for measuring sustained goal-driven attention, requiring participants to attend multiple target items as they move among distractors. Attentional load can be manipulated by increasing the number of objects the subject is requested to track; higher numbers of objects to track implies higher attentional load. Load manipulation allows for distinguishing between brain regions directly involved in attentional performance and showing load-dependent activity from regions activated by the task alone, giving a better measure for estimating neural activity in response to attentional demand rather than activity produced by task-relevant, but not load-dependent functions such as suppression of eye movement (Culham, Cavanagh, & Kanwisher, 2001). Tracking performance is reduced with age for trials with higher attentional load (Trick, Perl, & Sethi, 2005), and this reduction in performance may be specific to attentional function, as memory for object location was only marginally affected by age (Sekuler, McLaughlin & Yotsumoto, 2008). A recent event-related potentials (ERP) study reported age-related decreases in tracking performance with reduced attentional modulation of the visual P1 component (Störmer, Li, Heekeren, & Lindenberger, 2013; Trick et al., 2005), suggesting that MOT is sensitive to age-related differences in the neuronal machinery supporting attention.

While fMRI studies have documented robust DAN activation during MOT (Culham et al., 1998, 2001; Howe, Horowitz, Morocz, Wolfe, & Livingstone, 2009; Jovicich et al., 2001), age-related differences have not been studied. Further, little is known about DMN modulation during tracking (but see Alnæs et al., 2015; Tomasi et al., 2014), and to which degree network-specific activation and deactivations of different brain networks reflect independent and overlapping predictors of cognitive aging. Using independent component analysis (ICA)

and conventional voxel-wise time-series analyses, our main aims were to test for differences between a group of younger and older healthy volunteers in brain network activation and deactivation across a range of brain networks, including networks involved in motor, sensory, and cognitive functions, during MOT. Secondly, in order to explore to which degree activation of the various brain networks reflect unique and common mechanisms, we assessed the correlations between the brain networks' activations.

Based on current models of cognitive and brain aging (Cabeza, Anderson, Locantore, & McIntosh, 2002; Damoiseaux et al., 2008; Dennis & Cabeza, 2008; Grady et al., 2006; Li et al., 2015; Reuter-Lorenz & Park, 2010), we hypothesized:

1. MOT engages a range of brain networks, including but not limited to the DAN and DMN. Network responses are more pronounced with increasing load demand and there is an interaction effect of load and age, with stronger age-related differences at higher load levels.
2. Age differences are particularly manifested as reduced DMN deactivation and altered DAN activation, partly reflecting reduced tracking performance (Nagel et al., 2009). DAN effects may manifest either as increased activation in the old group, which—when accompanied by similar performance—indicate some form of compensation or increased mental effort associated with task demands (Cabeza et al., 2002; Reuter-Lorenz & Lustig, 2005), or as reduced activation, reflecting diminished brain network efficiency.
3. Based on the concept that cognition is enabled by the temporal synchronization of different brain networks and in line with the notion of dedifferentiation in cognitive aging (Andrews-Hanna et al., 2007; Baltes & Lindenberger, 1997; Chan, Park, Savalia, Petersen, & Wig, 2014; Lindenberger, 2014), we anticipated that age effects would additionally be revealed in a differential pattern of correlations in levels of task-related activations between the two age groups. The dedifferentiation theory posits that aging confers a loss of network specificity and disruptions within intrinsic functional networks, particularly implicating DMN and DAN (Andrews-Hanna et al., 2007). Thus, we anticipate stronger correlation in levels of co-activation between task-related components, particularly within the DAN and DMN for the younger group compared to the older group.

## 2 | MATERIALS AND METHODS

### 2.1 | Sample

We recruited 26 young (mean age: 24.2 years, *SD*: 4.9, 69% females) and 26 old (mean age: 66.2 years, *SD*: 7.4, 58% females) adults through a newspaper ad and social media. All subjects underwent neuropsychological screening (details below). Participants reported normal or corrected-to-normal vision. Exclusion criteria included estimated IQ < 70, previous history of alcohol- and substance abuse, history of neurological or psychiatric disease, participants presently on

any medication significantly affecting the nervous system and contraindications for MRI. All participants were self-sufficient and living independently, and reported no reason to suspect marked cognitive decline or undiagnosed dementia.

From the full dataset, we excluded participants due to excess motion during scanning ( $n = 2$ ) as well as poor MOT performance ( $n = 5$ ). Specifically, participants performing worse than chance during the low load condition (see below) or 2.5 standard deviations below the mean during the high load condition were excluded from analyses. Outliers in the high load condition were determined by boxplot graph visualization and verified using Grubbs' test for single outlier (Iglewicz & Hoaglin, 1993), yielding a final sample of 24 younger (mean age 24.42 years, *SD*: 5.06, 66.7% females) and 21 older adults (mean age 64.67, *SD*: 7.44, 53.4% females).

### 2.2 | Screening and neuropsychological assessment

Participants completed the matrices and vocabulary subtests from the Wechsler Abbreviated Scale of Intelligence (WASI; Wechsler, 1999) as a measure of general intellectual functioning, and the 4-trial version of the Stroop Color Word Interference test (CWIT) from the Delis-Kaplan Executive Function System (D-KEFS; Delis, Kaplan, & Kramer, 2001) to obtain a measure of cognitive speed, interference, and inhibition. CWIT comprises the following four conditions: (1) Color task—subject identifies the color of a series of squares (red, blue, green); (2) Word task—subject reads a series of color words (red, blue, green) written in black print; (3) Inhibition task—subject is presented with words written in congruent (e.g., red written in red ink) and incongruent (e.g., red written in blue ink) colors; (4) Inhibition/Switching—subject is presented with words written in congruent and incongruent colors. We used completion times as basis for analysis, with focus on the inhibition and inhibition/switching tasks.

Wechsler Abbreviated Scale of Intelligence subtest scores were converted to standardized scores from which full-scale IQ (FSIQ) was estimated. Two subjects (one young and one old) were native foreign language speakers and thus were not adequately able to perform the vocabulary subtest; their scores on this subtest were reported as missing and their FSIQ was calculated solely based on performance in the matrix reasoning subtest.

### 2.3 | MOT paradigm

All participants performed two versions of MOT in the MRI scanner during the same session, including one blocked run, and two runs comprising continuous tracking, in addition to one resting-state run following the protocol used by Alnæs et al. (2015). Here, we report data from the blocked runs. The level of attentional demand was set at two load conditions—load 1 (L1) and load 2 (L2) requiring the participants to track one or two targets, respectively, during the task. We restricted the load level to a maximum of L2 to ensure that both groups were able to perform at a high level, which is in particular pertinent for the subsequent utilization of the paradigm in clinical populations.

For both versions, the participant was looking through a mirror mounted on the head coil at a MR-compatible LCD screen (NNL LCD Monitor<sup>®</sup>, NordicNeuroLab, Bergen, Norway) placed in front of the scanner bore, with a screen resolution of 1920 × 1080@60 Hz. All stimuli were generated using MATLAB and the Psychophysics Toolbox extensions (Brainard, 1997; Pelli, 1997). Participants produced their responses using a MR-compatible subject response collection system (ResponseGrip<sup>®</sup>, NordicNeuroLab). A trigger pulse from the scanner synchronized the onset of the experiment to the beginning of the acquisition of an fMRI volume. The screen covered 32.43° of visual angle, and the tracking area covered 17.32° of visual angle at a viewing distance of 1.2 meters. The objects were circular disks with a diameter of 0.7° of visual angle moving at a speed of 4°/second. Objects changed direction when closer than 1° to another object or the edge of the tracking area, and also made random changes (one random turn per second on average) to make object movements unpredictable. A fixation circle of 0.5° of visual angle was located in the center of the tracking area. The participant's task consisted of covertly tracking target objects while fixating on the central fixation point. Detailed instructions were given before entering the scanner room as well as before each sequence.

The blocked run contained 18 trials divided into six blocks. Each block contained three different conditions: Passive Viewing (PV), one target object (L1), and two target objects (L2), followed by rest. The rest periods, which lasted 12 s were not explicitly modeled and thus constitute the implicit baseline. The order of the three conditions was random and counterbalanced so that each condition was followed by a rest period in two of the six parts, that is, PV was presented twice followed by rest, and so were L1 and L2. The run started with 1.5 s of instructions followed by 0.5 s fixation. Then, 10 identical objects were presented on a gray background. All objects were blue for 0.5 s, and then either zero (PV condition), one (L1) or two (L2) of the objects turned red (designating them as targets) for 2.5 s before turning color back to blue (during tracking all objects were identical). After another 1.5 s, the objects started moving randomly and independently of each other for 12 s. At the end of each trial, the objects stopped moving before one of the objects turned green (probe) for 2.5 s. The participant was instructed to respond as quickly and accurately as possible, "yes" or "no" to whether the green probe was one of the objects originally designated as a target. In passive viewing trials, there were no targets, nor probe, but the participants were still instructed to keep fixation during the length of the trial. Accuracy and response time (RT) were recorded for each button press.

## 2.4 | MRI acquisition

Magnetic resonance imaging scans were obtained from a General Electric (Signa HDxt) 3.0T scanner with an 8-channel head coil at Oslo University Hospital. Functional data were acquired with a T2\*-weighted 2D gradient echo planar imaging sequence (EPI) with 217 volumes (TR: 2,400 ms; TE: 30 ms; FA: 90°; voxel size: 3.75 × 3.75 × 3.2 mm; slices: 48; FOV: 240 × 240 mm; duration: 533 s). The first five volumes were discarded to allow for T1

equilibrium. In addition, a structural scan was acquired using a sagittal T1-weighted fast spoiled gradient echo (FSPGR) sequence (TR: 7.8 s; TE: 2.956 ms; TI: 450 ms; FA: 12°; voxel size: 1.0 × 1.0 × 1.2 mm; slices: 170; FOV: 256 mm<sup>2</sup>; duration: 428 s).

## 2.5 | fMRI processing and analysis

Functional MRI data were processed on single-subject level using the FMRI Expert Analysis Tool (FEAT) from the FMRIB Software Library (FSL; Smith et al., 2004), including spatial smoothing (FWHM = 6 mm), high-pass filtering (sigma = 64 s), motion correction (MCFLIRT), and single-session ICA using MELODIC (Beckmann & Smith, 2004).

We calculated in-scanner subject motion defined as the average root mean square of the displacement from one frame to its previous frame for each dataset, and used FMRIB's ICA-based Xnoiseifier (FIX; Salimi-Khorshidi et al., 2014) to identify and remove noise components (standard training set, threshold: 20), yielding a cleaned dataset for each subject. We used 24 motion parameters, including 6 raw realignment parameters and 24 extended parameters estimated from the realignment procedure. We did not regress out the global signal (GSR), nor the white matter or CSF. Instead, we used an ICA-based approach to selectively regress out noise components (FIX) from each dataset, in line with recent studies evaluating benefits of different noise reduction strategies (Pruim, Mennes, Buitelaar, & Beckmann, 2015). The older group showed significantly more in-scanner motion,  $t(43) = -3.9, p < .0001$ , and FIX removed a significantly higher number of components from the older group,  $t(19) = -2.2, p < .05$ , and also removed more of the variance from the raw fMRI data, both in terms of absolute and relative variance, both  $t(19) = -2.8, p < .05$ , which were significantly correlated with amount of subject motion across groups ( $r = .52, p < .0001$ ).

We used FreeSurfer (Fischl et al., 2002) for automated brain segmentation of the T1-weighted data to obtain brain masks used for coregistration to a standard coordinate system using FLIRT (Jenkinson & Smith, 2001), optimized using boundary-based registration (BBR; Greve & Fischl, 2009) and FNIRT (Andersson, Jenkinson, & Smith, 2007a,b).

## 2.6 | Voxel-wise GLMs

In the first-level general linear model (GLM), the onset and duration of the PV and tracking blocks (L1 and L2) were modeled with the fixation blocks as implicit baseline. The design matrix was filtered and convolved with a hemodynamic response function (HRF) before the model fit. A temporal derivative was added to the model to adjust for regional differences in the timing of the HRF. We included the following contrasts: Tracking (average of L1 and L2) versus PV, and L1 versus L2. The individual contrast parameter maps were then subjected to whole-brain group analysis based on a random effects model, testing for differences between the young and the old group. To correct for multiple comparisons across space, we performed cluster-level correction with voxel-wise  $Z > 2.3$  and a corrected cluster significance threshold of  $p < .05$  for all analyses.

## 2.7 | Group-independent component analysis and time-series analysis

The individually processed, filtered, cleaned, and normalized fMRI volumes were submitted to a group-level ICA using the temporal concatenation approach in MELODIC (Beckmann & Smith, 2004). The number of components was calculated using a Laplace approximation of the posterior probability of the model order (Beckmann & Smith, 2004), yielding 41 components. Next, the group-average spatial maps for the 28 non-noise components were used to generate subject-specific maps and associated time series using dual regression (Filippini et al., 2009). Dual-regression time series were submitted to time-series regression using the same individual-level GLM design matrices used for the voxel-wise analysis. The regression coefficients for the two tracking conditions were subtracted for each participant (L2-L1) for both DMN and DAN and submitted to group-level analysis assessing main effects of load across groups, as well as differences between the old and the young group. For visualization purposes, we calculated the group-average blocked time series for each of the three MOT conditions (PV, L1, L2) based on the z-normalized (within-run) dual-regression time series for each subject.

## 2.8 | Statistical analysis

Nonimaging data were analyzed in SPSS (IBM\_Corp, 2010). Between-group differences were assessed using Chi square tests (sex distribution) and linear models (age, neuropsychological performance, task performance). Group differences in MOT performance and estimated brain network beta values were assessed using two-by-two repeated-measures ANOVA with load (L1 and L2) as within subject factor and group (young and old) as between subject factor. Group differences in beta values were further explored using ANCOVA including gender and group as fixed factors. We used paired samples t-tests and ANCOVA

to test for load-dependent (L2-L1) differences in beta values. To test for association between task performance and beta estimates, we used an ANCOVA with gender and group as fixed factors and task accuracy during L2 as the dependent variable. We tested for association between neuropsychological performance and beta estimates using an ANCOVA with gender and group as fixed factors and performance scores for each neuropsychological subtest as the dependent variable. Lastly, we employed an ANCOVA to test for associations between the beta estimates for the respective networks at the given load conditions for the two groups, covarying for gender and age. In order to assess the between-network correlations of the task-related activations, we computed the Pearson's correlation between the betas of each of the component pairs, yielding a 28 by 28 correlation matrix for each group. Next, in order to test for group differences, the correlation coefficients were compared between groups using Fisher's r-to-z transformation. The resulting *p*-values were then adjusted using Bonferroni and FDR corrections. Raw *p*-values are also shown for transparency.

## 3 | RESULTS

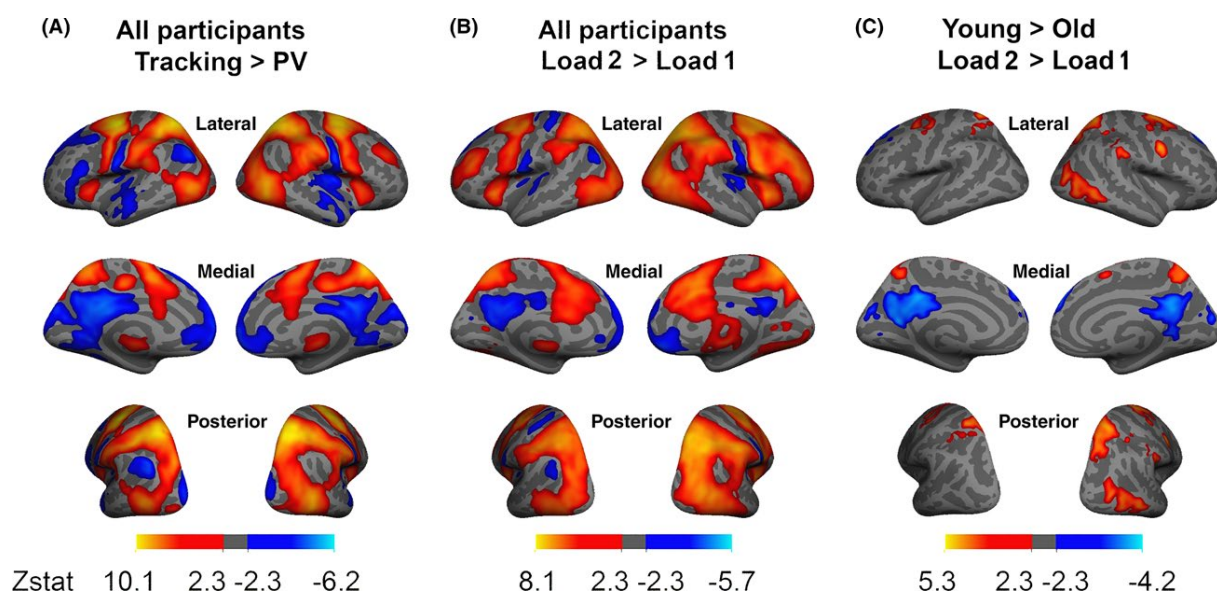
### 3.1 | Demographics, neuropsychology, and task performance

Table 1 summarizes demographic, neuropsychological, and MOT performance. Briefly, the younger subgroup performed significantly better on the matrix reasoning task of the WASI subtest as well as the inhibition and inhibition/switching parts of the Stroop test. No other significant differences were found. An ANCOVA exploring whether differences in performance on the neuropsychological tests correlated with activation levels in the selected DAN and DMN components revealed no significant correlation between WASI matrix reasoning and beta coefficients for either group. ANCOVA associating completion time during

**TABLE 1** Demographics and neuropsychological performance

	Young (SD)	Old (SD)	$\chi^2/t$ -score	<i>p</i>
N	24	21		
Age	24.42 (5.06)	64.67 (7.44)		
Age range	20–43	47–78		
Percent male	33.3	47.6	$\chi^2 = 0.95$	.33
Percent right handedness	91.7	85.7	$\chi^2 = 1.61$	.21
Years of education	15.50 (1.37)	15.12 (3.06)	<i>t</i> = 0.53	.603
WASI matrix reasoning	29.58 (2.17)	25.71 (6.48)	<i>t</i> = 2.61	<b>.015</b>
WASI vocabulary	65.91 (6.20)	66.10 (10.6)	<i>t</i> = -0.07	.943
Full scale IQ-2	120.04 (9.17)	119.95 (17.45)	<i>t</i> = 0.02	.983
Stroop word	30.36 (6.86)	34.36 (7.39)	<i>t</i> = -1.83	.074
Stroop color	22.79 (5.27)	25.33 (5.30)	<i>t</i> = -1.61	.115
Stroop inhibition	47.17 (11.26)	64.14 (22.35)	<i>t</i> = -3.15	<b>.004</b>
Stroop inhibition/switching	55.50 (11.73)	79.19 (45.94)	<i>t</i> = -2.30	<b>.031</b>
MOT accuracy on L1	97.9 (7.47)	94.4 (10.9)	<i>t</i> = 1.22	.230
MOT accuracy on L2	88.9 (14.5)	77.8 (20.6)	<i>t</i> = 2.063	<b>.047</b>

Significant group differences are shown in bold.



**FIGURE 1** Voxel-wise GLM analysis for the contrasts; (A) Tracking > passive viewing across groups; (B) L2 > L1 across groups; (C) Young > old group for L2 > L1. We employed Gaussian random field theory to carry out cluster-level corrections for multiple comparisons (voxel-level  $Z > 2.3$ ; cluster significance:  $p < .05$ , corrected)

the inhibition task from the Stroop task with activation levels for DAN L2 revealed a main effect of group [ $F(1,40) = 4.94$ ,  $p = .032$ , partial  $\eta^2 = .110$ ], but no main effect of DAN L2 [ $F(1,40) = .88$ ,  $p = .354$ , partial  $\eta^2 = .021$ ] and no interaction effect [ $F(1,40) = 3.88$ ,  $p = .056$ , partial  $\eta^2 = .088$ ]. No significant association was found between DMN L2 and performance on the inhibition subtest. ANCOVA associating completion time during the inhibition/switching task from the Stroop test with activation levels for DAN L2 revealed a main effect of group [ $F(1,40) = 5.88$ ,  $p = .020$ , partial  $\eta^2 = .128$ ], a main effect of DAN L2 [ $F(1,40) = 7.46$ ,  $p = .009$ , partial  $\eta^2 = .009$ ], and an interaction effect [ $F(1,40) = 5.42$ ,  $p = .025$ , partial  $\eta^2 = .119$ ], indicating better performance with increased DAN activation for the young group. Association between DMN L2 and the inhibition/switching subtest revealed no main effect of group [ $F(1,40) = .01$ ,  $p = .930$ , partial  $\eta^2 = .000$ ], but a main effect of DMN L2 [ $F(1,40) = 5.23$ ,  $p = .027$ , partial  $\eta^2 = .116$ ] and an interaction effect [ $F(1,40) = 4.94$ ,  $p = .032$ , partial  $\eta^2 = .110$ ], indicating better performance with increased DMN deactivation for the young group.

Mean tracking accuracy during the MOT task was 97.9% (L1) and 88.9% (L2) and 94.4% (L1) and 77.8% (L2) for the young and old group, respectively. A two-by-two repeated-measures ANOVA with load (L1 and L2) as within subject factor and group (young and old) as between subject factor yielded a significant effect of load [ $F(1,43) = 26.04$ ,  $p = 7.0E-6$ ] and group [ $F(1,43) = 4.69$ ,  $p = .04$ ], but no load by group interaction [ $F(1,43) = 2.30$ ,  $p = .137$ ].

## 3.2 | Functional MRI

### 3.2.1 | Voxel-wise analysis

In order to validate the MOT paradigm, we investigated whether patterns of activation in this study mirrored previously described findings

in MOT research. Figure 1A shows the main effects across groups for the tracking versus PV contrast. Tracking-related activation is seen in human motion area (MT+), FEF, IPS, SPL, and SMA. Tracking-related deactivation is seen within the DMN including the medial prefrontal cortex (mPFC), the precuneus, and the lateral temporal cortex (LTC).

Figure 1B shows the main effects across groups for the L2 versus L1 contrast. Increasing the task demand produces load-related activations and deactivations in areas overlapping the tracking versus PV contrast, including increased activations in FEF, lateral occipital cortices, and superior parietal lobules, decreases in activations are seen in medial prefrontal cortices and precuneus.

Figure 1C and Table 2 summarize the significant group differences in the L2 versus L1 contrast. Four clusters showed significantly greater load-dependent activity increases in the young compared to the old group, including the FEF, MT+ and SPL. Two clusters showed greater load-related deactivations in the young compared to the old group, including the precuneus and the mPFC.

### 3.2.2 | Independent component analysis

From the 41 components generated by the group-level ICA, 13 components were manually classified as noise components and discarded from further analysis, and the subsequent analyses were performed on the remaining 28 components (Fig. 2).

### 3.2.3 | Main effects of group and load and their interactions

Table 3 and Figure 2, panels A-C summarize the estimated contrast parameters for the L2 > L1 contrast and the young > old contrast at L2 > L1 using the individual-level GLMs and subject-specific

**TABLE 2** Cluster list with coordinates, cluster-level statistics for local maxima and associated brain regions for the main effects of the L2 > L1, young > old contrast. Positive Z-scores reflect increased differentiation between L2 and L1 in the young compared to the old group

Brain region	Voxels	<i>p</i>	$-\log_{10}(p)$	Z-max	Z-Max x, y, z (mm)
Right SPL	4,879	1.5E-08	7.81	5.03	62, -46, 52
Right FEF	2,285	8.66E-05	4.06	5.27	20, -6, 78
Left FEF	1,133	0.0115	1.94	4.2	-32, -4, 60
Right MT+	1,014	0.0206	1.69	4.48	40, -72, 6
Left precuneus	4,564	5.96E-08	7.22	-4.2	-6, -38, 34
Left mPFC	2,671	2.06E-05	4.69	-4.02	16, 42, 44

dual-regression times series, for the 28 independent components generated from the group ICA. Briefly, hierarchical clustering grouped the components into five clusters, largely corresponding to task-positive/DAN, DMN, somatosensory, brainstem/cerebellar, and frontoparietal clusters. The five strongest load effects were found for IC7 (DAN) ( $t = 12.21$ ,  $p < .001$ ), IC13 (posterior DAN) ( $t = 8.22$ ,  $p < .001$ ), IC 3 (DAN) ( $t = 7.83$ ,  $p < .001$ ), IC 1 (posterior DMN) ( $t = -7.02$ ,  $p < .001$ ), and IC11 (somatomotor) ( $t = -6.80$ ,  $p < .001$ ). The five strongest group effects at the L2 > L1 contrast were found for IC1 (posterior DMN) ( $t = -4.25$ ,  $p < .001$ ), IC3 (DAN) ( $t = 3.54$ ,  $p = .001$ ), IC 5 (anterior DMN) ( $t = -3.03$ ,  $p = .004$ ), IC 6 (posterior DMN) ( $t = -2.74$ ,  $p = .009$ ), and IC17 (somatomotor) ( $t = -2.70$ ,  $p = .01$ ), of which the two strongest (IC1 and IC3) remained significant after Bonferroni correction, indicating increased DAN activation and increased DMN deactivation in the young compared to the old group.

### 3.2.4 | DAN and DMN activations and associations between these networks

Figure 3A shows the two components showing significant group differences, representing the DMN (IC1) and the DAN (IC3), respectively. Figure 3C shows the average blocked time-series for the two components during L2. Table 4 summarizes the regression coefficients (betas) for each component for each of the load conditions.

A repeated-measures ANOVA with load as within subject factor and group as between subject factor revealed significant main effects of Load [ $F(1,43) = 72.97$ ,  $p = 8.21E-11$ , partial  $\eta^2 = .63$ ] and Group [ $F(1,43) = 18.1$ ,  $p = .0001$ , partial  $\eta^2 = .296$ ], and a significant Load by Group interaction [ $F(1,43) = 12.55$ ,  $p = .001$ , partial  $\eta^2 = .226$ ] on DAN activation. Post hoc group comparisons within the load conditions, using an ANCOVA with gender and group as fixed factors, revealed significant differences in DAN L1 [ $t(42) = 3.35$ ,  $p = .002$ ] and DAN L2 [ $t(42) = 5.13$ ,  $p = 7.0E-7$ ], indicating stronger DAN activations in the young group compared to the old, in both load conditions.

A repeated-measures ANOVA revealed a significant main effect of Load [ $F(1,43) = 63.46$ ,  $p = 5.29E-10$ , partial  $\eta^2 = .60$ ], no significant main effect of Group [ $F = (.005)$ ,  $p = .946$ , partial  $\eta^2 = .00011$ ], and a significant Load by Group interaction effect [ $F(1,43) = 18.05$ ,  $p = .00011$ , partial  $\eta^2 = .296$ ] on DMN deactivation. ANCOVA testing for group differences within the two load conditions in DMN activations revealed significant differences in DMN L1 [ $t(42) = 2.22$ ,

$p = .032$ ] as well as DMN L2 [ $t(42) = -2.30$ ,  $p = .027$ ], indicating increased and decreased DMN deactivation in the old group in the L1 and L2 condition, respectively.

Figure 3B summarizes the average difference between the L1 and L2 regression coefficients for the two groups. Paired samples t-tests revealed greater load-dependent DAN activations both in the young [mean difference = .804,  $SD = (.521)$ ,  $t(23) = 7.55$ ,  $p = 1.15E-7$ ] and the old [mean difference = .332,  $SD = .336$ ],  $t(19) = 4.53$ ,  $p = .00005$ ] group. Further, both the young [mean difference =  $-.796$ ,  $SE = .489$ ],  $t(23) = -7.97$ ,  $p = 4.58E-8$ ] and the old (mean difference =  $-.242$ ,  $SE .367$ ,  $t(19) = -3.04$ ,  $p = .007$ ) group showed greater DMN deactivations during L2 compared to L1.

ANCOVA revealed a significant [ $t(42) = 4.01$ ,  $p = .00025$ ] effect of group on the difference in DAN activation between L2 and L1, indicating larger load-dependent activations in the young compared to the old group. In addition, ANCOVA revealed a significant [ $t(42) = -4.27$ ,  $p = .00011$ ] effect of group on the difference in DMN deactivation between L2 and L1, indicating stronger load-dependent deactivations in the young compared to the old group.

ANCOVA testing for associations between betas for the DAN and the DMN within load conditions revealed no significant associations for either group during L1 [young:  $t(23) = .42$ ,  $p = .678$ ; old:  $t(19) = 1.81$ ,  $p = .088$ ] or L2 [young:  $t(23) = .27$ ,  $p = .792$ ; old:  $t(19) = 1.17$ ,  $p = .260$ ]. For the difference between L2 and L1, the ANCOVA revealed a significant association between DAN and DMN activation for the old group [ $t(19) = 2.18$ ,  $p = .042$ ], but not for the young [ $t(23) = -.65$ ,  $p = .526$ ], indicating a positive association between DAN and DMN activation when increasing load from L1 to L2 in the old group.

### 3.3 | Associations between component activation

We used the beta coefficients for all the 28 independent components generated from the group ICA to test for associations between component activation in both groups for the L2 > L1 contrast (Fig. 3, panel D). In a graph theoretical framework, the brain is modeled as a network that can be graphically represented by an assembly of nodes and edges. Here, the nodes represent the respective components and edges correspond to the temporal correlations between the said components. Across groups, positive correlations were primarily found between task-positive components within the DAN. Negative correlations were primarily found between subcortical

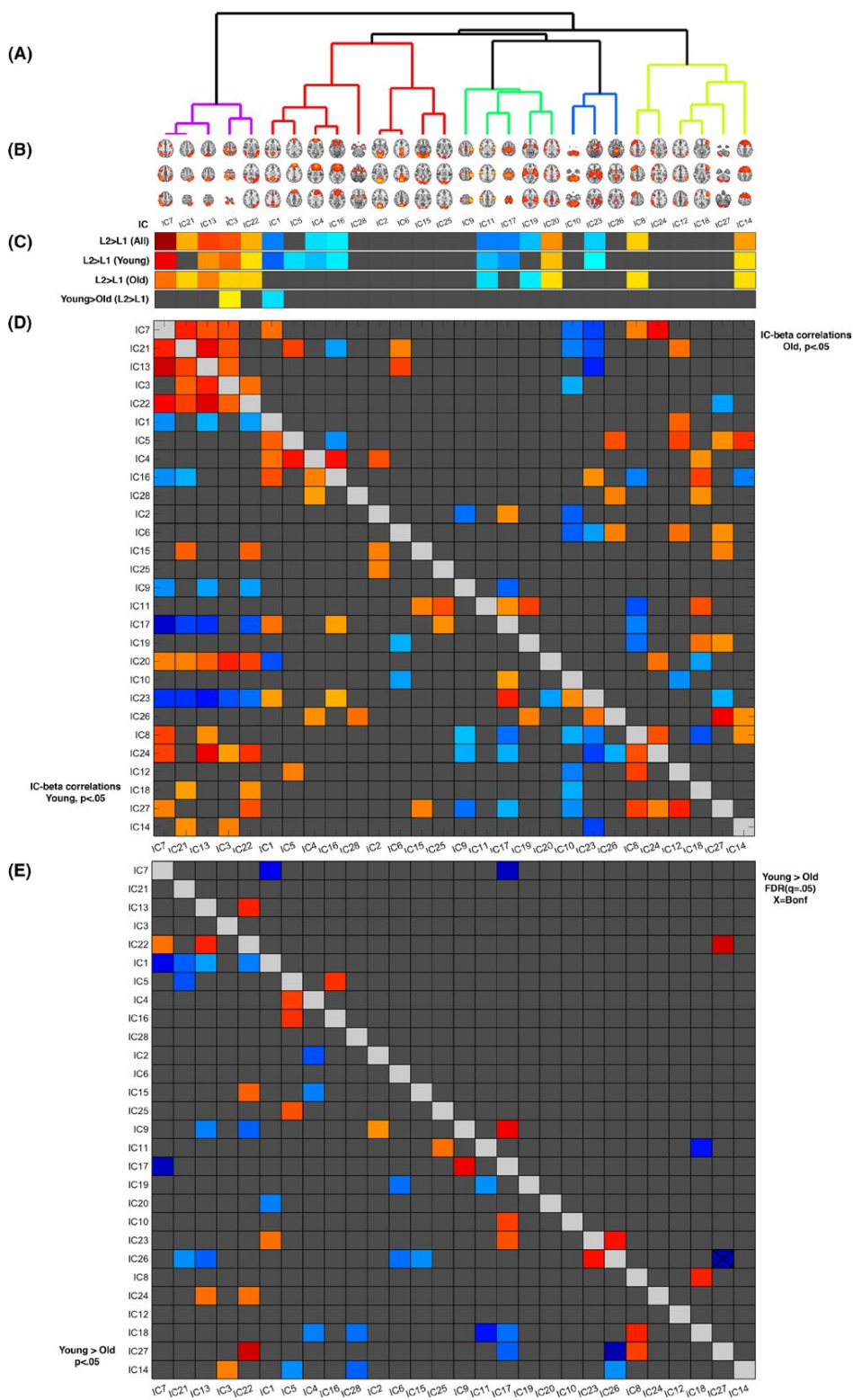


**FIGURE 2** Panel A: Dendrogram showing clustering of nodes for the 28 components from the group ICA. Panel B: The 28 nodes from the group ICA. Panel C: GLM for all the independent components at the given contrasts. Panel D: The nominally significant ( $p < 0.5$ ) beta correlations between the independent components, correlations in the old and young group are shown above and below the diagonal, respectively. Warm colors indicate high correlation, cold colors indicate low correlation. Panel E: Below the diagonal are the nominally ( $p < .05$ ) significant differences in correlation (Young > Old). Above the diagonal are the FDR ( $q = 0.05$ ) corrected differences in correlation (Young > Old). Warm colors indicate stronger correlations in the younger group, cold colors indicate stronger correlations in the older group. Squares marked with an X indicate the correlations surviving Bonferroni correction (378 independent tests)

**TABLE 3** Components sorted by main effect of load (L2 > L1) for all participants. Column 4 gives the *t*-score for the young versus old contrast at L2 > L1. The rightmost column gives the respective brain networks/regions corresponding to each component. Values that are significant after Bonferroni correction for multiple comparisons (28 tests) are shown in bold

IC no.	L2 > L1, all participants, <i>t</i> -score	<i>p</i> -value	L2 > L1, Young>Old, <i>t</i> -score	<i>p</i> -value	Brain network/region
7	<b>12.21</b>	<b>&lt;.001</b>	1.59	0.120	DAN
13	<b>8.22</b>	<b>&lt;.001</b>	1.67	0.102	Post-DAN
3	<b>7.83</b>	<b>&lt;.001</b>	<b>3.54</b>	<b>0.001</b>	DAN
1	<b>-7.02</b>	<b>&lt;.001</b>	<b>-4.25</b>	<b>&lt;0.001</b>	Post-DMN
11	<b>-6.80</b>	<b>&lt;.001</b>	-0.50	0.620	Somatomotor
17	<b>-6.75</b>	<b>&lt;.001</b>	-2.70	0.010	Somatomotor
20	<b>5.98</b>	<b>&lt;.001</b>	2.13	0.039	Supramarginal gyrus
14	<b>5.78</b>	<b>&lt;.001</b>	-0.98	0.332	Superior frontal gyrus
22	<b>5.30</b>	<b>&lt;.001</b>	1.68	0.100	Lateral occipital
21	<b>5.11</b>	<b>&lt;.001</b>	0.09	0.932	Left lateralized DAN
19	<b>-5.11</b>	<b>&lt;.001</b>	-0.35	0.729	Auditory/temporal
23	<b>-4.84</b>	<b>&lt;.001</b>	-1.27	0.211	Subcortical
4	<b>-4.54</b>	<b>&lt;.001</b>	-2.25	0.030	Ant. DMN
8	<b>4.49</b>	<b>&lt;.001</b>	-0.76	0.450	Right frontoparietal
16	<b>-4.06</b>	<b>&lt;.001</b>	-0.67	0.504	Ant. DMN
12	<b>-3.01</b>	<b>.004</b>	-2.29	0.027	Paracingulate
26	<b>2.98</b>	<b>.005</b>	-2.01	0.051	Brainstem
15	<b>2.97</b>	<b>.005</b>	0.10	0.922	Visual
28	<b>-2.30</b>	<b>.026</b>	-0.78	0.440	Insula
5	<b>-2.29</b>	<b>.027</b>	-3.03	0.004	Ant. DMN
9	<b>-1.80</b>	<b>.079</b>	-1.27	0.210	Somatomotor
18	<b>-1.79</b>	<b>.080</b>	-0.38	0.704	Left inferior frontal
25	<b>-1.44</b>	<b>.156</b>	-0.10	0.919	Visual
10	<b>1.42</b>	<b>.163</b>	0.48	0.634	Cerebellum
24	<b>1.23</b>	<b>.226</b>	0.09	0.927	Angular gyrus
27	<b>-0.86</b>	<b>.395</b>	-2.49	0.017	Cerebellum
2	<b>0.44</b>	<b>.663</b>	-1.78	0.083	Visual
6	<b>0.28</b>	<b>.784</b>	-2.74	0.009	Post-DMN

and task-positive DAN components and between somatomotor and task-positive DAN components. Component correlations within age groups revealed a higher number of correlated and anticorrelated components in the young compared to the old group; 92 out of 378 edges showed significant correlations at the nominal level in the young group; for the old group, 64 out of 378 edges were found nominally significant. Strongest positive correlations between components in the young group were found between IC7 (DAN) and IC13 (posterior DAN) ( $r = .82$ ,  $p = 1.22E-6$ ), IC13 (posterior DAN) and IC22 (lateral occipital) ( $r = .79$ ,  $p = 4.35E-6$ ), and between IC13 (posterior DAN) and IC24 (angular gyrus), ( $r = .76$ ,  $p = 1.63E-5$ ). Strongest negative correlations between components in the young group were found between IC7 (DAN) and IC17 (somatomotor) ( $r = -.87$ ,  $p = 3.88E-8$ ), IC13 (posterior DAN) and IC23 (subcortical) ( $r = -.73$ ,  $p = 4.36E-5$ ) and between IC13 (posterior DAN) and IC17 (somatomotor) ( $r = -.68$ ,  $p = 2.31E-4$ ). Strongest positive correlations

between components in the old group were found between IC13 (posterior DAN) and IC21 (left lateralized DAN) ( $r = .77$ ,  $p = 5.16E-5$ ), IC26 (brainstem) and IC27 (cerebellum) ( $r = .76$ ,  $p = 6.17E-5$ ) and between IC7 (DAN) and IC24 (angular gyrus) ( $r = .72$ ,  $p = 2.22E-4$ ). Strongest negative correlations between components in the old group were found between IC13 (posterior DAN) and IC23 (subcortical) ( $r = -.70$ ,  $p = 3.74E-4$ ), IC7 (DAN) and IC23 (subcortical) ( $r = -.63$ ,  $p = 2.30E-3$ ) and between IC8 (right frontoparietal) and IC18 (left inferior frontal) ( $r = -.63$ ,  $p = 2.30E-3$ ).

Figure 3E summarizes the age-related differences in correlations between the 28 independent components at nominal, FDR, and Bonferroni-corrected levels of significance for the L2 > L1 contrast, and Table 5 lists the edges with respective correlations coefficients within both groups and Fisher's *z*-scores comparing group differences. Using the more conservative Bonferroni correction, only one edge was significantly stronger in the older group, namely IC26 (brainstem)-IC27

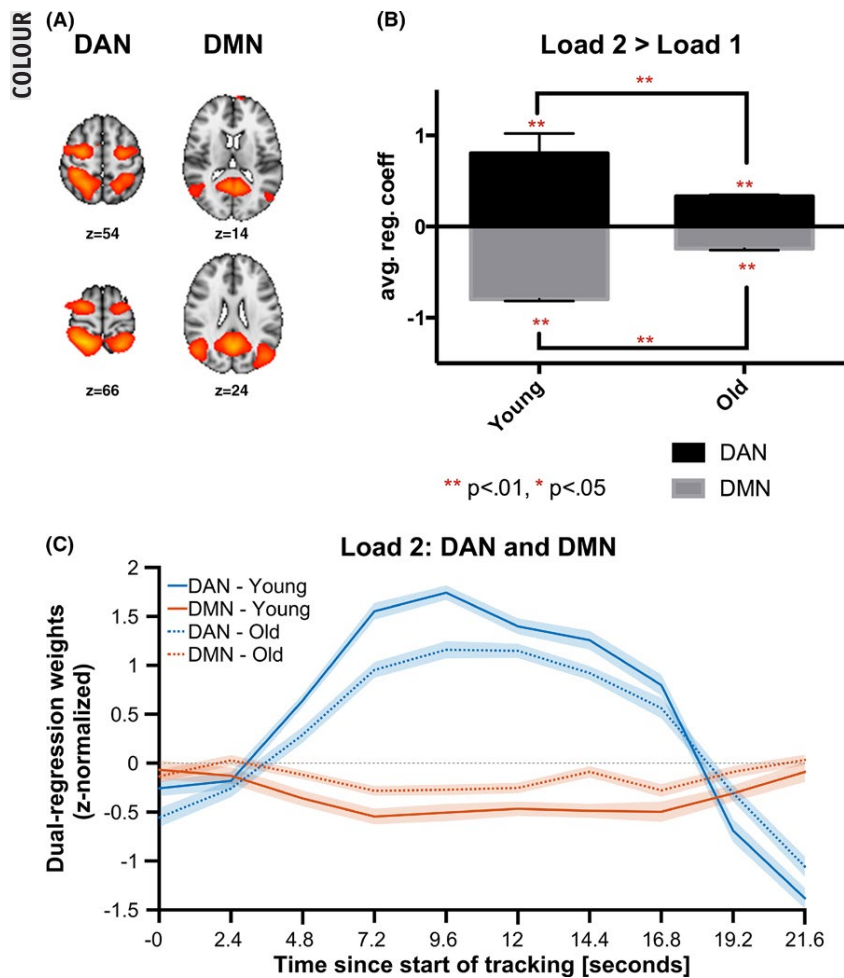


**FIGURE 3** ICA: (A) Spatial maps with selected components representing DAN (right) and DMN (left), (B) Average differences in beta estimates between L2 and L1 for the two networks, (C) Time series for DAN and DMN in both groups during L2

**TABLE 4** Beta coefficients reflecting the component time series model fit with the task design. Bold: Significantly ( $p < .05$ ) different from zero as indicated by one sample  $t$ -tests. Standard deviation is given in the parentheses

	Young		Old	
	L1	L2	L1	L2
DAN	<b>1.89</b> (0.44)	<b>2.70</b> (0.77)	<b>1.47</b> (0.45)	<b>1.80</b> (0.51)
DMN	0.15 (0.45)	<b>-0.65</b> (0.50)	-0.12 (0.51)	<b>-0.36</b> (0.33)

(cerebellum), and no edges were stronger in the younger group. Briefly, using FDR correction, stronger correlations were found between two DAN components (IC13-IC22) showing increased load-dependent activations (task positive) and within task-negative DMN components (IC5-IC16), in the young group. Stronger correlations were found between IC7 (DAN) and IC1 (posterior DMN), as well as between IC7 (DAN) and somatomotor IC17 (somatomotor), in the older group. Edges IC15 (visual)-IC18 (left inferior frontal) and IC22 (lateral occipital)-IC27 (cerebellum) were at a nominal significance level ( $p < .05$ , uncorrected) positively correlated in the young group and negatively correlated in the old group. The edge IC1 (posterior DMN)-IC7 (DAN) was

negatively correlated in the young group, but positively correlated in the old group.

### 3.3.1 | Associations with task performance

Two components corresponding to the DAN and the DMN showed significant load by group interaction effects. Based on these effects and a wealth of literature implicating these two networks as imperative to visual attention performance, the beta coefficients for the DAN and DMN were tested for correlations with task performance as indexed by the average percentage of correct responses for the two groups, respectively.

ANCOVAs assessing the relationship between the estimated betas (L2 and L2-L1) for DAN and DMN, and MOT tracking accuracy revealed for DAN L2, no main effect of group [ $F(1,40) = .15$ ,  $p = .700$ , partial  $\eta^2 = .004$ ], or DAN L2 activation [ $F(1,40) = 2.20$ ,  $p = .146$ , partial  $\eta^2 = .052$ ], and no interaction between group and DAN L2 activation [ $F(1,40) = .48$ ,  $p = .492$ , partial  $\eta^2 = .012$ ]. For DMN L2, there was a main effect of group [ $F(1,40) = 4.48$ ,  $p = .038$ , partial  $\eta^2 = .103$ ], but no main effect of DMN L2 [ $F(1,40) = .30$ ,  $p = .585$ , partial  $\eta^2 = .008$ ], and no interaction effect [ $F(1,40) = .32$ ,  $p = .572$ , partial  $\eta^2 = .008$ ]. No significant relationship was revealed between MOT tracking accuracy and the relative difference in load-dependent activations for either network (DAN and DMN L2-L1).

**TABLE 5** The 13 edges that showed FDR-corrected significant differences in correlations between the young and the old group for the L2 > L1 contrast, corresponding to Figure 2, panel E, above the diagonal. Columns to the left show the correlation coefficients and corresponding *p*-values within the young and the old group, respectively. The two rightmost columns give the Fisher's *r*-to-*z* values between the two groups' correlations coefficients with corresponding *p*-values. Bold indicates nominally significant component correlation within the groups

Edge	Young, <i>r</i>	Young, <i>p</i>	Old, <i>r</i>	Old, <i>p</i>	Fisher's <i>Z</i>	<i>p</i>
IC1-IC7	-.49	<b>0.01</b>	.50	<b>0.02</b>	-3.41	6.43E-4
IC7-IC17	-.87	<b>3.38E-3</b>	-.11	0.65	-3.79	1.50E-4
IC13-IC22	.79	<b>4.35E-6</b>	.16	0.49	2.84	4.51E-3
IC5-IC16	.35	0.09	-.48	<b>0.03</b>	2.78	5.40E-3
IC9-IC17	.36	0.09	-.59	<b>4.99E-3</b>	3.26	1.11E-3
IC23-IC26	.52	<b>8.88E-3</b>	-.36	0.11	2.96	3.05E-3
IC11-IC18	-.33	0.11	.58	<b>6.04E-3</b>	-3.12	1.79E-3
IC8-IC18	.18	0.40	-.62	<b>2.55E-3</b>	2.84	4.47E-3
IC15-IC18	.59	<b>2.57E-3</b>	-.77	<b>3.87E-5</b>	5.30	1.15E-7
I22-IC27	.56	<b>4.14E-3</b>	-.45	<b>0.04</b>	3.49	4.84E-4
IC26-IC27	-.24	0.26	.76	<b>6.17E-5</b>	-3.88	1.06E-4

### 3.3.2 | Motion correction

The dataset yielded significantly more in-scanner motion in the old group [(*df*)*t* = -3.9, *p* < .0001], and FIX removed a significantly higher number of components from the older group, *t*(19) = -2.2, *p* < .05, and also removed more of the variance from the raw fMRI data, both in terms of absolute and relative variance, both *t*(19) = -2.8, *p* < .05), which were significantly correlated with amount of subject motion across groups (*r* = .52, *p* < .0001).

In order to rule out that any group differences were induced by the cleaning procedure, we estimated load responses on the uncleaned dataset. The effects reported remained largely unchanged.

## 4 | DISCUSSION

Aging is associated with a manifold of changes in the brain structure and function resulting in altered behavioral performance and decline in cognitive faculties. Using a combination of fMRI-based voxel and multivariate analyses across a range of large-scale brain networks obtained during multiple object tracking, we have demonstrated age-related differences in tracking performance and associated brain network recruitment, in particular related to task-related activation and deactivations of the DAN and DMN, respectively. Compared to the young participants, the older subjects showed reduced tracking accuracy. Voxel and brain network-level fMRI analyses converged on decreased load-dependent activation of the DAN, and decreased load-related deactivations of the DMN during tracking in the old group, suggesting differential age-related alterations in task-positive and task-negative brain networks. Investigating the age- and load-dependent effects in all of the 28 components generated from the group ICA, we found a significant group by load interaction in two components representing the DAN and the DMN, respectively. This suggests that these two brain networks are engaged during the MOT task as well as sensitive to aging effects.

Furthermore, we have demonstrated significantly stronger correlations between the levels of activation in components within both the

DAN and the DMN for younger adults. Conversely, task-positive DAN and DMN components were positively correlated in older adults and negatively correlated in younger adults.

### 4.1 | Effects of task and age on task-positive networks

Studies investigating the brain network involvement in visual attention consistently report task-related activations in the DAN (Corbetta & Shulman, 2002; Kastner & Ungerleider, 2000). This frontoparietal network is hypothesized to be involved in the goal-directed (top-down), endogenous component of attentional processing as opposed to the exogenous, stimulus-driven (bottom-up) component (Shulman et al., 1997). Less consistent findings have been reported when studying the age-related effects on DAN activation; some studies have found a relative increase in activation for older adults, possibly reflecting functional compensation for inefficient bottom-up processing (Cabeza et al., 2004; Madden, 2007). However, a longitudinal study by Nyberg et al. (2010) reported age-related reduced activations in the same areas, complicating a straight-forward interpretation of the DAN in relation to neurocognitive aging.

With diverging literature in mind, we hypothesized an altered DAN response in older relative to younger adults without making strong predictions with regard to the specifics of these alterations. We observed strong DAN activation in both age groups when subjects were engaged in the task, and increasing load demand from one to two targets resulted in a further increased DAN activation. Group comparison revealed significantly stronger DAN activation for younger relative to older adults, and this activation pattern amplified with increasing task demand. Furthermore, the relative increase in DAN activation observed with increasing load demand was significantly greater for younger adults, possibly representing a greater capacity for DAN recruitment in response to increased attentional demand for younger adults. Thus, results obtained from this study support an age-related diminished activation pattern for the DAN along with less capability for load-dependent activation increase for older adults.

## 4.2 | Effects of task and age on task-negative networks

Mediating introspection and self-referential thought, the DMN represents an antagonistic function to that of the task-driven DAN. Also known as the task-negative network, the DMN is deactivated in response to tasks involving selective visual attention reflecting a reallocation of resources from monitoring of the self and the environment to external and goal-oriented behavior. Although the DMN is not task-negative *per se* in that the DMN is indeed engaged in active cognitive processes requiring internal focusing (Golland et al., 2007), the value in dichotomizing these two networks stems from studies where attention demanding tasks engage the DAN and passive fixation relative to task reliably engages the DMN (Raichle et al., 2001; Shulman et al., 1997). Our results are in line with the existing literature; we observed strong task-related DMN deactivations for both groups with diminished deactivations for the older relative to the younger group. Similar (although with opposite direction) to the activation pattern observed for the DAN—increasing task demand resulted in stronger DMN deactivations for both groups with the younger group having a significantly stronger load-dependent response compared to the older group.

These findings are in line with several previous observations (Grady et al., 2006; Persson et al., 2007), and suggest that reduced DMN modulation with increasing age can negatively affect attentional processing by increasing vulnerability to irrelevant distractions.

The ICA approach we employed in this study parsed the DMN into five components, the DMN component (IC 1) showing load and group interaction effects and that was included in the subsequent analyses, corresponded anatomically to the posterior DMN (precuneus and angular gyrus). Our findings fall in line with a number of studies in healthy aging and Alzheimer's disease, that have observed the posterior DMN to have an increased susceptibility to decreases in task-induced deactivations (Hafkemeijer, van der Grond, & Rombouts, 2012; Mevel, Chételat, Eustache, & Desgranges, 2011). The same areas are also particularly vulnerable to amyloid deposits (Sperling et al., 2009), a proposed cause of functional disruption and aberrant network activity, even in clinically healthy subjects (Sperling et al., 2010).

## 4.3 | Association between brain network activation

Based on the interlinked and dynamic relationship between various brain networks during the execution of cognitive tasks, in particular between the DAN and DMN, a critical aim of this study was to investigate the associations between the levels of activation of different brain networks and how their relationship is affected in aging. Importantly, if the level of task-related activation in one network (e.g., the DAN) is highly correlated with the level of activation in another network (e.g., the DMN), this may indicate that the activation levels of the two networks are reflecting partly overlapping mechanisms. We found no such significant association between two selected components representing the DAN and the DMN at the L1 or the L2 load conditions for either of the age groups, a finding that could suggest that the mechanisms of brain network level activation in cognitive aging,

for these two networks are relatively independent. However, this interpretation might be an oversimplification of the complex network dynamics underlying attentional processing. Considering the engagement of the DMN in goal-directed internally focused tasks such as autobiographical planning, recent studies (Di & Biswal, 2014; Spreng, Stevens, Chamberlain, Gilmore, & Schacter, 2010) have elucidated the confounding role of an anatomically interposed frontoparietal executive control network and its function in flexibly coupling with the DAN or DMN when engaged in external or internal oriented tasks, respectively. Further, investigating aging effects, Spreng and Schacter (2012) found for older compared to younger adults a relative inability to decouple the control network from the default network during a visuospatial task. The researchers attributed the failure of DMN deactivation not to intrinsic DMN dysfunction, but rather reduced network flexibility and range of dynamic network modulation in response to different task demands. The magnitude of load-dependent activations (L2-L1) in a range of components was significantly correlated across groups. In particular, we found strong positive correlations within task-positive components, between visual and task-positive components and within two DMN components, indicating that subjects with strong load-dependent increase in activation in one component also showed strong load-dependent activation in the other components and subjects with strong load-dependent decrease in activation in one component also showed load-dependent deactivation in another component. Similarly, we observed strong negative correlations between task-positive and task-negative components and between subcortical and task-positive components, indicating the opposite relationship. The level of co-activation across components pertains to the system-level coordination of brain networks during cognitive processing, and comparing the correlation between groups yields a window into the age-related differences in this brain network coordination. Interestingly, we identified significantly stronger correlations within DAN as well as within DMN components in the younger group and conversely, stronger correlations between DAN and DMN components in the older group, indicating a load-dependent response shifting from increased within-network specificity in younger adults to a more between-network dependence in older adults. Disrupted functional connectivity with advancing age has been proposed to reflect a reduction in specialization and segregation of brain systems (Chan et al., 2014). This brain dedifferentiation and reduction in diversity (Ferreira et al., 2015) may reduce the flexibility and dynamic repertoire of large-scale brain networks, which in turn contribute to age-related cognitive decline (Chou, Chen, & Madden, 2013). Along with the robust group effects on the load-dependent activation of the DMN and DAN, these results suggest altered coordination of brain networks during cognitive processing in aging.

## 4.4 | Associations between task performance and DAN and DMN activation

As expected, we observed a significant group difference in MOT performance accuracy between younger and older adults, as well as a significant effect of load, but no interactions.

Investigating the relationship between MOT accuracy and component beta estimates (DAN and DMN L2 and L2-L1), we found for DMN L2, a significant main effect of age group, but no significant effect of DMN deactivation and no interaction effect on performance accuracy. No significant associations were found for DMN L2-L1, DAN L2, or DAN L2-L1. The weak relationship between activation levels and performance accuracy could be due to the relatively low task demand. Investigating age differences in the MOT task, Sekuler, McLaughlin, and Yotsumoto (2008) demonstrated that younger adults were able to track up to four target objects simultaneously while older adults managed to track only three. Our implementation of the MOT task was limited to tracking a maximum of two target objects to ensure that participants of both groups were able to maintain task-focus throughout each trial. However, this restriction prevented participants from achieving maximal attentional load demand, allowing for ceiling effects and limited our capacity to make any strong inferences about how specific network properties relate to task performance at high load.

#### 4.5 | Limitations

This study does not come without limitations. Head movement is a ubiquitous concern in studies of network properties, and we found significantly more in-scanner motion in the old group. We used a sensitive approach for denoising of fMRI data by automated classification of ICA components on an individual level (FIX; Salimi-Khorshidi et al., 2014). Although there inevitably will be an effect of motion in any given fMRI experiment, using such a validated approach (Pruim et al., 2015) minimizes noise contamination. However, since the cleaning procedure removed more variance from the old participants, we estimated both DAN and DMN load-responses on the uncleaned datasets in order to rule out that any age differences was induced by the cleaning procedure. The effects reported remained largely unchanged.

Since we included healthy subject on both ends of the adult age spectrum, we do not have data covering a continuous age range. Therefore, our data cannot determine whether changes in network patterns follow a linear or nonlinear curve or if there is a critical age at which a cut-off point is reached and dramatic decline in attentional ability is observed. Full-scale IQ observed for both groups were above average. Considering that the sample was not drawn randomly from the population, but rather based on convenience—this was not an unexpected finding, yet it does influence generalizability. A study by Dixon et al. (2004) investigating episodic memory retrieval found a similar, gradual age-related decline in an advantaged convenience sample and a low-education population-based sample, suggesting that although population-based samples are more representative, the same pattern of age-related changes in higher cortical functions is retained in convenience samples.

As previously addressed, the restriction to two MOT load conditions was done to ensure that the participants indeed were engaged in the MOT task and that neuronal activity more accurately reflected attentional effort and not mind wandering due to loss of focus. For some of the participants, especially in the young group, the task demand might have been insufficient to elicit a strong network response, and we cannot exclude that including higher load conditions

would have revealed stronger group effects and possibly group by load interactions. However, using tracking accuracy as an index of attentional performance, this design proved sensitive to group and load effects validating its use within the scope of our investigation.

## 5 | CONCLUSION

Using MOT as means of measuring visual attention, our results further support a substantial amount of research reporting an age-related attentional decline. fMRI analysis including a range of large-scale brain networks revealed age-related alterations in network recruitment during mental tracking consisting of diminished activations of the DAN and diminished deactivations of the DMN in older relative to younger participants. Although these brain network level reductions may reflect a general signature of the aged brain, we did not observe any robust associations with task performance in the older group, possibly due to the relatively low task demands. Lastly, we identified several robust correlations in brain network activations, and also significant group differences in a subsample of these brain network activation correlations; we found stronger correlations within DMN and within DAN components for younger adults and stronger correlations between DAN and DMN components for older adults, indicating age-related alterations in the coordinated network-level activation during attentional processing. The correlation between DAN and DMN activation was low, suggesting that while some dependencies indeed exist between several of the estimated brain networks, the age-related alterations in DAN and DMN responses to attentional demands may reflect independent mechanisms.

## FUNDING INFORMATION

This work was funded by the Research Council of Norway (204966/F20), the South-Eastern Norway Regional Health Authority (2013054, 2014097, 2015073), and the Norwegian Extra Foundation for Health and Rehabilitation (2015/FO5146).

## CONFLICT OF INTERESTS

None declared.

## REFERENCES

- Alain, C., & Woods, D. L. (1999). Age-related changes in processing auditory stimuli during visual attention: Evidence for deficits in inhibitory control and sensory memory. *Psychology and Aging, 14*, 507.
- Alnæs, D., Kaufmann, T., Richard, G., Duff, E. P., Sneve, M. H., Endestad, T., ... Westlye, L. T. (2015). Attentional load modulates large-scale functional brain connectivity beyond the core attention networks. *NeuroImage, 109*, 260–272.
- Andersson, J. L., Jenkinson, M., & Smith, S. (2007a). *Non-linear optimisation. FMRIB technical report TR07JA1*. Oxford, UK: FMRIB Centre.
- Andersson, J. L., Jenkinson, M., & Smith, S. (2007b). *Non-linear registration, aka Spatial normalisation FMRIB technical report TR07JA2*. Oxford, UK: FMRIB Analysis Group of the University of Oxford.

- Andrews-Hanna, J. R., Snyder, A. Z., Vincent, J. L., Lustig, C., Head, D., Raichle, M. E., & Buckner, R. L. (2007). Disruption of large-scale brain systems in advanced aging. *Neuron*, *56*, 924–935.
- Baltes, P. B., & Lindenberger, U. (1997). Emergence of a powerful connection between sensory and cognitive functions across the adult life span: A new window to the study of cognitive aging? *Psychology and Aging*, *12*, 12.
- Bar, M. (2003). A cortical mechanism for triggering top-down facilitation in visual object recognition. *Journal of Cognitive Neuroscience*, *15*, 600–609.
- Beckmann, C. F., DeLuca, M., Devlin, J. T., & Smith, S. M. (2005). Investigations into resting-state connectivity using independent component analysis. *Philosophical Transactions of the Royal Society B: Biological Sciences*, *360*, 1001–1013.
- Beckmann, C. F., & Smith, S. M. (2004). Probabilistic independent component analysis for functional magnetic resonance imaging. *IEEE Transactions on Medical Imaging*, *23*, 137–152.
- Brainard, D. H. (1997). The psychophysics toolbox. *Spatial Vision*, *10*, 433–436.
- Cabeza, R., Anderson, N. D., Locantore, J. K., & McIntosh, A. R. (2002). Aging gracefully: Compensatory brain activity in high-performing older adults. *NeuroImage*, *17*, 1394–1402.
- Cabeza, R., Daselaar, S. M., Dolcos, F., Prince, S. E., Budde, M., & Nyberg, L. (2004). Task-independent and task-specific age effects on brain activity during working memory, visual attention and episodic retrieval. *Cerebral Cortex*, *14*, 364–375.
- Chan, M. Y., Park, D. C., Savalia, N. K., Petersen, S. E., & Wig, G. S. (2014). Decreased segregation of brain systems across the healthy adult lifespan. *Proceedings of the National Academy of Sciences of the United States of America*, *111*, E4997–E5006.
- Chou, Y.-H., Chen, N.-K., & Madden, D. J. (2013). Functional brain connectivity and cognition: Effects of adult age and task demands. *Neurobiology of Aging*, *34*, 1925–1934.
- Corbetta, M., Kincade, J. M., Ollinger, J. M., McAvoy, M. P., & Shulman, G. L. (2000). Voluntary orienting is dissociated from target detection in human posterior parietal cortex. *Nature Neuroscience*, *3*, 292–297.
- Corbetta, M., Patel, G., & Shulman, G. L. (2008). The reorienting system of the human brain: From environment to theory of mind. *Neuron*, *58*, 306–324.
- Corbetta, M., & Shulman, G. L. (2002). Control of goal-directed and stimulus-driven attention in the brain. *Nature Reviews Neuroscience*, *3*, 201–215.
- Culham, J. C., Brandt, S. A., Cavanagh, P., Kanwisher, N. G., Dale, A. M., & Tootell, R. B. (1998). Cortical fMRI activation produced by attentive tracking of moving targets. *Journal of Neurophysiology*, *80*, 2657–2670.
- Culham, J. C., Cavanagh, P., & Kanwisher, N. G. (2001). Attention response functions: Characterizing brain areas using fMRI activation during parametric variations of attentional load. *Neuron*, *32*, 737–745.
- Czigler, I., Csibra, G., & Ambró, Á. (1996). Aging, stimulus identification and the effect of probability: An event-related potential study. *Biological Psychology*, *43*, 27–40.
- Damoiseaux, J., Beckmann, C., Arigita, E. S., Barkhof, F., Scheltens, P., Stam, C., ... Rombouts, S. (2008). Reduced resting-state brain activity in the “default network” in normal aging. *Cerebral Cortex*, *18*, 1856–1864.
- Delis, D. C., Kaplan, E., & Kramer, J. H. (2001). *Delis-Kaplan executive function system (D-KEFS)*. San Antonio, TX: Psychological Corporation.
- Dennis, N. A., & Cabeza, R. (2008). Neuroimaging of healthy cognitive aging. *The Handbook of Aging and Cognition*, *3*, 1–54.
- Di, X., & Biswal, B. B. (2014). Modulatory interactions between the default mode network and task positive networks in resting-state. *PeerJ*, *2*, e367.
- Dixon, R. A., Wahlin, Å., Maitland, S. B., Hultsch, D. F., Hertzog, C., & Bäckman, L. (2004). Episodic memory change in late adulthood: Generalizability across samples and performance indices. *Memory & Cognition*, *32*, 768–778.
- Duncan, J. (2013). The structure of cognition: Attentional episodes in mind and brain. *Neuron*, *80*, 35–50.
- Eposito, F., Aragri, A., Pesaresi, I., Cirillo, S., Tedeschi, G., Marciano, E., ... Di Salle, F. (2008). Independent component model of the default-mode brain function: Combining individual-level and population-level analyses in resting-state fMRI. *Magnetic Resonance Imaging*, *26*, 905–913.
- Ferreira, L. K., Regina, A. C. B., Kovacevic, N., Martin, M. D. G. M., Santos, P. P., de Godoi Carneiro, C., ... Busatto, G. F. (2015). Aging effects on whole-brain functional connectivity in adults free of cognitive and psychiatric disorders. *Cerebral Cortex*, doi:10.1093/cercor/bhv190
- Filippini, N., MacIntosh, B. J., Hough, M. G., Goodwin, G. M., Frisoni, G. B., Smith, S. M., ... Mackay, C. E. (2009). Distinct patterns of brain activity in young carriers of the APOE-ε4 allele. *Proceedings of the National Academy of Sciences of the United States of America*, *106*, 7209–7214.
- Fischl, B., Salat, D. H., Busa, E., Albert, M., Dieterich, M., Haselgrove, C., ... Dale, A. M. (2002). Whole brain segmentation: Automated labeling of neuroanatomical structures in the human brain. *Neuron*, *33*, 341–355.
- Fox, M. D., Snyder, A. Z., Vincent, J. L., Corbetta, M., Van Essen, D. C., & Raichle, M. E. (2005). The human brain is intrinsically organized into dynamic, anticorrelated functional networks. *Proceedings of the National Academy of Sciences of the United States of America*, *102*, 9673–9678.
- Gazzaley, A., Cooney, J. W., Rissman, J., & D'Esposito, M. (2005). Top-down suppression deficit underlies working memory impairment in normal aging. *Nature Neuroscience*, *8*, 1298–1300.
- Gitelman, D. R., Nobre, A. C., Parrish, T. B., LaBar, K. S., Kim, Y.-H., Meyer, J. R., & Mesulam, M.-M. (1999). A large-scale distributed network for covert spatial attention: Further anatomical delineation based on stringent behavioural and cognitive controls. *Brain*, *122*, 1093–1106.
- Golland, Y., Bentin, S., Gelbard, H., Benjamini, Y., Heller, R., Nir, Y., ... Malach, R. (2007). Extrinsic and intrinsic systems in the posterior cortex of the human brain revealed during natural sensory stimulation. *Cerebral Cortex*, *17*, 766–777.
- Grady, C., Springer, M., Hongwanishkul, D., McIntosh, A., & Winocur, G. (2006). Age-related changes in brain activity across the adult lifespan. *Journal of Cognitive Neuroscience*, *18*, 227–241.
- Greve, D. N., & Fischl, B. (2009). Accurate and robust brain image alignment using boundary-based registration. *NeuroImage*, *48*, 63–72.
- Hafkemeijer, A., van der Grond, J., & Rombouts, S. A. (2012). Imaging the default mode network in aging and dementia. *Biochimica et Biophysica Acta (BBA)-Molecular Basis of Disease*, *1822*, 431–441.
- Howe, P. D., Horowitz, T. S., Morocz, I. A., Wolfe, J., & Livingstone, M. S. (2009). Using fMRI to distinguish components of the multiple object tracking task. *Journal of Vision*, *9*, 10.
- Hugdahl, K., Raichle, M. E., Mitra, A., & Specht, K. (2015). On the existence of a generalized non-specific task-dependent network. *Frontiers in Human Neuroscience*, *9*, 430.
- IBM\_Corp, R. (2010). *IBM SPSS statistics for windows*. IBM Corp, Armonk, NY.
- Iglewicz, B., & Hoaglin, D. C. (1993). *How to detect and handle outliers (Vol. 16)*. Milwaukee, WI: Asq Press.
- Jenkinson, M., & Smith, S. (2001). A global optimisation method for robust affine registration of brain images. *Medical Image Analysis*, *5*, 143–156.
- Jovicich, J., Peters, R., Koch, C., Braun, J., Chang, L., & Ernst, T. (2001). Brain areas specific for attentional load in a motion-tracking task. *Journal of Cognitive Neuroscience*, *13*, 1048–1058.
- Kastner, S., & Ungerleider, L. G. (2000). Mechanisms of visual attention in the human cortex. *Annual Review of Neuroscience*, *23*, 315–341.
- Li, H.-J., Hou, X.-H., Liu, H.-H., Yue, C.-L., Lu, G.-M., & Zuo, X.-N. (2015). Putting age-related task activation into large-scale brain networks: A meta-analysis of 114 fMRI studies on healthy aging. *Neuroscience & Biobehavioral Reviews*, *57*, 156–174.
- Lindenberger, U. (2014). Human cognitive aging: Corriger la fortune? *Science*, *346*, 572–578.
- Logan, J. M., Sanders, A. L., Snyder, A. Z., Morris, J. C., & Buckner, R. L. (2002). Under-recruitment and nonselective recruitment: Dissociable neural mechanisms associated with aging. *Neuron*, *33*, 827–840.
- Lustig, C., Snyder, A. Z., Bhakta, M., O'Brien, K. C., McAvoy, M., Raichle, M. E., ... Buckner, R. L. (2003). Functional deactivations: Change with age and dementia of the Alzheimer type. *Proceedings of the National Academy of Sciences of the United States of America*, *100*, 14504–14509.

- Madden, D. J. (2007). Aging and visual attention. *Current Directions in Psychological Science*, 16, 70–74.
- McDowd, J. M., & Shaw, R. J. (2000). Attention and aging: A functional perspective. In F. I. M. Craik & T. A. Salthouse (Eds.), *The Handbook of Aging and Cognition*, (pp. 221–292). Mahwah, NJ: Erlbaum.
- Mckiernan, K. A., Kaufman, J. N., Kucera-Thompson, J., & Binder, J. R. (2003). A parametric manipulation of factors affecting task-induced deactivation in functional neuroimaging. *Journal of Cognitive Neuroscience*, 15, 394–408.
- Mevel, K., Chételat, G., Eustache, F., & Desgranges, B. (2011). The default mode network in healthy aging and Alzheimer's disease. *International Journal of Alzheimer's Disease*, 2011, 535816–535825.
- Miller, S. L., Celone, K., DePeau, K., Diamond, E., Dickerson, B. C., Rentz, D., ... Sperling, R. A. (2008). Age-related memory impairment associated with loss of parietal deactivation but preserved hippocampal activation. *Proceedings of the National Academy of Sciences of the United States of America*, 105, 2181–2186.
- Mowinckel, A. M., Espeseth, T., & Westlye, L. T. (2012). Network-specific effects of age and in-scanner subject motion: A resting-state fMRI study of 238 healthy adults. *NeuroImage*, 63, 1364–1373.
- Nagel, I. E., Preuschhof, C., Li, S. C., Nyberg, L., Backman, L., Lindenberger, U., & Heekeren, H. R. (2009). Performance level modulates adult age differences in brain activation during spatial working memory. *Proceedings of the National Academy of Sciences of the United States of America*, 106, 22552–22557.
- Nyberg, L., Salami, A., Andersson, M., Eriksson, J., Kalpouzos, G., Kauppi, K., ... Nilsson, L.-G. (2010). Longitudinal evidence for diminished frontal cortex function in aging. *Proceedings of the National Academy of Sciences of the United States of America*, 107, 22682–22686.
- Parks, E. L., & Madden, D. J. (2013). Brain connectivity and visual attention. *Brain Connectivity*, 3, 317–338.
- Pelli, D. G. (1997). The VideoToolbox software for visual psychophysics: Transforming numbers into movies. *Spatial Vision*, 10, 437–442.
- Persson, J., Lustig, C., Nelson, J. K., & Reuter-Lorenz, P. A. (2007). Age differences in deactivation: A link to cognitive control? *Journal of Cognitive Neuroscience*, 19, 1021–1032.
- Pessoa, L., Kastner, S., & Ungerleider, L. G. (2003). Neuroimaging studies of attention: From modulation of sensory processing to top-down control. *The Journal of Neuroscience*, 23, 3990–3998.
- Pruim, R. H., Mennes, M., Buitelaar, J. K., & Beckmann, C. F. (2015). Evaluation of ICA-AROMA and alternative strategies for motion artifact removal in resting state fMRI. *NeuroImage*, 112, 278–287.
- Pylshyn, Z. W., & Storm, R. W. (1988). Tracking multiple independent targets: Evidence for a parallel tracking mechanism. *Spatial Vision*, 3, 179–197.
- Raichle, M. E., MacLeod, A. M., Snyder, A. Z., Powers, W. J., Gusnard, D. A., & Shulman, G. L. (2001). A default mode of brain function. *Proceedings of the National Academy of Sciences of the United States of America*, 98, 676–682.
- Reuter-Lorenz, P. A., & Lustig, C. (2005). Brain aging: Reorganizing discoveries about the aging mind. *Current Opinion in Neurobiology*, 15, 245–251.
- Reuter-Lorenz, P. A., & Park, D. C. (2010). Human neuroscience and the aging mind: A new look at old problems. *The Journals of Gerontology Series B: Psychological Sciences and Social Sciences*, 65, 405–415.
- Ruff, C. C., Bestmann, S., Blankenburg, F., Bjoertomt, O., Josephs, O., Weiskopf, N., ... Driver, J. (2008). Distinct causal influences of parietal versus frontal areas on human visual cortex: Evidence from concurrent TMS–fMRI. *Cerebral Cortex*, 18, 817–827.
- Salimi-Khorshidi, G., Douaud, G., Beckmann, C. F., Glasser, M. F., Griffanti, L., & Smith, S. M. (2014). Automatic denoising of functional MRI data: Combining independent component analysis and hierarchical fusion of classifiers. *NeuroImage*, 90, 449–468.
- Sekuler, R., McLaughlin, C., & Yotsumoto, Y. (2008). Age-related changes in attentional tracking of multiple moving objects. *Perception*, 37, 867–876.
- Shulman, G. L., Fiez, J. A., Corbetta, M., Buckner, R. L., Miezin, F. M., Raichle, M. E., & Petersen, S. E. (1997). Common blood flow changes across visual tasks: II. Decreases in cerebral cortex. *Journal of Cognitive Neuroscience*, 9, 648–663.
- Smith, S. M., Jenkinson, M., Woolrich, M. W., Beckmann, C. F., Behrens, T. E., Johansen-Berg, H., ... Flitney, D. E. (2004). Advances in functional and structural MR image analysis and implementation as FSL. *NeuroImage*, 23, S208–S219.
- Sperling, R. A., Dickerson, B. C., Pihlajamaki, M., Vannini, P., LaViolette, P. S., Vitolo, O. V., ... Selkoe, D. J. (2010). Functional alterations in memory networks in early Alzheimer's disease. *Neuromolecular Medicine*, 12, 27–43.
- Sperling, R. A., LaViolette, P. S., O'Keefe, K., O'Brien, J., Rentz, D. M., Pihlajamaki, M., ... Hedden, T. (2009). Amyloid deposition is associated with impaired default network function in older persons without dementia. *Neuron*, 63, 178–188.
- Spreng, R. N., Mar, R. A., & Kim, A. S. (2009). The common neural basis of autobiographical memory, prospection, navigation, theory of mind, and the default mode: A quantitative meta-analysis. *Journal of Cognitive Neuroscience*, 21, 489–510.
- Spreng, R. N., & Schacter, D. L. (2012). Default network modulation and large-scale network interactivity in healthy young and old adults. *Cerebral Cortex*, 22, 2610–2621.
- Spreng, R. N., Stevens, W. D., Chamberlain, J. P., Gilmore, A. W., & Schacter, D. L. (2010). Default network activity, coupled with the frontoparietal control network, supports goal-directed cognition. *NeuroImage*, 53, 303–317.
- Störmer, V. S., Li, S.-C., Heekeren, H. R., & Lindenberger, U. (2013). Normal aging delays and compromises early multifocal visual attention during object tracking. *Journal of Cognitive Neuroscience*, 25, 188–202.
- Szczepanski, S. M., Pinsk, M. A., Douglas, M. M., Kastner, S., & Saalmann, Y. B. (2013). Functional and structural architecture of the human dorsal frontoparietal attention network. *Proceedings of the National Academy of Sciences of the United States of America*, 110, 15806–15811.
- Tomasi, D., Wang, R., Wang, G.-J., & Volkow, N. D. (2014). Functional connectivity and brain activation: A synergistic approach. *Cerebral Cortex*, 24, 2619–2629.
- Toro, R., Fox, P. T., & Paus, T. (2008). Functional coactivation map of the human brain. *Cerebral Cortex*, 18, 2553–2559.
- Trick, L. M., Perl, T., & Sethi, N. (2005). Age-related differences in multiple-object tracking. *The Journals of Gerontology Series B: Psychological Sciences and Social Sciences*, 60, P102–P105.
- Uddin, L. Q., Clare Kelly, A., Biswal, B. B., Xavier Castellanos, F., & Milham, M. P. (2009). Functional connectivity of default mode network components: Correlation, anticorrelation, and causality. *Human Brain Mapping*, 30, 625–637.
- Wechsler, D. (1999). *The Wechsler Abbreviated Scale of Intelligence (WASI)*. USA, San Antonio, TX: Psychological Corporation.
- Wojciulik, E., & Kanwisher, N. (1999). The generality of parietal involvement in visual attention. *Neuron*, 23, 747–764.

## SUPPORTING INFORMATION

Additional Supporting Information may be found online in the supporting information tab for this article.

**How to cite this article:** Dørum, E. S., Alnæs, D., Kaufmann, T., Richard, G., Lund, M. J., Tønnesen, S., Sneve, M. H., Mathiesen, N. C., Rustan, Ø. G., Gjertsen, Ø., Vatn, S., Fure, B., Andreassen, O. A., Nordvik, J. E., and Westlye, L. T. (2016). Age-related differences in brain network activation and co-activation during multiple object tracking. *Brain and Behavior*, 6: 1–15. e00533, doi: 10.1002/brb3.533



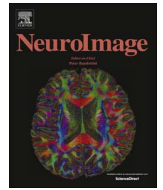






Contents lists available at ScienceDirect

NeuroImage

journal homepage: [www.elsevier.com/locate/neuroimage](http://www.elsevier.com/locate/neuroimage)

## Increased sensitivity to age-related differences in brain functional connectivity during continuous multiple object tracking compared to resting-state

Erlend S. Dørum<sup>a,b,c</sup>, Tobias Kaufmann<sup>b</sup>, Dag Alnæs<sup>b</sup>, Ole A. Andreassen<sup>b</sup>,  
Geneviève Richard<sup>a,b,c</sup>, Knut K. Kolskår<sup>a,b,c</sup>, Jan Egil Nordvik<sup>a</sup>, Lars T. Westlye<sup>b,c,\*,1</sup>

<sup>a</sup> Sunnaas Rehabilitation Hospital HT, Nesodden, Norway

<sup>b</sup> NORMENT, KG Jebsen Centre for Psychosis Research, Division of Mental Health and Addiction, Oslo University Hospital & Institute of Clinical Medicine, University of Oslo, Norway

<sup>c</sup> Department of Psychology, University of Oslo, Norway

### ARTICLE INFO

#### Keywords:

fMRI  
Aging  
Brain network connectivity  
Machine learning  
SDSA

### ABSTRACT

Age-related differences in cognitive agility vary greatly between individuals and cognitive functions. This heterogeneity is partly mirrored in individual differences in brain network connectivity as revealed using resting-state functional magnetic resonance imaging (fMRI), suggesting potential imaging biomarkers for age-related cognitive decline. However, although convenient in its simplicity, the resting state is essentially an unconstrained paradigm with minimal experimental control. Here, based on the conception that the magnitude and characteristics of age-related differences in brain connectivity is dependent on cognitive context and effort, we tested the hypothesis that experimentally increasing cognitive load boosts the sensitivity to age and changes the discriminative network configurations. To this end, we obtained fMRI data from younger ( $n=25$ , mean age  $24.16 \pm 5.11$ ) and older ( $n=22$ , mean age  $65.09 \pm 7.53$ ) healthy adults during rest and two load levels of continuous multiple object tracking (MOT). Brain network nodes and their time-series were estimated using independent component analysis (ICA) and dual regression, and the edges in the brain networks were defined as the regularized partial temporal correlations between each of the node pairs at the individual level. Using machine learning based on a cross-validated regularized linear discriminant analysis (rLDA) we attempted to classify groups and cognitive load from the full set of edge-wise functional connectivity indices.

While group classification using resting-state data was highly above chance (approx. 70% accuracy), functional connectivity (FC) obtained during MOT strongly increased classification performance, with 82% accuracy for the young and 95% accuracy for the old group at the highest load level. Further, machine learning revealed stronger differentiation between rest and task in young compared to older individuals, supporting the notion of network dedifferentiation in cognitive aging. Task-modulation in edgewise FC was primarily observed between attention- and sensorimotor networks; with decreased negative correlations between attention- and default mode networks in older adults. These results demonstrate that the magnitude and configuration of age-related differences in brain functional connectivity are partly dependent on cognitive context and load, which emphasizes the importance of assessing brain connectivity differences across a range of cognitive contexts beyond the resting-state.

### Introduction

Individual life-span trajectories in brain and cognition are shaped by a dynamic interplay between genetic and environmental factors (Lindenberger, 2014). Aging confers a notable increase in

inter-individual variability in cognitive functions (Buckner, 2004; Singh-Manoux et al., 2012), and developing sensitive and specific *in vivo* biomarkers for identification of individuals at risk for cognitive impairment and dementia is a key challenge for clinical neuroscience.

\* Corresponding author at: NORMENT, KG Jebsen Centre for Psychosis Research, Division of Mental Health and Addiction, Oslo University Hospital & Institute of Clinical Medicine, University of Oslo, Norway.

E-mail address: [l.t.westlye@psykologi.uio.no](mailto:l.t.westlye@psykologi.uio.no) (L.T. Westlye).

<sup>1</sup> postal address: Oslo University Hospital, PoBox 4956 Nydalen, 0424 OSLO, Norway.

The brain is intrinsically organized into neuronal networks or nodes of which continuous cross-talk enables cognition and complex behaviors (Sporns et al., 2004). Functional connectivity (FC) measured by functional magnetic resonance imaging (fMRI) refers to the synchronization between nodes, reflecting an organizational principle of the brain (Van Den Heuvel and Pol, 2010). In line with this system-level view of brain function, aging studies converge on less specialized and segregated brain networks, supporting the theory of cognitive and neuronal dedifferentiation in aging (Baltes and Lindenberger, 1997; Chan et al., 2014; Daselaar et al., 2005; Lindenberger, 2014; Park et al., 2012).

Age-related FC differences have been extensively studied, implicating a range of networks including the executive control (ECN), dorsal attention (DAN), default mode (DMN), frontoparietal (FPN) and hippocampal networks (Salami et al., 2014; Voss et al., 2010; Zhang et al., 2014), and links between DMN connectivity and cognitive aging (Andrews-Hanna et al., 2007; Sambataro et al., 2010) corroborate the notion of network-level vulnerability to advancing age (Mowinckel et al., 2012; Salami et al., 2012).

In line with the selective vulnerability of brain networks, age-related cognitive decline is not uniform across domains (Glisky, 2007). Whereas crystallized functions including vocabulary and general knowledge remain relatively unaffected, a commonly reported impairment relates to deficient selective attention (Quigley and Müller, 2014) which manifests as reduced ability to selectively attend to and ignore information based on relevance (Kensinger and Corkin, 2009; Murray and Kensinger, 2012). Whereas resting-state fMRI has provided an opportunity to test specific hypotheses regarding the underlying brain connectivity alterations, the selective cognitive vulnerability suggests that attention-demanding tasks may comprise a more sensitive and informative context for the study of age-related brain network alterations. Thus, in order to characterize the brain functional connectomic signature of cognitive aging in different cognitive contexts, we compare fMRI brain connectivity indices obtained during rest and during two load levels of a continuous multiple object tracking (MOT) task (Pylyshyn and Storm, 1988) between young and older healthy adults.

MOT requires the subject to attend to multiple target items as they move among distractor items, which is a basic feature of sustained multifocal visual attention (Cavanagh and Alvarez, 2005). Alnæs et al. (2015) reported widespread connectivity modulations during MOT in young adults, and machine learning revealed high classification accuracy when discriminating between task and rest, demonstrating successful decoding of cognitive load using FC features. Here, we utilize a similar decoding approach to describe the neuronal characteristics of cognitive aging by comparing two groups of healthy adults at both ends of the adult lifespan. We hypothesized that (1) multivariate classification would yield robust discrimination between resting state and data collected during MOT as well as between younger and older adults, reflecting age and cognitive context related changes in brain network configuration. Higher task classification accuracy in young compared to older adults would support the notion of cognitive and neuronal dedifferentiation in aging. Additionally, we anticipated stronger group differences with higher load, resulting in improved group classification with increasing load. On edge-level, we hypothesized (2) that the most discriminative edges for rest and task are found in connections between attention networks and somatosensory and motor nodes (Alnæs et al., 2015; Tomasi et al., 2014). With regards to age-related edgewise effects in response to attentional demand and keeping with the theory of dedifferentiation, we hypothesized a system-level loss in network segregation, reflected in decreased FC within modular networks and in particular within the DMN as well as increased connectivity between large-scale brain networks, in particular during continuous tracking, which would support a relative inability to selectively inhibit competing neural processes during task engagement.

Finally, since any effects on edgewise functional connectivity may be partly driven by nodal increases or decreases in activity, we probe temporal variability on node level by computing the standard deviation

of signal amplitude (SDSA) (Garrett et al., 2010). Brain signal variability has been shown to reveal distinct patterns not captured by mean-based analyses (Garrett et al., 2011), and increased signal variability is thought to be indicative of a more sophisticated and complex neural machinery (McIntosh et al., 2008), offering greater dynamic range and facilitating the brain's ability to explore different network states. When applied to aging studies, reduced SDSA has proved to be a better predictor of advancing age and poorer task performance than the mean measure (Grady and Garrett, 2014). Additionally, in a study investigating age-related variability changes in response to cognitive demand, Garrett et al. (2012) observed a broad increase in SDSA on task compared to fixation for both age groups, the magnitude and spatial extent of this variability increase was comparatively reduced for the older group. Based on this, we hypothesize (3) task related modulations of signal variability that is network selective, reflected in increased and decreased SDSA in task-positive and task-negative/irrelevant networks, respectively. Further, reflecting reduced dynamic repertoire in response to cognitive state-transition, we anticipate group differences in signal variability manifested as diminished task-related SDSA changes for older compared to younger adults.

## Materials and methods

### Sample

We recruited 26 young and 26 older adults through a newspaper ad and social media. The sample is overlapping with a previous publication (Dorum et al., 2016) reporting results from the blocked MOT runs (see below). All subjects provided an informed consent and underwent neuropsychological screening (details below). Participants reported normal or corrected-to-normal vision. Exclusion criteria included estimated IQ < 70, previous history of alcohol- and substance abuse, history of neurologic or psychiatric disease, medications significantly affecting the nervous system and counter indications for MRI. All participants were self-sufficient and living independently, and reported no reason to suspect marked cognitive decline or undiagnosed dementia.

From the full dataset, we excluded participants due to excess in-scanner motion where image artifacts persisted after running FSL FIX (FMRIB's ICA-based Xnoiseifier) (n=2), as well as due to chance-level or below-chance level performance on the one load condition MOT task (n=3), yielding a final sample of 47 subjects, including 25 young (mean age: 24.2 years, SD: 5.1, 68% females) and 22 old individuals (mean age: 65.1, SD: 7.5, 55% females).

### Screening and neuropsychological assessment

Participants completed the matrices and vocabulary subtests from the Wechsler Abbreviated Scale of Intelligence (WASI) (Wechsler, 1999). Results from the subtests were converted to standardized scores from which full scale IQ (FSIQ) was estimated. Two subjects were native foreign language speakers and thus not adequately able to perform the vocabulary subtest, and their FSIQ was calculated based on matrix reasoning.

### fMRI paradigms

All participants underwent one resting state run and two versions of MOT, including one blocked and two continuous tracking runs, performed in the MRI scanner during the same session (Alnæs et al., 2015). Here we report data from the continuous MOT runs (Supplementary material). The level of attentional demand was set at two load conditions – load 1 (L1) and load 2 (L2) requiring the participants to track one or two targets respectively during the task. We restricted the load level to a maximum of 2 to ensure that both groups were able to perform at a high level.

Participants were looking through a mirror mounted on the head coil at a calibrated MR-compatible LCD screen (NNL LCD Monitor®, NordicNeuroLab, Bergen, Norway) placed in front of the scanner bore, with a screen resolution of 1920×1080 at 60 Hz. All stimuli were generated using MATLAB and the Psychophysics Toolbox extensions (Brainard, 1997; Pelli, 1997). Participants responded to the tasks using a MR-compatible subject response collection system (ResponseGrip®, NordicNeuroLab, Bergen, Norway). A trigger pulse from the scanner synchronized the onset of the experiment to the beginning of the acquisition of an fMRI volume. The screen covered 32.43° of visual angle, and the tracking area covered 17.32° of visual angle at a viewing distance of 1.2 m. The objects were circular disks with a diameter of 0.7° of visual angle moving at a speed of 4°/s. Objects changed direction when closer than 1° to another object or the edge of the tracking area, and also made random changes (one random turn per second on average) to make object movements unpredictable. Colors used for the objects were isoluminant (as measured using Spyder 4, Datacolor, Lawrenceville, NJ). A fixation circle of 0.5° of visual angle was located in the center of the tracking area. The participant's task consisted of covertly tracking target objects while fixating on the central fixation point. Detailed instructions were given before entering the scanner room as well as before each sequence.

Each participant performed two runs of continuous MOT task, one with tracking load of 1 object, and the other with 2 objects. Each continuous tracking block lasted 7.5 min and contained 14 trials. The continuous tracking versions started with 1.5 s instruction, followed by 0.5 s fixation. After that, 10 identical blue objects were presented on a grey background screen, and after another 0.5 s the objects started moving. The first cued object(s), or target(s), turned red after the first 0.5 s, and remained red for a duration of 2.5 s. The tracking period lasted on average 32 s (range, 27–37) after which the participants were instructed to respond to a probe (green object), “yes” or “no” to whether the green probe was one of the objects originally designated as a target, before a new target assignment took place. The colors of the distractor (blue), cued (red) and probe (green) objects, were set for the whole task. The duration of the target and the probe presentation was 2.5 s. The participants were instructed to fixate on the centrally presented fixation point during the length of the run. Accuracy and reaction times were recorded.

#### MRI acquisition

MRI scans were obtained from a General Electric (Signa HDxt) 3.0 T scanner with an 8-channel head coil at Oslo University Hospital. Functional data were acquired with a T2\*-weighted 2D gradient echo planar imaging sequence (EPI) with 140 volumes (TR: 2400 ms; TE: 30 ms; FA: 90°; voxel size: 3.75×3.75×3.2 mm; slices: 48; FOV: 240×240 mm; duration: 533 s). The first five volumes were discarded. In addition, a structural scan was acquired using a sagittal T1-weighted fast spoiled gradient echo (FSPGR) sequence (TR: 7.8 s; TE: 2.956 ms; TI: 450 ms; FA: 12°; voxel size: 1.0×1.0×1.2 mm; slices: 170; FOV: 256 mm<sup>2</sup>; duration: 428 s).

#### fMRI processing and network estimation

fMRI data was processed on single-subject level using the FMRI Expert Analysis Tool (FEAT) from the FMRIB Software Library (FSL) (Smith et al., 2004) including motion correction (MCFLIRT), high-pass filtering (sigma=64 s), spatial smoothing (FWHM=6 mm), and single-session independent component analysis (ICA) using MELODIC (Beckmann and Smith, 2004).

We calculated in-scanner subject motion defined as the average root mean square of the displacement from one frame to its previous frame for each dataset. Repeated measures ANOVA revealed no significant effect of run (resting state, C1 and C2) ( $F=2.23$ ,  $p=.113$ ) or group ( $F=1.91$ ,  $p=.17$ ) on motion, but a significant condition by group

interaction effect ( $F=6.81$ ,  $p=.002$ ). Independent samples t-tests revealed no significant group differences in motion during rest [ $\text{mean}(\text{SD})_{\text{young}}=.084$  (.098),  $\text{mean}(\text{SD})_{\text{old}}=.072$  (.034),  $t=-.533$ ,  $p>.596$ ]; but the old group showed significantly more motion during L1 [ $\text{mean}(\text{SD})_{\text{old}}=.126$  (.099),  $\text{mean}(\text{SD})_{\text{young}}=.072$  (.068),  $t=2.20$ ,  $p=.033$ ]; and during L2 ( $\text{mean}(\text{SD})_{\text{old}}=.104$  (.066),  $\text{mean}(\text{SD})_{\text{young}}=.069$  (.055),  $t=2.02$ ,  $p<.049$ ).

We used FSL FIX (FMRIB's ICA-based Xnoiseifier) (Salimi-Khorshidi et al., 2014) to identify and remove noise components (standard training set, threshold: 20), which has been shown superior to other conventional methods for denoising fMRI data (Pruim et al., 2015), and regressed out the estimated motion parameters from MCFLIRT from the voxel-wise time series.

We used FreeSurfer (Fischl et al., 2002) for automated brain segmentation of the T1-weighted data to obtain brain masks used for co-registration using FLIRT (Jenkinson and Smith, 2001), optimized using boundary-based registration (BBR) (Greve and Fischl, 2009) and FNIRT (Andersson et al., 2007a, b).

Next, we used a group-PCA approach (Smith et al., 2014) in MELODIC with an automated estimation of model order ( $n=55$ ). We discarded noise components based on the spatial distribution of the component maps and/or the frequency spectrum of the components' time series (Kelly et al., 2010), resulting in a final set of 32 components. Thereafter, for each subject we estimated individual time series and component spatial maps using dual regression (Filippini et al., 2009) for the full set of components. Finally, we regressed out the time-series of noise components from the time-series of the remaining components and estimated functional connectivity matrices using FSLNets (Smith et al., 2011b). To ensure reliable network estimation, we computed regularized partial correlations of the time series, with an automated estimation of lambda on the individual level (Ledoit and Wolf, 2003; Schäfer and Strimmer 2005). Such data-driven, automatic lambda optimization on the single subject level yields well-conditioned networks that do not depend on a preselected, global lambda value (Brier et al., 2015; Deligianni et al., 2014; Kaufmann et al., 2016). Components were hierarchically clustered based on the Euclidean distance metrics using the ward linkage function in Matlab (The Mathworks Inc.), as implemented in FSLNets (Smith et al., 2011a). Ward's linkage uses the incremental sum of squares; that is, the increase in the total within-cluster sum of squares as a result of joining two clusters. The within-cluster sum of squares is defined as the sum of the squares of the distances between all objects in the cluster and the centroid of the cluster. The sum of squares measure is equivalent to the distance between the cluster's centroids. The linkage procedure maximizes the distance between centroids while minimizing the within-sum of squares for each cluster. For each dataset we also computed the SDSA of each component's time series as a measure of nodal strength (Garrett et al., 2010; Kaufmann et al., 2015).

#### Multivariate classification of condition and group

The regularized partial correlation based networks each comprised 32 nodes yielding 496 unique edges. We used these edges in several classification tasks using a regularized linear discriminant analysis classifier (shrinkage LDA) (Friedman, 1989; Schäfer and Strimmer, 2005). We classified between (1) young and old individuals within resting state and load conditions and between (2) resting state and load conditions within and across groups utilizing leave-one-out (LOO) cross validation procedures, and assessed reliability across 10,000 permutations, in line with a previous publication (Alnæs et al., 2015).

#### Univariate statistical analysis

Non-imaging data were analyzed in SPSS (IBM Corp R, 2010). Between-group differences were assessed using Chi square tests (sex distribution) and linear models (age, neuropsychological performance,

MOT task performance). Group differences in MOT performance were assessed using two-by-two repeated measures ANOVA with load (L1 and L2) as within subject factor and group (young and old) as between subject factor.

For each edge in the connectivity matrix, we performed repeated measures ANOVA to test for effects of group while accounting for sex. We computed edgewise partial eta-squared effect sizes, and adjusted the alpha level using false discovery rate (FDR) for each test separately with a false discovery rate level  $q=0.05$  and a threshold based on the assumption of independence or positive dependence (Nichols, 2009; Nichols and Hayasaka, 2003).

Whereas the main analysis is targeting the connections between the nodes, the cumulative involvement of each of the nodes is also of interest. To assess the importance of each network node in distinguishing between groups and conditions, we calculated nodewise eigenvector centrality (EC) (Bonacich, 2007) based on edgewise effect sizes, in line with a previous publication (Skåtun et al., in press). A high EC indicates altered connectivity with several other nodes, indicating a relative importance of this node in discriminating between groups or load condition. Finally, for each dataset we computed the standard deviation of signal amplitude (SDSA) for each component's time series, as a measure of nodal activity. Group differences in SDSA were tested using ANCOVAs, covarying for sex.

## Results

### Neuropsychology and demographics

Table 1 summarizes key demographics and WASI and MOT performance. Briefly, the younger group performed significantly better on the matrix reasoning subtest of the WASI. Repeated measures ANOVA revealed significant main effects of load ( $F=17.58$ ,  $p < .001$ ) and group ( $F=4.11$ ,  $p=.049$ ) on MOT accuracy, indicating higher accuracy during L1 compared to L2 and for young compared to old, but no group by load interaction ( $F=.35$ ,  $p=.56$ ). No other significant differences were found.

### Classification analysis

Fig. 1 shows the confusion matrices from all classification analyses. The algorithm distinguished resting state from both load conditions with high accuracy (mean classification accuracy across groups:  $M=93.62\%$ ,  $p_{\text{perm}} < 0.0001$ ). Classification of load conditions (L1 vs L2) yielded higher accuracy in the young group (L1 and L2: both 72%,  $p_{\text{perm}} < 0.0001$ ) than the older group (L1: 59.09%,  $p_{\text{perm}}=0.003$ , L2: 54.55%,  $p_{\text{perm}}=0.011$ ).

We further trained the classifier to distinguish old from young individuals based on data from resting state or each of the two load conditions separately. Using resting state data, we achieved 72% classification accuracy for identifying the young group ( $p_{\text{perm}}=0.025$ ) and 68.18% accuracy for identifying the old group ( $p_{\text{perm}}=0.0035$ ).

**Table 1**  
Demographics and neuropsychological performance.

	Young (SD)	Old (SD)	$\chi^2$ /t-score	p
N	25	22		
Age	24.16 (5.11)	65.09 (7.53)		
Age range	18–43	47–78		
Percent male	32.00	45.45	$\chi^2=0.90$	.34
Percent right handedness	92.00	86.36	$\chi^2=0.39$	.53
Years of education	15.43 (1.47)	15.07 (2.99)	$t=0.51$	.613
WASI matrix reasoning	30.32 (2.79)	25.64 (6.38)	$t=3.18$	<b>.004</b>
WASI vocabulary	65.80 (5.97)	66.27 (10.16)	$t=-0.20$	.845
Full scale IQ-2	119.60 (9.25)	120.18 (17.06)	$t=-0.14$	.888
MOT accuracy on L1	90.00 (13.54)	82.27 (16.88)	$t=1.74$	.089
MOT accuracy on L2	80.40 (18.81)	69.55 (22.57)	$t=1.80$	.079

Accuracy when using L1 was 80.77% and 80.95% for the young and old group, respectively (both  $p_{\text{perm}}=0.0001$ ). Accuracy using L2 was 82.76% ( $p_{\text{perm}} < 0.0001$ ) for the young and 94.44% ( $p_{\text{perm}}=0.0001$ ) for the old group.

### Edgewise univariate analysis

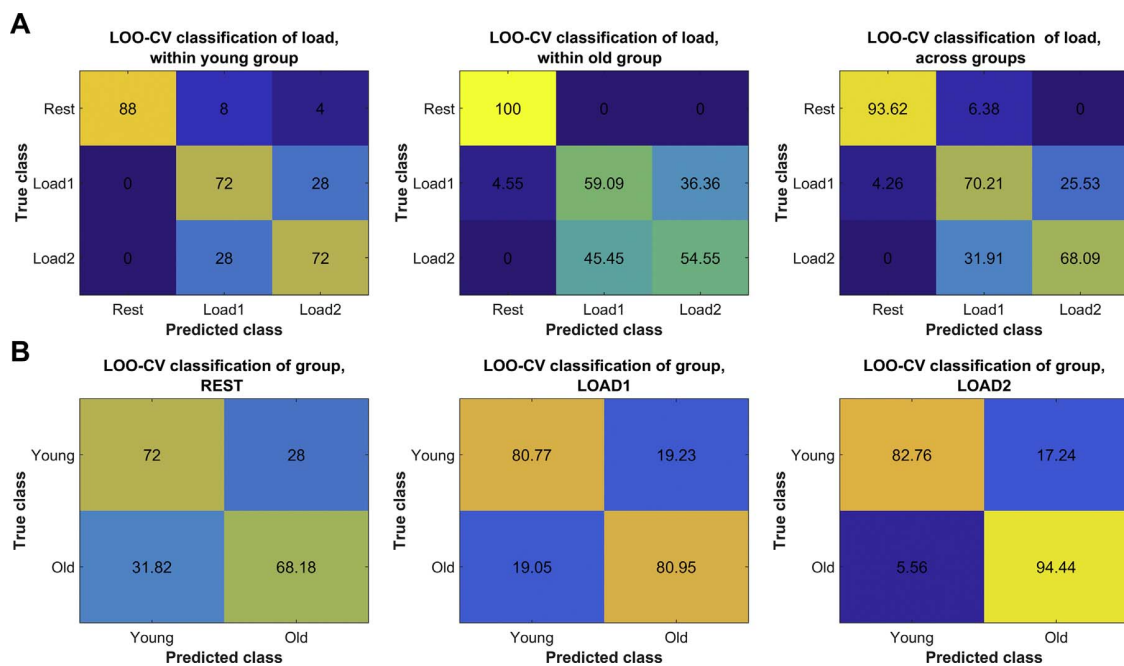
Fig. 2A shows the results from the edgewise repeated measures ANOVAs. Briefly, we identified 41 edges showing significant effects of load, 25 edges showing significant effects of group and 1 edge showing a significant interaction effect (all  $p < .05$ , FDR corrected).

The node with most edges showing effect of condition was the DAN (IC4), involved in 9 out of the 41 significant edges. The 5 strongest effects of condition were found between another node of the DAN (IC9) and a right occipital node (IC23) ( $F=64.09$ ,  $p < .0001$ ), connectivity between these nodes became less positive going from rest to the task conditions; between DAN (IC4) and an occipital node (IC28) ( $F=48.64$ ,  $p < .0001$ ), this edge was weakly negative at rest and positively correlated during task; between DAN (IC4) and a visual node (IC13) ( $F=44.70$ ,  $p < .0001$ ), this edge was weakly positive at rest and negatively correlated during task; between DAN (IC4) and a sensorimotor node (IC17) ( $F=29.07$ ,  $p < .0001$ ), this edge was positively correlated during rest and showed a linear decrease in connectivity strength with increasing load demand; and between two nodes within the DMN (IC6 - IC19), ( $F=26.46$ ,  $p < .0001$ ), this edge was positively correlated for both groups at rest, during task engagement the connectivity became markedly less positive for the young group, whereas in the older group, this edge showed a minimal decrease in connectivity in response to task engagement. With the exception of the edge within the DMN, there were no significant group differences for the other listed edges.

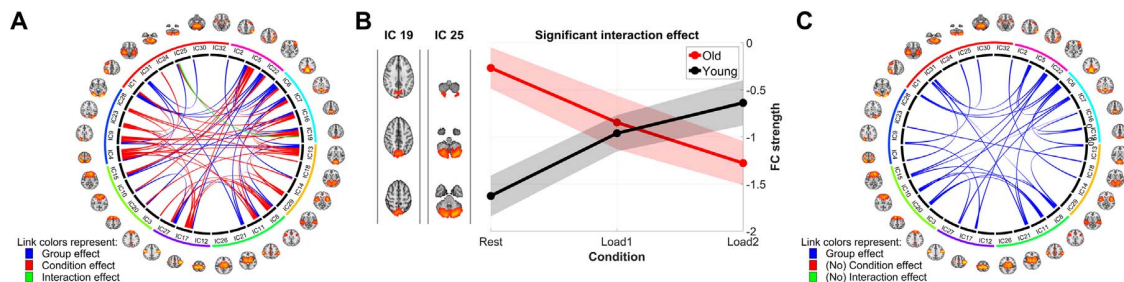
Seven of the 25 edges showing significant effect of group implicated the DMN (IC6), which was the node with the highest number of age effects. The 5 strongest effects of group were; between the left frontoparietal network (IC2) and insula (IC14) ( $F=24.8$ ,  $p < .0001$ ), connectivity between these nodes was positive during rest for the old and weakly negative for the young group, with task engagement, this edge became less positive for the old group with little change in connectivity strength for the young group; between the thalami (IC21) and temporal cortices (IC31) ( $F=24.5$ ,  $p < .0001$ ), connectivity strength for this edge was positive at rest for the old group, becoming slightly more positive with task engagement. For the young group, this edge was uncorrelated at rest and slightly more negative when increasing task load; between the DAN (IC5) and DMN (IC6) ( $F=24.3$ ,  $p < .0001$ ), connectivity for this edge at rest was negative for the young and positive for the old group. During task, connectivity became less negative for the young and more positive for the old group; between DMN (IC7) and sensorimotor cortex (IC27) ( $F=20.9$ ,  $p < .0001$ ), for the old group these nodes were uncoupled during rest with minimal connectivity change during task. For the young group, connectivity at rest was negative, with task engagement connectivity became more negative, and again less negative when increasing load demand from L1 to L2; and between the right frontoparietal network (IC1) and the DMN (IC6) ( $F=20.8$ ,  $p < .0001$ ), resting connectivity for this edge was negative for the young and positive for the old group, with increasing attentional demand connectivity strength became more positive and less negative for the old and young group, respectively.

Fig. 2B illustrates the significant interaction effect, which implicated IC19 (DMN) and IC25 (cerebellum). For this particular edge, resting state connectivity was stronger in the young participants compared to the old. Task engagement caused a decrease in connectivity in the young group whereas connectivity strength increased in the old group. These connectivity changes were further amplified when increasing load demand from L1 to L2.

Fig. 2C shows results from edgewise repeated measures ANOVAs after removing resting state runs, revealing 30 edges showing effect of



**Fig. 1.** Confusion matrices from various classification tasks. (A) Classification of the three conditions (rest, L1 and L2) within the young group, the old group and across groups. (B) Classification of the two groups (old and young) within resting state, load 1 and load 2.



**Fig. 2.** The components grouped into 8 clusters largely corresponding to motor/somatosensory components (purple); frontal pole (light green); dorsal attention and visual components (blue); temporal and cerebellar components (red); frontoparietal (pink); default mode (turquoise); visual and auditory components (yellow); and subcortical components (green). (A) Circular connectivity plot showing effect of condition, group and interaction during all conditions; (B) Changes in functional connectivity (FC) strength for both groups during the three conditions for the edge showing interaction effect; (C) Connectivity plot with the resting state session removed. (For interpretation of the references to color in this figure legend, the reader is referred to the web version of this article.)

group (FDR corrected), and no load or interaction effects. Strongest age effects were found for frontoparietal-DMN (IC1-6), frontoparietal-frontal pole (IC1-22), DAN-insula (IC2-14) and DAN-temporal (IC4-31).

#### Nodewise eigenvector centrality

**Fig. 3** summarizes the nodewise EC obtained from each of the relevant statistical analyses. For group effects, highest centrality was found for IC6 (DMN), IC5 (DAN), and IC16. For load effects, highest EC was found for IC4 (DAN), IC9 (DAN) and IC13 (visual). For the interaction effect, highest EC was found for IC19 (DMN), IC6 (DMN) and IC10 (cingulum).

#### Nodewise SDSA analyses

**Fig. 4** shows the results from the nodewise SDSA analysis. Overall, greater SDSA was observed in more numerous nodes in younger compared to older participants, during rest (50.00% versus 31.25%); during L1 (62.50% versus 34.38%); as well as during L2 (53.13% versus 40.63%). Briefly, repeated measured ANOVA revealed 12 significant ( $p < .05$ , FDR corrected) effects of load, 4 effects of group

and one group by load interaction effect. Load effects showing an increase in task-related variability for both groups were observed in DAN (IC4), frontal (IC15) and sensorimotor (IC17) nodes; task-related decreases in SDSA for both groups were seen in DMN (IC6, IC7, IC16, IC19), DAN (IC5, IC9), visual (IC23, IC28) and sensorimotor (IC11) nodes ([Supplementary material](#)).

Group effects comprised the cerebellum (IC24, IC25 and IC30), with higher variability in the old group in all runs, and a node in the left frontal lobe (IC22) where amplitude variability was higher for the young group in all runs. The interaction effect implicated the DMN (IC7), where resting SDSA was higher for the older group than the younger. During L1 there was a sharp decrease for the older group and a slighter decrease from L1 to L2. For the young group, SDSA for IC7 did not show any marked changes from rest to L2. Comparing variability between group within runs, we found; during resting state two cerebellar nodes (IC 24 and 25) and two frontal nodes (IC 3 and 22) with greater variability in the older and younger group, respectively; during L1, a somatosensory node (IC 11) had higher SDSA in the young and a cerebellar node (IC 30) was more variable in the older group; during L2 there were no significant group differences in signal variability.

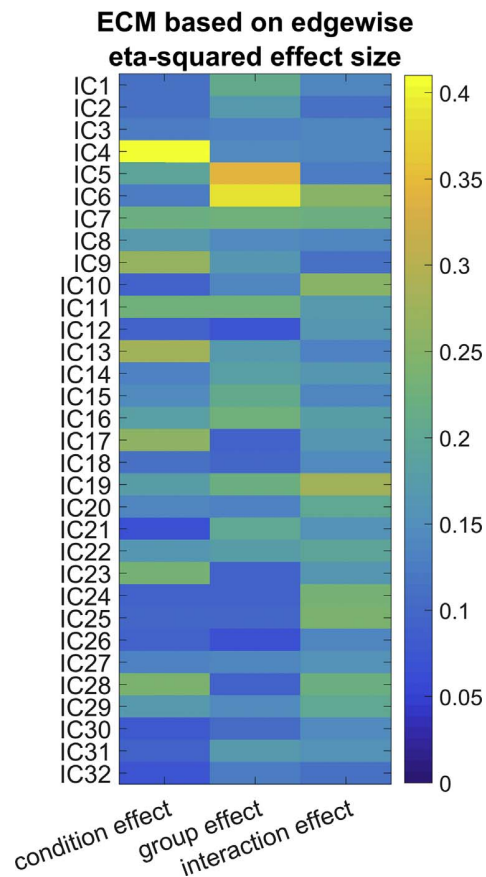


**Fig. 3.** Nodewise eigenvector centrality based on edgewise effect sizes for main effect of load, group, and their interactions.

**Discussion**

The heterogeneity in cognitive aging across cognitive domains is mirrored in a differential vulnerability of brain network connectivity, which has been proposed as a candidate imaging biomarker for age-related cognitive decline and risk and progression of dementia. Since previous studies have primarily utilized resting-state fMRI, we assessed the generalizability of the predictive FC patterns across the resting-state and constrained contexts characterized by higher cognitive load. In line with our main hypothesis, FC patterns discriminated between

young and old individuals using the full range of connections with increasing accuracies from resting state to higher constraint and load. Further, we discriminated resting-state from task runs, with accuracy approaching 100% across groups. Importantly, whereas we significantly discriminated between the MOT load levels for young participants, these were indistinguishable among the older group, providing FC support for decreased network modularity in cognitive aging.

*Classification of group and run*

Using multivariate machine learning techniques, we have demonstrated robust discrimination between state of rest and state of attentional effort as well as between younger and older adults, using brain connectivity indices. In agreement with our hypotheses, distinguishing between resting state and task engagement is done with high accuracy in both age groups (93.6% classification accuracy across groups), distinguishing between the two levels of attentional load is done with moderate accuracy, with better discrimination in the young group compared to the old. Furthermore, classification between young and old age groups is more accurate during MOT than during resting state, and increasing load yields a further increase in classification accuracy.

Our findings of lower discrimination between the two load levels in old individuals corroborate the notion of less distinctive neural representations with advanced age, which has been conceptualized through theories of cognitive and neural dedifferentiation in aging (Baltes and Lindenberger, 1997; Ghisletta and Lindenberger, 2003; Park et al., 2004), postulating that specialized neural networks lose fidelity with age with additional recruitment of non-selective brain regions (Goh, 2011). In line with this, we have in an overlapping sample recently demonstrated stronger correlations in the task-related activation between DAN and DMN during the blocked MOT runs in the older compared to the younger group, indicating stronger between-network dependence or lower differentiation in older adults (Dorum et al., 2016).

An alternative but not mutually exclusive theory termed compensation-related utilization of neural circuits (CRUNCH) (Reuter-Lorenz and Cappell, 2008; Reuter-Lorenz and Lustig, 2005) proposes that at low levels, specialized neural resources are recruited and as task demand increases, the specialized machinery becomes exhausted, requiring the utilization of more task-general resources. Due to neural inefficiency, older individuals reach their resource ceiling at lower task-demand than younger subjects and thus CRUNCH predicts that distinctiveness in neural representation becomes more pronounced. Conversely, at higher task demand when older subjects recruit more

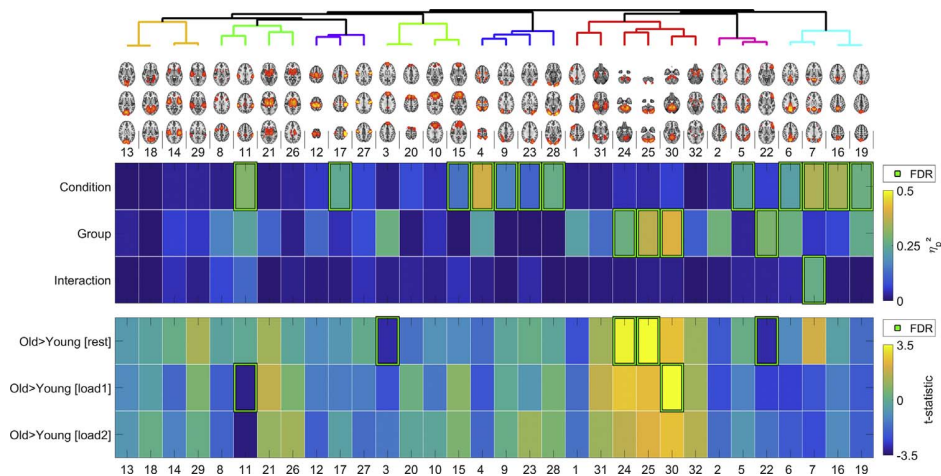


**Fig. 4.** Nodewise SDSA analysis. Top panel shows the hierarchical clustering of nodes. Middle panel shows the significant effect of condition, group and interaction effect across groups. Lower panel shows the group differences within each condition. FDR-significant effects are highlighted.

task-general resources, neural representations become less discriminable. Thus, our observations that discriminating between task engagement and rest is done with superior accuracy in the older group and discriminating between the two levels of task demand is more accurate for the younger group are consistent with CRUNCH, although an all-encompassing model on cognitive aging does not exist, it would likely to incorporate features from both dedifferentiation and CRUNCH.

#### Edgewise univariate analysis

The temporal correlations between fMRI time series in anatomically separated regions represent channels of functional communication. As such, the human brain can be understood as an integrative network of communicating brain regions where the coordinated activity of distributed brain systems underlies complex behavior. The continuous MOT task allows us to discern the differential connectivity patterns induced by sustained attentional effort, from the network configurations of the brain at rest. By comparing connectivity features in a group of older and a group of younger adults, we investigate age-related dynamic brain network alterations in response to cognitive demand.

Exploring the edgewise connectivity changes between network nodes during states of rest and effortful attention, we found the most predictive information about cognitive states in edges involving the DAN. A task-dependent decrease in connectivity was found for an edge connecting the DAN to a sensorimotor node, suggesting a disconnection of task-irrelevant networks. Both increased and decreased connectivity could be observed in edges between the DAN and the occipital cortex, this differential coupling and decoupling between the DAN and visual system directly replicates a recent publication using a similar approach (Alnæs et al., 2015) and could possibly reflect the selective retinotopic representation of tracked objects in the central visual field. Decreased functional connectivity was also observed between two nodes within the DMN. Whereas there were minimal group differences in the other aforementioned edges, this within-DMN edge showed a marked decrease in connectivity strength for the old group and little task-related connectivity changes in the young group. Age-related reductions in DMN connectivity has been widely reported in resting state (Damoiseaux et al., 2008; Ferreira et al., 2015b; Hafkemeijer et al., 2012) and task based studies (Chen et al., 2013), however a recent task-based fMRI study found age differences in DMN connectivity during rest but not during task (Grady et al., 2016).

The most discriminative edges when comparing age groups were primarily found in nodes involving the DMN and manifested as an age-related increase in between-network connectivity. Edges connecting the DAN to the DMN were negatively correlated in younger adults and positively correlated in older adults across conditions, possibly reflecting an age-related loss in maintaining the anticorrelated relationship between these networks, as it serves to prevent interference between internal and external processing of information (Fox et al., 2005). The FPN is thought to mediate the flexible coupling and decoupling between these networks based on specific task demands, serving as a cognitive “switch” by exerting top-down influence on large-scale network reconfiguration (Di and Biswal, 2014). FPN and DMN nodes were positively correlated in older and negatively correlated in younger adults, supporting the notion of an age-related decrease in large-scale network segregation. Relative to the young group, older adults also showed stronger connectivity in FPN-insula, DMN-sensorimotor and thalamic-temporal connections, supporting the notion of a system-level loss of network specificity with advancing age.

Nodewise eigenvector centrality based on the univariate edgewise effect sizes suggested strongest involvement for group discrimination in nodes comprising the DMN and DAN, indicating widespread age-related connectivity alterations in these nodes. Altered network dynamics between these interdependent networks is commonly reported in aging studies (Ferreira et al., 2015a; Spreng et al., 2016) and,

supported by the results from the edgewise connectivity analysis, the present findings suggests reduced DMN-DAN anticorrelation to be a signature feature in cognitive aging.

For effects of condition, we found strongest involvement of DAN and visual nodes, suggesting nodes within these networks to be central when visually attentive, reflecting dynamic network alterations in response to task goals. An interaction effect between age and condition was primarily observed for the DMN, reflecting the role of the DMN as a connectivity hub, its selective vulnerability to aging effects and relevance in task processing.

#### SDSA

More than simple “noise” – brain signal variability has been shown to reveal biologically relevant brain patterns distinct from mean-based patterns (Garrett et al., 2010, 2011). We tested effects of group and condition on the brain network node-level SDSA. Overall, greater SDSA was observed in more numerous nodes in younger compared to older participants across conditions. Significant effects of load were most pronounced in DAN, DMN, frontal and sensorimotor nodes, reflecting network selective modulation in SDSA with increased load and task engagement. Contrary to the unidirectional increase in brain signal variability reported by Garrett et al. (2012), we observed both task-related increases and decreases changes in variability. In agreement with our initial hypothesis, that task-positive networks would exhibit higher signal variation in response to cognitive load, we note that the node showing strongest load effect represented the canonical DAN, and SDSA changes manifested as a linear increase in variability with increasing load for both groups with more variability seen across conditions for the young group. However, task-induced SDSA decreases were also observed for DAN nodes, and similarly, somatosensory nodes also exhibited both increased and decreased SDSA in response to the MOT task. For DMN and visual nodes, we observed consistent reductions in signal variability during task. Significant group differences were found in a frontal pole node where SDSA was greater for the younger participants, and in three nodes encompassing the cerebellum where the older group showed greater signal variability. Interestingly, two previous studies (Garrett et al., 2010, 2011) using a blocked design, several cognitive tasks and voxel-based signal SD analyses, also reported an age-related increase in signal variability in cerebellar regions. The significance of this finding is unknown and requires further research. A single load by group interaction effect was found in a DMN node, reflecting greater SDSA at rest for the older group, with a marked reduction during attentional effort, whilst for the younger group variability remained unaffected by task demand.

As an index of neural complexity, research into the variability in temporal signal fluctuations supplements temporal signal synchronicity (FC) in understanding the governing principles underlying information processing between local and distributed brain networks (McDonough and Nashiro, 2014). Evidence from developmental (Bunge, 2009; McIntosh et al., 2008) and aging studies (Garrett et al., 2010, 2012) suggests that lifespan signal variability changes follow an inverted U-shaped trajectory with greatest variability observed in early adulthood and lower variability seen in infancy and senescence, a pattern which is corroborated by recent evidence of reduced resting-state fMRI dynamic functional connectivity with disease severity across the Alzheimer's disease spectrum (Córdova-Palomera et al., 2017). A similar lifespan developmental trajectory has been described for functional (Wang et al., 2012) and white matter microstructural properties (Westlye et al., 2009). Along with the results from the connectivity analyses, the present findings from the SDSA analysis extend the notion of a strong vulnerability of the DMN to aging effects, and reveal that age-related network changes can be reflected in reduced signal variation in addition to previously described findings of diminished deactivation and decreased FC.

### Strengths and limitations

The current study does not come without limitations. Our findings should be interpreted in the light of the relatively modest size of our final sample ( $n=47$ ). Sample size limits statistical power and thus reduces both the chance of detecting true effects and the likelihood that the significant results indeed reflect true effects. We attempted to overcome this limitation by applying advanced statistics on node and edge-level and used cross-validated machine learning techniques along with permutation testing to assess the robustness of our findings. In-scanner motion is a universal problem in fMRI studies, and the present study is no exception. Further, in light of a recent study documenting increased head motion during rest relative to task (Huijbers et al., 2016), accounting for movement is especially relevant for the present study. We observed more movement during the task conditions for the older compared to the younger group, but the reported group differences in functional connectivity remained largely unchanged when adding mean estimated motion as an additional covariate. The limitations imposed by a cross-sectional study design are well known, and large-scale longitudinal studies are needed to establish the dynamic changes in functional connectivity with increasing age. Finally, BOLD signal group comparisons rely on the assumption that neurovascular coupling is similar between the groups; any differences in cerebrovascular dynamics will have an effect on neurovascular coupling and thus complicate the interpretation of the measured signal (D'Esposito et al., 2003). This confound is particularly relevant when comparing individuals on both ends of the adult age spectrum, as vascular changes accumulate throughout the course of a lifespan. There are several approaches to estimate differences in vasculature, including breath-holding induced hypercapnia (which might be poorly tolerated in older adults) (Lu et al., 2010) and scaling for resting state fluctuation amplitude (RSFA) along with electroencephalographic (EEG) recordings (Tsvetanov et al., 2015). However, vascular alteration is a ubiquitous feature in the aging brain and it's likely that cognitive changes are in part caused by age-related changes in vasculature. Accordingly, the findings in this study should be interpreted in light of its scope in classifying and describing age differences regardless of origin, without attempting to disentangle the neuronal effects of age from the vascular.

### Conclusion

Our main findings demonstrate that FC during a constrained continuous tracking task strongly increases sensitivity to age compared to the conventional resting-state paradigm, and secondly, that data obtained during rest and task is more distinguishable in young compared to older individuals, providing further neuronal support of the conjecture of cognitive and neuronal dedifferentiation in aging. Complementary connectivity analyses on node and edge level, as well as nodal signal variability indices suggests widespread modular disruptions in distributed brain systems and loss of signal complexity with advancing age, with a selective susceptibility of the DMN to aging effects. Further large-scale longitudinal studies are needed to test the clinical utility for predicting cognitive decline and potential link to development of dementia, and for assessing the generalization to other neuropsychiatric disorders. A continuous multiple object tracking task may yield great value in approaching these goals.

### Acknowledgements

This work was funded by the Research Council of Norway (204966/F20), the South-Eastern Norway Regional Health Authority (2013054, 2014097, 2015073), and the Norwegian Extra Foundation for Health and Rehabilitation (2015/FO5146).

### Appendix A. Supporting information

Supplementary data associated with this article can be found in the online version at doi:10.1016/j.neuroimage.2017.01.048.

### References

- Alnaes, D., Kaufmann, T., Richard, G., Duff, E.P., Sneve, M.H., Endestad, T., Nordvik, J.E., Andreassen, O.A., Smith, S.M., Westlye, L.T., 2015. Attentional load modulates large-scale functional brain connectivity beyond the core attention networks. *NeuroImage* 109, 260–272 (<http://www.sciencedirect.com/science/article/pii/S1053811915000403>).
- Alnaes, D., Sneve, M.H., Richard, G., Skatun, K.C., Kaufmann, T., Nordvik, J.E., Andreassen, O.A., Endestad, T., Laeng, B., Westlye, L.T., 2015b. Functional connectivity indicates differential roles for the intraparietal sulcus and the superior parietal lobule in multiple object tracking. *Neuroimage* 123, 129–137.
- Andersson, J.L., Jenkinson, M., Smith, S., 2007a. Non-linear optimisation. FMRIB technical report TR07JA1. FMRIB Centre, Oxford (UK).
- Andersson, J.L., Jenkinson, M., Smith, S., 2007b. Non-linear registration, aka Spatial normalisation FMRIB technical report TR07JA2. FMRIB Analysis Group of the University of Oxford.
- Andrews-Hanna, J.R., Snyder, A.Z., Vincent, J.L., Lustig, C., Head, D., Raichle, M.E., Buckner, R.L., 2007. Disruption of large-scale brain systems in advanced aging. *Neuron* 56, 924–935.
- Baltes, P.B., Lindenberger, U., 1997. Emergence of a powerful connection between sensory and cognitive functions across the adult life span: a new window to the study of cognitive aging? *Psychol. Aging* 12, 12.
- Beckmann, C.F., Smith, S.M., 2004. Probabilistic independent component analysis for functional magnetic resonance imaging. *IEEE Trans. Med. Imaging* 23, 137–152.
- Bonacich, P., 2007. Some unique properties of eigenvector centrality. *Social. Netw.* 29, 555–564.
- Brainard, D.H., 1997. The psychophysics toolbox. *Spat. Vision* 10, 433–436.
- Brier, M.R., Mitra, A., McCarthy, J.E., Ances, B.M., Snyder, A.Z., 2015. Partial covariance based functional connectivity computation using Ledoit–Wolf covariance regularization. *NeuroImage* 121, 29–38.
- Buckner, R.L., 2004. Memory and executive function in aging and AD: multiple factors that cause decline and reserve factors that compensate. *Neuron* 44, 195–208.
- Bunge, S., 2009. Differential maturation of brain signal complexity in the human auditory and visual system. *Dev. Human Brain*, 6.
- Cavanagh, P., Alvarez, G.A., 2005. Tracking multiple targets with multifocal attention. *Trends Cogn. Sci.* 9, 349–354.
- Chan, M.Y., Park, D.C., Savalia, N.K., Petersen, S.E., Wig, G.S., 2014. Decreased segregation of brain systems across the healthy adult lifespan. *Proceedings of the National Academy of Sciences* 111, E4997–E5006.
- Chen, S.A., Wu, C.-Y., Lua, R.-p., Akoshi, M.M., Nakai, T., 2013. Age-related changes in resting-state and task-activated functional MRI networks. In: *Proceedings of the IEEE 2013 7th International Symposium on Medical Information and Communication Technology (ISMICT)*. pp. 218–222.
- Córdova-Palamera, A., Kaufmann, T., Persson, K., Alnaes, D., Doan, N., Moberget, T., Lund, M., Barca, M., Engvig, A., Brækhus, A., Engedal, K., Andreassen, O., Selbæk, G., Westlye, L. Disrupted global metastability and static and dynamic brain connectivity across individuals in the Alzheimer's disease continuum. *Scientific Reports*. 2017, <http://www.nature.com/articles/srep40268>.
- D'Esposito, M., Deouell, L.Y., Gazzaley, A., 2003. Alterations in the BOLD fMRI signal with ageing and disease: a challenge for neuroimaging. *Nat. Rev. Neurosci.* 4, 863–872.
- Damoiseaux, J., Beckmann, C., Arigita, E.S., Barkhof, F., Scheltens, P., Stam, C., Smith, S., Rombouts, S., 2008. Reduced resting-state brain activity in the "default network" in normal aging. *Cereb. Cortex* 18, 1856–1864.
- Daselaar, S.M., Veltman, D.J., Rombouts, S.A., Raaijmakers, J.G., Jonker, C., 2005. Aging affects both perceptual and lexical/semantic components of word stem priming: an event-related fMRI study. *Neurobiol. Learn. Mem.* 83, 251–262.
- Deligianni, F., Centeno, M., Carmichael, D.W., Clayden, J.D., 2014. Relating resting-state fMRI and EEG whole-brain connectomes across frequency bands. *Front Neurosci.* 8.
- Di, X., Biswal, B.B., 2014. Modulatory interactions between the default mode network and task positive networks in resting-state. *PeerJ* 2, e367.
- Dørum, E.S., Alnaes, D., Kaufmann, T., Richard, G., Lund, M.J., Tønnesen, S., Sneve, M.H., Mathiesen, N.C., Rustan, Ø.G., Gjertsen, Ø., Vatn, S., Fure, B., Andreassen, O.A., Nordvik, J.E., Westlye, L.T., 2016. Age-related differences in brain network activation and co-activation during multiple object tracking. *Brain Behav.* (<https://www.ncbi.nlm.nih.gov/pubmed/27843692>).
- Ferreira, L.K., Regina, A.C., Kovacevic, N., Martin, M.D., Santos, P.P., Carneiro, C.G., Kerr, D.S., Amaro, E., Jr, McIntosh, A.R., Busatto, G.F., 2015a. Aging effects on whole-brain functional connectivity in adults free of cognitive and psychiatric disorders. *Cereb. Cortex* bhv1, 90.
- Ferreira, L.K., Regina, A.C.B., Kovacevic, N., Martin, M.D., Santos, P.P., Carneiro, C.G., Kerr, D.S., Amaro, E., McIntosh, A.R., Busatto, G.F., 2015b. Aging effects on whole-brain functional connectivity in adults free of cognitive and psychiatric disorders. *Cereb. Cortex*.
- Filippini, N., MacIntosh, B.J., Hough, M.G., Goodwin, G.M., Frisoni, G.B., Smith, S.M., Matthews, P.M., Beckmann, C.F., Mackay, C.E., 2009. Distinct patterns of brain activity in young carriers of the APOE-epsilon 4 allele. In: *Proceedings of the National Academy of Sciences of the United States of America* 106, 7209–7214.

- Fischl, B., Salat, D.H., Busa, E., Albert, M., Dieterich, M., Haselgrove, C., van der Kouwe, A., Killiany, R., Kennedy, D., Klaveness, S., Montillo, A., Makris, N., Rosen, B., Dale, A.M., 2002. Whole brain segmentation: automated labeling of neuroanatomical structures in the human brain. *Neuron* 33, 341–355.
- Fox, M.D., Snyder, A.Z., Vincent, J.L., Corbetta, M., Van Essen, D.C., Raichle, M.E., 2005. The human brain is intrinsically organized into dynamic, anticorrelated functional networks. *Proceedings of the National Academy of Sciences of the United States of America* 102, 9673–9678.
- Friedman, J.H., 1989. Regularized discriminant analysis. *J. Am. Stat. Assoc.* 84, 165–175.
- Garrett, D.D., Kovacevic, N., McIntosh, A.R., Grady, C.L., 2010. Blood oxygen level-dependent signal variability is more than just noise. *J. Neurosci.* 30, 4914–4921.
- Garrett, D.D., Kovacevic, N., McIntosh, A.R., Grady, C.L., 2011. The importance of being variable. *J. Neurosci.* 31, 4496–4503.
- Garrett, D.D., Kovacevic, N., McIntosh, A.R., Grady, C.L., 2012. The modulation of BOLD variability between cognitive states varies by age and processing speed. *Cereb. Cortex* bhs0, 55.
- Ghisletta, P., Lindenberger, U., 2003. Age-based structural dynamics between perceptual speed and knowledge in the Berlin Aging Study: direct evidence for ability dedifferentiation in old age. *Psychol. Aging* 18, 696.
- Glisky, E.L., 2007. Changes in cognitive function in human aging. *Brain Aging: Model. Methods Mech.*, 3–20.
- Goh, J.O., 2011. Functional dedifferentiation and altered connectivity in older adults: neural accounts of cognitive aging. *Aging Dis.* 2, 30.
- Grady, C., Sarraf, S., Saverino, C., Campbell, K., 2016. Age differences in the functional interactions among the default, frontoparietal control, and dorsal attention networks. *Neurobiol. Aging* 41, 159–172.
- Grady, C.L., Garrett, D.D., 2014. Understanding variability in the BOLD signal and why it matters for aging. *Brain Imaging Behav.* 8, 274–283.
- Greve, D.N., Fischl, B., 2009. Accurate and robust brain image alignment using boundary-based registration. *NeuroImage* 48, 63–72.
- Hafkemeijer, A., van der Grond, J., Rombouts, S.A., 2012. Imaging the default mode network in aging and dementia. *Biochim. Biophys. Acta (BBA)-Mol. Basis Dis.* 1822, 431–441.
- Huijbers, W., Van Dijk, K.R., Boenniger, M.M., Stirnberg, R., Breteler, M.M., 2016. Less head motion during MRI under task than resting-state conditions. *NeuroImage*. IBM Corp, R, 2010. IBM SPSS Statistics for Windows. IBM Corp, Armonk, NY.
- Jenkinson, M., Smith, S., 2001. A global optimisation method for robust affine registration of brain images. *Med. Image Anal.* 5, 143–156.
- Kaufmann, T., Elvsashagen, T., Alnaes, D., Zak, N., Pedersen, P.O., Norbom, L.B., Quraishi, S.H., Tagliazucchi, E., Laufs, H., Bjørnerud, A., Malt, U.F., Andreassen, O.A., Roussos, E., Duff, E.P., Smith, S.M., Groote, I.R., Westlye, L.T., 2016. The brain functional connectome is robustly altered by lack of sleep. *Neuroimage* 127, 324–332.
- Kaufmann, T., Skåtun, K.C., Alnaes, D., Doan, N.T., Duff, E.P., Tønnesen, S., Roussos, E., Ueland, T., Aminoff, S., Lagerberg, T.V., Agartz, I., Melle, I., Smith, S.M., Andreassen, O.A., Westlye, L.T., 2015. Disintegration of sensorimotor brain networks in schizophrenia. *Schizophr. Bull.* (<https://www.ncbi.nlm.nih.gov/pmc/articles/PMC4601711/>).
- Kelly, R.E., Jr, Alexopoulos, G.S., Wang, Z., Gunning, F.M., Murphy, C.F., Morimoto, S.S., Kanellopoulos, D., Jia, Z., Lim, K.O., Hoptman, M.J., 2010. Visual inspection of independent components: defining a procedure for artifact removal from fMRI data. *J. Neurosci. Methods* 189, 233–245.
- Kensinger, E.A., Corkin, S., 2009. Cognition in aging and age related disease. *Handb. Neurosci. Aging*, 249–256.
- Ledoit, O., Wolf, M., 2003. Improved estimation of the covariance matrix of stock returns with an application to portfolio selection. *Journal of empirical finance* 10 (5), 603–621 (<http://www.sciencedirect.com/science/article/pii/S0927539803000070>).
- Lindenberger, U., 2014. Human cognitive aging: corrigere la fortune? *Science* 346, 572–578.
- Lu, H., Xu, F., Rodrigue, K.M., Kennedy, K.M., Cheng, Y., Flicker, B., Hebrank, A.C., Uh, J., Park, D.C., 2010. Alterations in cerebral metabolic rate and blood supply across the adult lifespan. *Cereb. Cortex* bhq2, 24.
- McDonough, I.M., Nashiro, K., 2014. Network complexity as a measure of information processing across resting-state networks: evidence from the Human Connectome Project. *Front Hum. Neurosci.*, 8.
- McIntosh, A.R., Kovacevic, N., Itier, R.J., 2008. Increased brain signal variability accompanies lower behavioral variability in development. *PLoS Comput. Biol.* 4, e1000106.
- Mowinckel, A.M., Espeseth, T., Westlye, L.T., 2012. Network-specific effects of age and in-scanner subject motion: a resting-state fMRI study of 238 healthy adults. *Neuroimage* 63, 1364–1373.
- Murray, B.D., Kensinger, E.A., 2012. Cognitive aging. In: Seel, N.M. (Ed.), *Encyclopedia of the Sciences of Learning*. Springer, US, Boston, MA, 560–563.
- Nichols, T., 2009. FDR implementation provided online by Tom Nichols at (<http://www-personal.umich.edu/~nichols/FDR/>).
- Nichols, T., Hayasaka, S., 2003. Controlling the familywise error rate in functional neuroimaging: a comparative review. *Stat. Methods Med. Res.* 12, 419–446.
- Park, D.C., Polk, T.A., Park, R., Minear, M., Savage, A., Smith, M.R., 2004. Aging reduces neural specialization in ventral visual cortex. *Proceedings of the National Academy of Sciences of the United States of America* 101, 13091–13095.
- Park, J., Carp, J., Kennedy, K.M., Rodrigue, K.M., Bischof, G.N., Huang, C.M., Rieck, J.R., Polk, T.A., Park, D.C., 2012. Neural broadening or neural attenuation? Investigating age-related dedifferentiation in the face network in a large lifespan sample. *J. Neurosci.* 32, 2154–2158.
- Pelli, D.G., 1997. The VideoToolbox software for visual psychophysics: transforming numbers into movies. *Spat. Vision* 10, 437–442.
- Pruim, R.H., Mennes, M., Buitelaar, J.K., Beckmann, C.F., 2015. Evaluation of ICA-AROMA and alternative strategies for motion artifact removal in resting state fMRI. *Neuroimage* 112, 278–287.
- Pylyshyn, Z.W., Storm, R.W., 1988. Tracking multiple independent targets: evidence for a parallel tracking mechanism. *Spat. Vision* 3, 179–197.
- Quigley, C., Müller, M.M., 2014. Feature-selective attention in healthy old age: a selective decline in selective attention? *J. Neurosci.* 34, 2471–2476.
- Reuter-Lorenz, P.A., Cappell, K.A., 2008. Neurocognitive aging and the compensation hypothesis. *Curr. Dir. Psychol. Sci.* 17, 177–182.
- Reuter-Lorenz, P.A., Lustig, C., 2005. Brain aging: reorganizing discoveries about the aging mind. *Curr. Opin. Neurobiol.* 15, 245–251.
- Salami, A., Eriksson, J., Nyberg, L., 2012. Opposing effects of aging on large-scale brain systems for memory encoding and cognitive control. *J. Neurosci.* 32, 10749–10757.
- Salami, A., Pudas, S., Nyberg, L., 2014. Elevated hippocampal resting-state connectivity underlies deficient neurocognitive function in aging. *Proc. Natl. Acad. Sci. USA* 111, 17654–17659.
- Salimi-Khorshidi, G., Douaud, G., Beckmann, C.F., Glasser, M.F., Griffanti, L., Smith, S.M., 2014. Automatic denoising of functional MRI data: combining independent component analysis and hierarchical fusion of classifiers. *NeuroImage* 90, 449–468.
- Sambataro, F., Murty, V.P., Callicott, J.H., Tan, H.-Y., Das, S., Weinberger, D.R., Mattay, V.S., 2010. Age-related alterations in default mode network: impact on working memory performance. *Neurobiol. Aging* 31, 839–852.
- Schäfer, J., Strimmer, K., 2005. A shrinkage approach to large-scale covariance matrix estimation and implications for functional genomics. *Stat. Appl. Genet. Mol. Biol.* 4, 1–12.
- Singh-Manoux, A., Kivimaki, M., Glymour, M.M., Elbaz, A., Berr, C., Ebmeier, K.P., Ferrie, J.E., Dugravot, A., 2012. Timing of onset of cognitive decline: results from Whitehall II prospective cohort study. *Bmj* 344, d7622.
- Skåtun, K., Kaufmann, T., Doan, N., Alnaes, D., Córdova-Palomera, A., Jönsson, E., Fatouros-Bergman, H., Flyckt, L., consortium, K.S.P.K., Melle, I., Andreassen, O., Agartz, I., Westlye, L., in press. Consistent functional connectivity alterations in schizophrenia spectrum disorder: a multi-site study. *Schizophrenia Bulletin*.
- Smith, S.M., Hyvarinen, A., Varoquaux, G., Miller, K.L., Beckmann, C.F., 2014. Group-PCA for very large fMRI datasets. *Neuroimage* 101, 738–749.
- Smith, S.M., Jenkinson, M., Woolrich, M.W., Beckmann, C.F., Behrens, T.E.J., Johansen-Berg, H., Bannister, P.R., De Luca, M., Drobnjak, I., Flitney, D.E., Niazy, R.K., Saunders, J., Vickers, J., Zhang, Y.Y., De Stefano, N., Brady, J.M., Matthews, P.M., 2004. Advances in functional and structural MR image analysis and implementation as FSL. *Neuroimage* 23, S208–S219.
- Smith, S.M., Miller, K.L., Salimi-Khorshidi, G., Webster, M., Beckmann, C.F., Nichols, T.E., Ramsey, J.D., Woolrich, M.W., 2011a. Network modelling methods for FMRI. *NeuroImage* 54, 875–891.
- Smith, S.M., Miller, K.L., Salimi-Khorshidi, G., Webster, M., Beckmann, C.F., Nichols, T.E., Ramsey, J.D., Woolrich, M.W., 2011b. Network modelling methods for FMRI. *Neuroimage* 54, 875–891.
- Sporns, O., Chialvo, D.R., Kaiser, M., Hilgetag, C.C., 2004. Organization, development and function of complex brain networks. *Trends Cogn. Sci.* 8, 418–425.
- Spreng, R.N., Stevens, W.D., Viviano, J.D., Schacter, D.L., 2016. Attenuated anticorrelation between the default and dorsal attention networks with aging: evidence from task and rest. *Neurobiol. Aging*.
- Tomasi, D., Wang, R., Wang, G.-J., Volkow, N.D., 2014. Functional connectivity and brain activation: a synergistic approach. *Cereb. Cortex* 24, 2619–2629.
- Tsvetanov, K.A., Henson, R.N., Tyler, L.K., Davis, S.W., Shafto, M.A., Taylor, J.R., Williams, N., Rowe, J.B., 2015. The effect of ageing on fMRI: correction for the confounding effects of vascular reactivity evaluated by joint fMRI and MEG in 335 adults. *Human. Brain Mapp.* 36, 2248–2269.
- Van Den Heuvel, M.P., Pol, H.E.H., 2010. Exploring the brain network: a review on resting-state fMRI functional connectivity. *Eur. Neuropsychopharmacol.* 20, 519–534.
- Voss, M.W., Prakash, R.S., Erickson, K.I., Basak, C., Chaddock, L., Kim, J.S., Alves, H., Heo, S., Szabo, A.N., White, S.M., 2010. Plasticity of brain networks in a randomized intervention trial of exercise training in older adults. *Front. Aging Neurosci.* 2.
- Wang, L., Su, L., Shen, H., Hu, D., 2012. Decoding lifespan changes of the human brain using resting-state functional connectivity MRI. *PLoS One* 7, e44530.
- Wechsler, D., 1999. The Wechsler Abbreviated Scale of Intelligence (WASI). 1999. USA, Psychological Corporation.
- Westlye, L.T., Walhovd, K.B., Dale, A.M., Bjørnerud, A., Due-Tønnessen, P., Engvig, A., Grydeland, H., Tamnes, C.K., Østby, Y., Fjell, A.M., 2009. Life-span changes of the human brain white matter: diffusion tensor imaging (DTI) and volumetry. *Cereb. Cortex* bhq2, 80 (<https://www.ncbi.nlm.nih.gov/pubmed/20032062>).
- Zhang, H.-Y., Chen, W.-X., Jiao, Y., Xu, Y., Zhang, X.-R., Wu, J.-T., 2014. Selective vulnerability related to aging in large-scale resting brain networks. *PLoS One* 9, e108807.









## Research article

## Functional brain network modeling in sub-acute stroke patients and healthy controls during rest and continuous attentive tracking



Erlend S. Dørum<sup>a,b,c,\*</sup>, Tobias Kaufmann<sup>a</sup>, Dag Alnæs<sup>a</sup>, Geneviève Richard<sup>a</sup>,  
Knut K. Kolskår<sup>a,b,c</sup>, Andreas Engvig<sup>d</sup>, Anne-Marthe Sanders<sup>a,b,c</sup>, Kristine Ulrichsen<sup>a,b,c</sup>,  
Hege Ihle-Hansen<sup>e</sup>, Jan Egil Nordvik<sup>f</sup>, Lars T. Westlye<sup>a,b,g,\*\*</sup>

<sup>a</sup> NORMENT, Division of Mental Health and Addiction, Oslo University Hospital & Institute of Clinical Medicine, University of Oslo, Norway

<sup>b</sup> Department of Psychology, University of Oslo, Norway

<sup>c</sup> Sunnaas Rehabilitation Hospital HT, Nesodden, Norway

<sup>d</sup> Department of Internal Medicine, Oslo University Hospital, Norway

<sup>e</sup> Department of Geriatric Medicine, Oslo University Hospital, Norway

<sup>f</sup> CatoSenteret Rehabilitation Center, Son, Norway

<sup>g</sup> KG Jebsen Centre for Neurodevelopmental Disorders, University of Oslo, Norway

## ARTICLE INFO

## Keywords:

Cerebral stroke  
fMRI  
Brain network connectivity  
Machine learning  
Behavioral neuroscience  
Cognitive neuroscience  
Systems neuroscience  
Neurology  
Medical imaging

## ABSTRACT

A cerebral stroke is characterized by compromised brain function due to an interruption in cerebrovascular blood supply. Although stroke incurs focal damage determined by the vascular territory affected, clinical symptoms commonly involve multiple functions and cognitive faculties that are insufficiently explained by the focal damage alone. Functional connectivity (FC) refers to the synchronous activity between spatially remote brain regions organized in a network of interconnected brain regions. Functional magnetic resonance imaging (fMRI) has advanced this system-level understanding of brain function, elucidating the complexity of stroke outcomes, as well as providing information useful for prognostic and rehabilitation purposes.

We tested for differences in brain network connectivity between a group of patients with minor ischemic strokes in sub-acute phase ( $n = 44$ ) and matched controls ( $n = 100$ ). As neural network configuration is dependent on cognitive effort, we obtained fMRI data during rest and two load levels of a multiple object tracking (MOT) task. Network nodes and time-series were estimated using independent component analysis (ICA) and dual regression, with network edges defined as the partial temporal correlations between node pairs. The full set of edgewise FC went into a cross-validated regularized linear discriminant analysis (rLDA) to classify groups and cognitive load.

MOT task performance and cognitive tests revealed no significant group differences. While multivariate machine learning revealed high sensitivity to experimental condition, with classification accuracies between rest and attentive tracking approaching 100%, group classification was at chance level, with negligible differences between conditions. Repeated measures ANOVA showed significantly stronger synchronization between a temporal node and a sensorimotor node in patients across conditions. Overall, the results revealed high sensitivity of FC indices to task conditions, and suggest relatively small brain network-level disturbances after clinically mild strokes.

## 1. Introduction

Unlike the insidious onset and progressive neurological decline observed in most neurodegenerative diseases, a cerebral stroke is characterized by instant damage to brain tissue due to a compromise in cerebrovascular blood supply. Although stroke incurs focal damage determined by the vascular territory affected, clinical symptoms

commonly involve multiple functions and cognitive faculties that are insufficiently explained by the focal damage alone (Carter et al., 2012; Ovadia-Caro et al., 2013).

The brain is organized in a network of connected brain regions that are spatially dispersed, yet functionally linked (Bullmore and Sporns, 2009; Damoiseaux et al., 2006; Power et al., 2011; Van Den Heuvel and Pol, 2010), thus even a well localized stroke can give rise to a complex

\* Corresponding author.

\*\* Corresponding author.

E-mail addresses: [erlendsd@hotmail.com](mailto:erlendsd@hotmail.com) (E.S. Dørum), [l.t.westlye@psykologi.uio.no](mailto:l.t.westlye@psykologi.uio.no) (L.T. Westlye).

<https://doi.org/10.1016/j.heliyon.2020.e04854>

Received 10 November 2019; Received in revised form 25 April 2020; Accepted 2 September 2020

2405-8440/© 2020 The Authors. Published by Elsevier Ltd. This is an open access article under the CC BY license (<http://creativecommons.org/licenses/by/4.0/>).

clinical picture of symptoms owing to the highly interconnected organization of the cerebral cortex. Contemporary brain network connectivity models go beyond traditional lesion-symptom mapping, and advanced imaging techniques like functional magnetic resonance imaging (fMRI) can be used to capture disruptions of connectivity following stroke. fMRI has shown great promise in probing alterations in brain activity for a range of neurodegenerative (Cordova-Palomera et al., 2017; Dickerson et al., 2016; Paulsen et al., 2004) and neuropsychiatric (Kaufmann et al., 2015; Skåtun et al., 2016; Yu et al., 2015) conditions. These techniques may provide novel understanding of brain function, and potentially, clinical information used to predict patient recovery, outcome and aid in tailoring individual rehabilitation strategies.

Functional connectivity (FC) refers to the temporal correlation of blood-oxygen-level dependent (BOLD) signal between brain regions (Hampson et al., 2002). Resting state fMRI has revealed the brain to be organized into functional networks of distributed brain systems, where an orchestra of synchronous activity underlies even the simplest behaviors (Van Den Heuvel and Pol, 2010). Task based fMRI studies have shown that functional connections at rest are similarly engaged during various cognitive tasks (Raichle, 2010; Smith et al., 2009) and the increase in joint BOLD activations in spatially dispersed brain regions has revealed networks engaged during attention (Alnæs et al., 2015; Szczepanski et al., 2013), working memory (Compte et al., 2000), language (Ferstl et al., 2008) and motor task (Hanakawa et al., 2008), as well as various other cognitive operations.

Most studies relating the effect of stroke on fMRI-based FC to behavioral deficits have used unconstrained resting state data. Siegel et al. (2016) showed that FC was superior in predicting certain memory deficits, whilst visual and motor impairments were best predicted by lesion topography. Attention and language deficits were well predicted by both. He et al. (2007) demonstrated that the severity of spatial neglect was correlated with the degree of disruption within the contralateral attention network connectivity.

The present work builds on a previous study that examined age differences in functional connectivity in healthy controls during 1) an unconstrained resting-state condition and 2) two load levels of a constrained multiple object tracking (MOT) task (Dørum et al., 2017). Briefly, our previous findings demonstrated that a machine learning approach based on FC resulted in robust discrimination between a group of younger and a group of older healthy participants, as well as between states of rest and effortful attention, with higher sensitivity to age group observed during continuous tracking compared to resting state. In the present study, we aim to apply a similar prediction model on data from 44 patients with stroke and 100 healthy controls, in order to test whether the functional brain data alone would be sufficient to accurately identify the stroke patients, and whether the group classification varied between load levels. We also investigated edge-level main effects of experimental condition and group, as well as their interactions, using repeated measures ANOVA. Lastly, since edge-level FC ultimately reflects nodal signal changes, temporal activity on node-level was probed by computing the standard deviation of signal amplitude (SDSA) (Garrett et al., 2010). Brain signal variability reflects neural complexity and the ability to dynamically transition between a range of network states (Garrett et al., 2011), and a reduction in signal variability has been reported with advancing age (Grady and Garrett, 2014), in patients with schizophrenia (Kaufmann et al., 2015), and in acute stroke patients (Zappasodi et al., 2014), indicating global loss of complexity and neurological dysfunction.

Based on the studies reviewed above and current models of brain network dysfunction after stroke, we hypothesized 1) that multivariate classification would yield robust discrimination between a group of sub-acute stroke patients and healthy controls, as well as between states of rest and task engagement. Next, we anticipated that 2) FC during task would yield higher classification accuracy when classifying between stroke patients and healthy controls. We accompanied the multivariate analyses with edgewise repeated measures ANOVAs to test for effects of group, task condition (rest, L1, L2) and their interactions. Lastly, we hypothesized 3)

decreased SDSA for stroke patients compared to healthy controls, with group differences more prominent during task compared to rest.

## 2. Methods and material

### 2.1. General study design

In this cross-sectional study, stroke patients and healthy controls underwent MRI examination, including a resting state and task-based functional image acquisition as well as cognitive and neuropsychological assessment.

### 2.2. Study material and recruitment procedures

Patients were recruited from the stroke units at Oslo University hospital (OUS), Diakonhjemmet hospital and Bærum hospital, Norway. Inclusion criteria were: (i) age 18 or older, (ii) clinically and radiologically documented stroke of ischemic, hemorrhagic or subarachnoid origin, (iii) time of enrolment within 14 days of admittance. Exclusion criteria were: (i) clinical condition of impaired consciousness leading to inability to actively participate and maintain wakefulness psychiatric condition (e.g. schizophrenia, bipolar disorder) as well as alcohol or substance abuse that potentially could impact the interpretation of the behavioral/imaging data, (iii) contraindication for MRI including incompatible metal implants, claustrophobia or pregnancy.

Clinical assessment quantifying stroke severity was performed according to the National Institute of Health Stroke Scale (NIHSS) at the respective stroke units by an attending physician specialized in internal medicine, neurology or geriatric medicine at the time of discharge. Cognition was assessed using the Montreal Cognitive Assessment (MoCA) test after the patients were clinically stable and before discharge. The ischemic strokes were classified according to the TOAST classification (Adams et al., 1993). The patients were treated in accordance with national guidelines (Helsedirektoratet, 2017).

Healthy controls were recruited from social media and newspaper ads. Inclusion criteria were: (i) age 18 years or older, (ii) absence of neurologic, psychiatric condition as well as alcohol or substance abuse, (iii) abnormal radiological findings requiring medical follow-up (e.g. silent stroke, tumor). From a pool of 341 healthy controls recruited to a parallel study (Richard et al., 2018), we selected  $n = 100$  adults based on a group-level matching with the patient sample with regards to age, sex, education and handedness.

Written informed consent was obtained from all participants, and the Regional Committees for Medical Research Ethics South East Norway approved the study protocol.

### 2.3. MRI acquisition

MRI scans were obtained using a General Electric Medical Systems (Discovery MR750) 3.0T scanner with a 32-channel head coil at Oslo University Hospital. fMRI data was acquired with a T2\*-weighted 2D gradient echo planar imaging sequence (EPI) (TR: 2250 ms; TE: 30 ms; FA: 79°; voxel size: 2.67 × 2.67 × 3.0 mm; slices: 43; FOV: 96 × 96 × 129 mm). We collected 200 volumes for the resting-state condition and 152 volumes for the two MOT load conditions, after discarding the first five volumes. We collected a structural scan using a sagittal T1-weighted fast spoiled gradient echo (FSPGR) sequence (TR: 8.16 ms; TE: 3.18 ms; TI: 450 ms; FA: 12°; voxel size: 1.0 × 1.0 × 1.0 mm; slices: 188; FOV: 256 × 256 × 188 mm; duration: 288 s), and a T2-FLAIR (TR: 8000 ms; TE: 127 ms, TI: 2240; voxel size: 1.0 × 1.0 × 1.0 mm; duration 443 s) for lesion demarcation.

### 2.4. fMRI paradigms

Participants underwent one resting state run and three versions of MOT, including one blocked and two continuous tracking runs, performed in the MRI scanner during the same session (Alnæs et al., 2015).

Here we report results from the resting-state and the two continuous load conditions. The level of attentional demand was set at two load conditions – load 1 (L1) and load 2 (L2) requiring the participants to track one or two targets, respectively. We restricted the load level to 2 to ensure that both groups were able to perform at a high level.

The task was presented on a calibrated MR-compatible LCD screen (NNL LCD Monitor®, NordicNeuroLab, Bergen, Norway) with a screen resolution of  $1920 \times 1080$  at 60Hz, placed in front of the scanner bore. The experimental set-up and technical specifications were performed as described in a previous publication (Alnæs et al., 2015).

Each participant performed two runs of continuous MOT task, one with tracking load of 1 object, and the other with 2 objects. Each continuous tracking block lasted 7.5 min and contained 14 trials. Detailed outline of the task is described in our previous study (Dørum et al., 2017). Briefly, 10 identical blue objects were presented on a grey background screen, and after another 0.5 s the objects started moving. The first cued object(s), or target(s), turned red after the first 0.5 s, and remained red for a duration of 2.5 s. The tracking period lasted on average 32 s (range, 27–37) after which the participants were instructed to respond to a probe (green object), “yes” or “no” to whether the green probe was one of the objects originally designated as a target, before a new target assignment took place. The participants were instructed to fixate on a central fixation point during the length of the run. Accuracy and reaction times were recorded.

### 2.5. Lesion demarcation

Individual lesions were defined based on visible damage and hyperintensities on FLAIR images as well as guided by independent neuroradiological descriptions using DWI/FLAIR images. The lesions were semi-automatically delineated in native space using the Clusterize toolbox (de Haan et al., 2015) used with SPM8, running under Matlab R2013b (The Mathworks, Inc., Natick, MA). The FLAIR images were registered with the high-resolution T1 images using a linear transformation with 6 degrees-of-freedom. Subsequently, each T1 image was registered to the MNI152 standard space by computing 12 degrees-of-freedom linear affine transformation. To obtain each registered lesion mask in standard space, the native-to-standard transformation matrices were applied using the nearest neighbor interpolation. Figure 1 shows a probabilistic lesion heat-map displaying lesion overlap across patients.

### 2.6. fMRI analysis

fMRI data was processed on single-subject level using the FMRI Expert Analysis Tool (FEAT) from the FMRIB Software Library (FSL) (Smith et al., 2004) including spatial smoothing (FWHM = 6 mm), high-pass filtering (sigma = 64 s), motion correction (MCFLIRT) and

single-session independent component analysis (ICA) using MELODIC (Beckmann and Smith, 2004). In-scanner motion was calculated as the average root mean square of the displacement from one frame to its previous frame for each dataset.

We used FSL FIX (FMRIB's ICA-based Xnoiseifier) (Salimi-Khorshidi et al., 2014) to identify and remove noise components at the individual level (standard training set, threshold: 20), and regressed out the estimated motion parameters from MCFLIRT from the voxel-wise time series.

Next, we employed a group-level PCA approach (Smith et al., 2014) in MELODIC to estimate group-level spatial maps representing the nodes in our networks. We used a model order of 40 and discarded 10 noise components based on the spatial distribution of the component maps and/or the frequency spectrum of the components' time series (Kelly et al., 2010), resulting in a final set of 30 components (see Figure 2). Next, the full set of spatial maps from the group analysis was used to generate subject-specific versions of the spatial maps, and associated timeseries, using dual regression (Nickerson et al., 2017). First, for each subject, the group-average set of spatial maps is regressed (as spatial regressors in a multiple regression) into the subject's 4D space-time dataset. This results in a set of subject-specific timeseries, one per group-level spatial map. Next, those timeseries are regressed (as temporal regressors, again in a multiple regression) into the same 4D dataset, resulting in a set of subject-specific spatial maps, one per group-level spatial map. Here, in order to remove common variance with the lesion, we included the segmented lesion mask as an additional component in individual dual regression runs.

After discarding the estimated time-series from the lesion, we used the components' time series for network modeling (Smith et al., 2011). Here, the spatial maps are considered nodes in an extended brain network, and the edges are defined as the temporal correlation between each pair of nodes. Based on our previous work (Kaufmann et al., 2016), we estimated the temporal correlations using regularized partial correlations with an automated lambda estimation (Brier et al., 2015; Ledoit and Wolf, 2003). For each individual, this approach resulted in 435 unique edges, each reflecting the strength of a node-by-node connection represented as indexed by the regularized correlation coefficient from the current network modeling approach, which were submitted to further group-level univariate and multivariate analyses (see below).

For each dataset, we also computed the individual level SDSA of each component's time series as a measure of nodal volatility or strength (Garrett et al., 2010; Kaufmann et al., 2015).

### 2.7. Statistical analysis

Demographics, behavioral and clinical data were analyzed in SPSS (IBM\_Corp, 2010). Between-group differences were assessed using Chi square tests (sex distribution) and linear models (age, neuropsychological performance, MOT task performance).

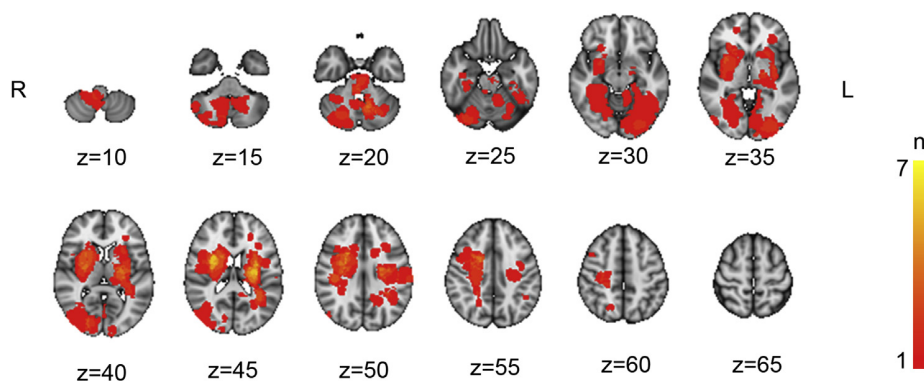
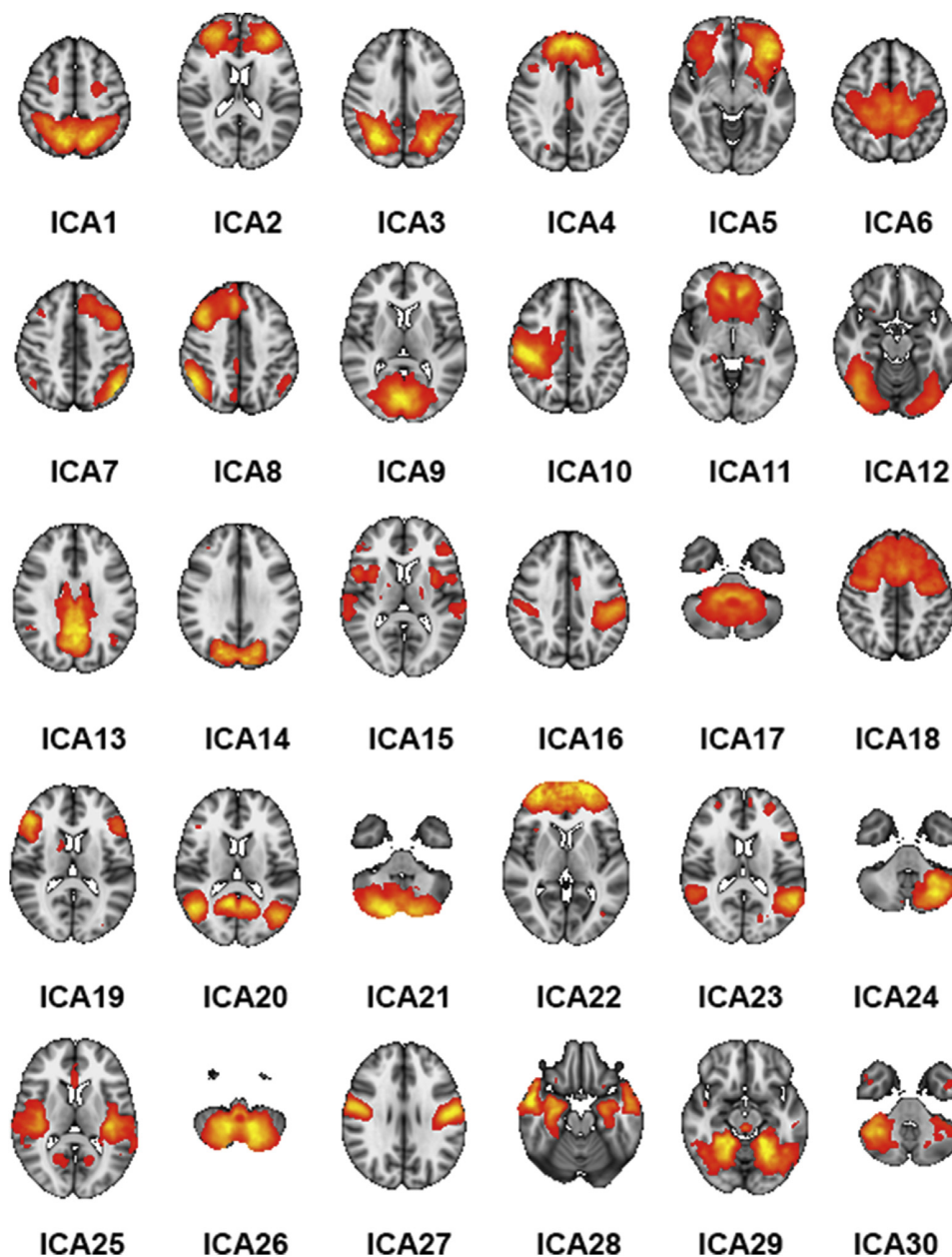


Figure 1. Probabilistic lesion heat-map across all stroke patients with coordinates in MNI-space. Colors towards the yellow range indicate higher degree of lesion overlap across the stroke group.



**Figure 2.** The 30 networks derived from the ICA numbered from top left to bottom right. The color scale refers to z-scores, and all maps were thresholded at  $z > 3$ .

In order to assess the predictive value of the FC measures on the individual level we employed a multivariate machine learning approach based on our previous work (Alnæs et al., 2015; Dørum et al., 2017). We used the network edges to classify task condition across and within groups, and also classified group (case/control) across and within task conditions, using a regularized linear discriminant classifier (shrinkage LDA) (Friedman, 1989; Schäfer and Strimmer, 2005). To avoid bias due to the uneven group sizes, we performed the group classification within a nested loop of 100 iterations, in which we each time randomly picked healthy controls to match the sample size of the patient group. The robustness of the models was assessed using leave-one-out cross-validation to avoid overfitting and permutation testing across 10,000 iterations to compare the predictive value to empirical null distributions.

In order to assess the univariate associations at the edge level, we performed repeated measures ANOVA to test for effects of group, task

condition (rest, L1, L2) for each edge, and their interactions. We computed edgewise F-stats and adjusted the alpha level using false discovery rate (FDR) for each test separately with an FDR level  $q = 0.05$  and a threshold based on the assumption of independence or positive dependence (Nichols, 2009; Nichols and Hayasaka, 2003).

### 3. Results

#### 3.1. Sample descriptives

We included 44 patients with ischemic stroke in the present analyses. Of the 54 patients initially enrolled in the study, 10 were excluded (3 were diagnosed with diseases other than stroke, 3 had stroke-related visual and/or motor impairments rendering them incapable of performing the MOT task, 4 were unable to complete the MRI protocol and/or the neuropsychological tests). Table 1 provides individual patient level

information regarding lesion location, stroke classification and days between stroke incident and MRI scan.

Table 2 summarizes key demographics, neuropsychological data and MOT performance for both groups, as well as stroke severity for the patient group as assessed by NIHSS. There were no significant group differences in any demographic variables, MoCA scores or MOT performance between patients and healthy controls.

### 3.2. Group difference in head motion

Independent samples t-tests revealed no significant difference in motion during rest [mean (SD)<sub>controls</sub> = .09 (.05), mean (SD)<sub>patients</sub> = .11 (.08), t = -1.54 p = .13]; during L1 [mean (SD)<sub>controls</sub> = .11 (.08), mean (SD)<sub>patients</sub> = .13 (.09), t = -1.50, p = .14]; and during L2 [mean (SD)<sub>controls</sub> = .14 (.14), mean (SD)<sub>patients</sub> = .15 (.09), t = -.65, p = .52].

### 3.3. Classification analysis

Figure 3 shows the confusion matrices from all classification analyses. The algorithm distinguished resting state from both load conditions with high accuracy (mean classification accuracy across groups: 95.83%,  $p_{perm} < .0001$ , chance level = 30%). Classification of load conditions revealed minimal group differences, specifically L1 yielded slightly higher accuracy in the control group (L1: 67%  $p_{perm} < .0001$ ) than in the stroke group (L1: 61.36%,  $p_{perm} < .0001$ ), for load condition L2 classification accuracy was slightly higher for the stroke group (L2: 63.64%,  $p_{perm} < .0001$ ) than the healthy control group (L2: 58.00%,  $p_{perm} < .0001$ ).

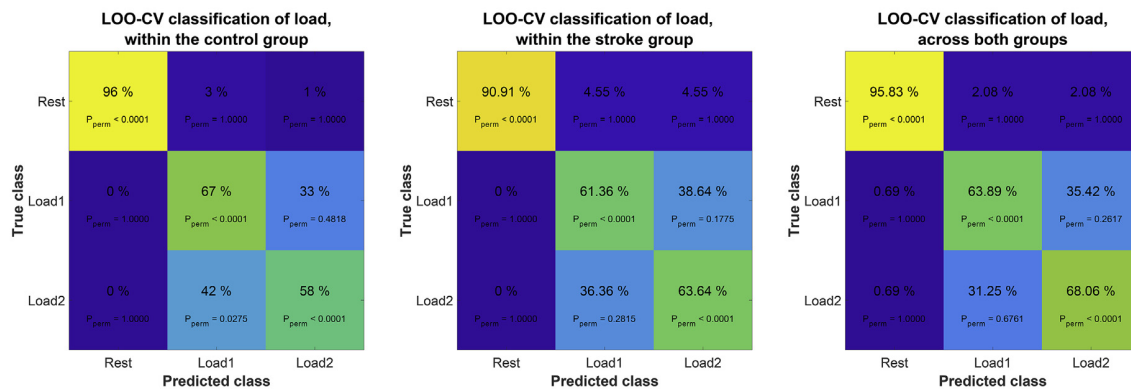
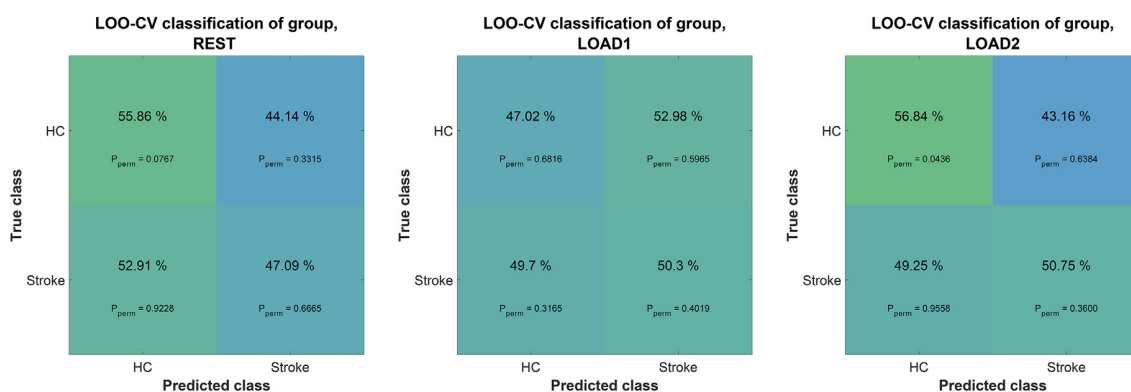
We further trained the classifier to distinguish stroke patients from healthy controls based on data from resting state or each of the two load conditions separately. Briefly, classification performance was low, and, except for stroke group accuracy at L2, none of the classification tasks

**Table 1.** Patient sample with classification according to TOAST, lesion location, lesion size and days between stroke incident and MRI scan.

Patient	Lesion classification	Lesion location	Lesion size (in mm <sup>3</sup> )	Days between stroke and MRI
1	Cardioembolism	Right temporooccipital cortex	25592	5
2	Large artery atherosclerosis	Right cerebellum	1216	1
3	Cardioembolism	Right sided subcortical stroke	36624	3
4	Small vessel occlusion	Left corona radiata	167416	8
5	Large artery atherosclerosis	Right precentral gyrus, right external capsule and left postcentral gyrus	3176	3
6	Large artery atherosclerosis	Right frontoparietal cortex	10808	6
7	Cardioembolism	Right cerebellum	15232	2
8	Large artery atherosclerosis	Pons	4664	5
9	Large artery atherosclerosis	Left frontoparietal cortex	7560	8
10	Large artery atherosclerosis	Right occipital cortex	7480	8
11	Small vessel occlusion	Right basal ganglia	1336	8
12	Large artery atherosclerosis	Left cerebellum	9680	11
13	Large artery atherosclerosis	Left cerebellum	6072	8
14	Large artery atherosclerosis	Left occipital cortex	7256	13
15	Large artery atherosclerosis	Right middle frontal gyrus	1456	23
16	Large artery atherosclerosis	Right frontal cortex	5000	5
17	Cardioembolism	Right frontoparietal cortex	15904	2
18	Cardioembolism	Left occipital cortex	3584	8
19	Cardioembolism	Left centrum semiovale	2736	7
20	Small vessel occlusion	Right basal ganglia	20128	7
21	Stroke of undetermined etiology	Left parietal cortex	5584	12
22	Large artery atherosclerosis	Left frontal cortex	19624	17
23	Cardioembolism	Multiple emboli in right frontotemporooccipital cortex	27848	6
24	Large artery atherosclerosis	Right occipital cortex	2392	7
25	Large artery atherosclerosis	Three cortical and subcortical emboli left hemisphere	21624	11
26	Small vessel occlusion	Left external capsule	1160	7
27	Small vessel occlusion	Left thalamus	1736	4
28	Cardioembolism	Right precentral gyrus	19384	8
29	Small vessel occlusion	Right internal capsule	9720	11
30	Cardioembolism	Right cella media	13944	9
31	Small vessel occlusion	Right cerebellum	15432	11
32	Cardioembolism	Medulla oblongata	2240	11
33	Small vessel occlusion	Right cerebellum	12520	9
34	Small vessel occlusion	Pons and left splenium of corpus callosum	5712	6
35	Small vessel occlusion	Left caudate nucleus	93752	2
36	Cardioembolism	Left insula and left corona radiata	10432	11
37	Cardioembolism	Left temporal cortex	5072	8
38	Small vessel occlusion	Bilateral cerebellum	12840	12
39	Small vessel occlusion	Left temporooccipital cortex	19096	16
40	Small vessel occlusion	Medulla oblongata and multiple frontoparietooccipital emboli	1552	6
41	Small vessel occlusion	Pons	10712	7
42	Stroke of undetermined etiology	Right postcentral gyrus and middle frontal gyrus	2504	5
43	Small vessel occlusion	Left corona radiata	6152	8
44	Small vessel occlusion	Left internal capsule	6728	9

**Table 2.** Demographics, stroke severity, and neuropsychologic performance. Standard deviations in parentheses.

	Stroke	Healthy controls	$\chi^2 / t$	p
N	44	100		
Age	63.11 (14.8)	63.12 (11.2)	$t = .00$	.99
Age range	34–87	35–81		
Percent male	75.0	60.0	$\chi^2 = 3.00$	.08
Percent righthanded	92.0	90.90	$\chi^2 = .48$	.83
Years of education	15.18 (2.0)	15.82 (2.9)	$t = 1.52$	.13
MoCA	26.91 (2.6)	27.65 (1.7)	$t = 1.75$	.09
NIHSS	.73 (1.17)	NA		
MOT accuracy L1	77.7 (24.9)	84.0 (24.0)	$t = 1.42$	.16
MOT response time L1	1.13 (0.2)	1.16 (0.2)	$t = .66$	.51
MOT accuracy L2	66.5 (23.9)	71.7 (23.5)	$t = 1.22$	.23
MOT response time L2	1.17 (0.3)	1.22 (0.2)	$t = 1.04$	.30

**A****B****Figure 3.** Confusion matrices from various classification tasks. A) Classification of the three conditions (rest, L1 and L2) within the stroke group, the healthy control group and across groups. B) Classification of the two groups (stroke and healthy controls) within resting state, load 1 and load 2.

performed substantially better than chance level as estimated using permutation testing. Using resting state data, we achieved 47.09 % classification accuracy for identifying the stroke group ( $p_{perm} = .67$ ) and 55.86% accuracy for identifying healthy controls ( $p_{perm} = .08$ ). Accuracy when using L1 was 50.3% ( $p_{perm} = .40$ ) and 47.02% ( $p_{perm} = .68$ ) for the stroke and healthy control group, respectively. Accuracy using L2 was 50.75% ( $p_{perm} < .36$ ) for patients and 56.84% ( $p_{perm} = .04$ ) for controls.

### 3.4. Edgewise univariate analysis

Figure 4 and Figure 5 summarize the results from the repeated measures ANOVA testing for A) main effect of condition, B) main effect of group and C) group by condition interaction effect. Repeated measures ANOVA

revealed 210 edges showing significant main effect of condition. The edges showing strongest effect of condition were observed between nodes 14–20 (visual-DMN;  $F = 122.62$ ,  $p < .001$ ), nodes 1–7 (DAN-left frontoparietal;  $F = 119.53$ ,  $p < .001$ ), nodes 1–16 (DAN-supramarginal gyrus;  $F = 117.76$ ,  $p < .001$ ), nodes 1–27 (DAN-sensorimotor;  $F = 113.56$ ,  $p < .001$ ) and nodes 10–13 (right sensorimotor-DMN;  $F = 96.78$ ,  $p < .001$ ).

Among 41 edges showing nominally significant group differences, one edge remained significant after correction for multiple comparisons ( $p < .05$ , adjusted using FDR). The significant edge connected nodes 23 and 27 (temporal-sensorimotor;  $F = 23.08$ ,  $p < .001$ ), and showed a task-dependent increase in connectivity strength for both groups, with significantly higher connectivity in the stroke group during resting state and both task loads.

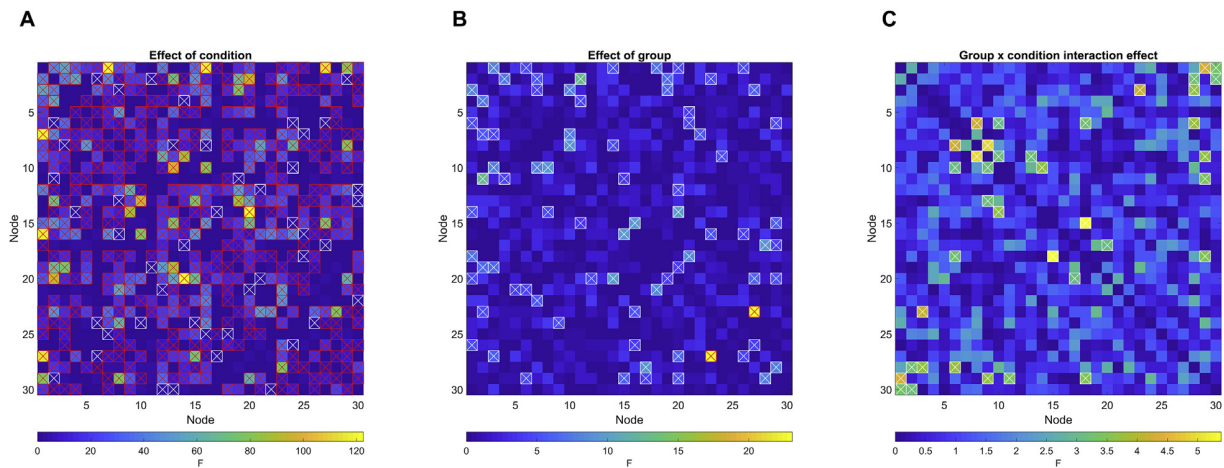


**Figure 4.** Edgewise repeated measures ANOVA. A) Main effect of condition, B) Main effect of group, C) Group by condition interaction effect. Red-crossed boxes denotes FDR-significant edges; white-crossed boxes denote nominally significant ( $p < .05$ ) edges.

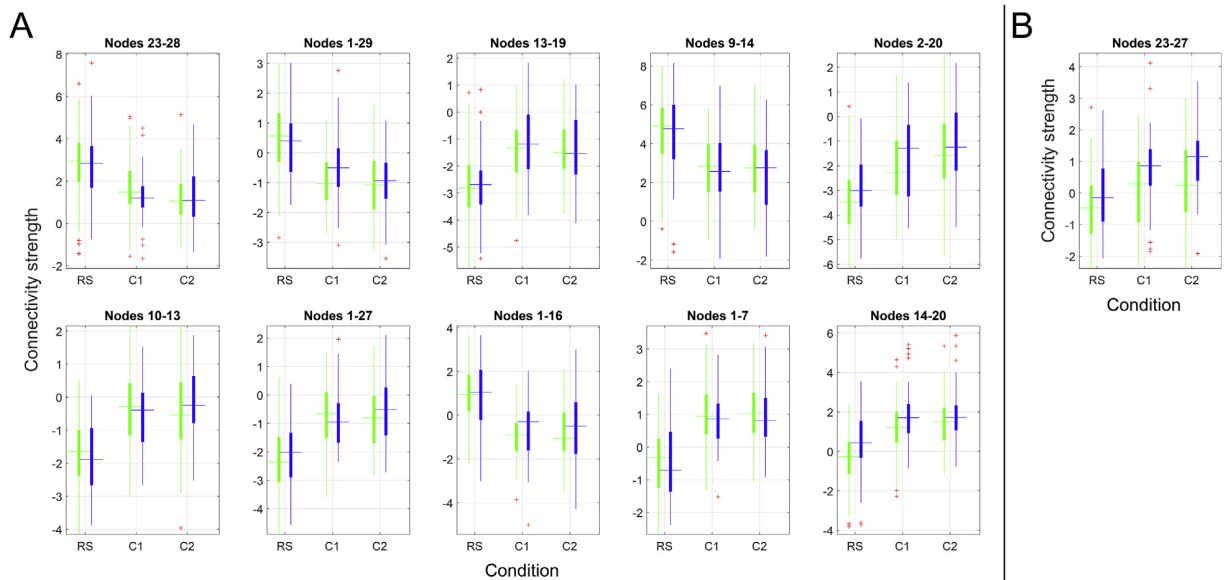


**Figure 5.** Differences in functional connectivity for stroke patients (blue) and healthy controls (green) during the three conditions for A) the 10 edges showing strongest effect of condition and B) the single edge showing FDR-significant group effect. The values on the y-axes represent the strength of the relevant node-by-node connection, as indexed by the regularized correlation coefficient from the current network modeling approach.

18 edges showed nominally significant group by condition interactions, however none survived FDR correction.

### 3.5. SDSA

Figure 6 visualizes the results of the nodewise SDSA analysis. Repeated measures ANOVA revealed a significant ( $p < .05$ , FDR corrected) main effect of condition for 19 nodes. Strongest effect of condition was observed in node 20 [(inferior frontal gyrus),  $F = 205.96$ ,  $p < .001$ ], node 15 [(DAN),  $F = 150.00$ ,  $p < .001$ ], node 13 [(DMN),  $F = 104.98$ ,  $p < .001$ ], node 24 [(cerebellum),  $F = 57.85$ ,  $p < .001$ ] and node 23 [(temporal lobe),  $F = 48.64$ ,  $p < .001$ ]. Briefly, the frontal gyrus, DAN, DMN and temporal lobe nodes showed a task-related decrease in signal variability whereas a task-related increase was observed in the cerebellar node. FDR adjustment revealed no significant main effects of group and no significant interaction between group and condition on node-wise SDSA.

## 4. Discussion

Identifying sensitive imaging markers for early evaluation of severity and prognosis is important for improving patient stratification and personalized approaches in stroke care. In an attempt to classify patients with sub-acute strokes from healthy controls, we used fMRI-based brain network approaches to estimate indices of brain functional connectivity during an unconstrained resting state, and during two load levels of a multiple object tracking task. In line with our previous studies (Dörum et al., 2017), the classification analysis successfully distinguished between resting state and attentive tracking, with accuracies approaching 100% across groups. Despite the high sensitivity to experimental condition, and contrary to our initial hypothesis, the algorithm was not able to robustly distinguish between patients and healthy controls. Based on a notion of effort-dependent aberrations in brain functional organization, we had anticipated that increasing cognitive demand would increase the ability to discriminate between groups, however, the results did not

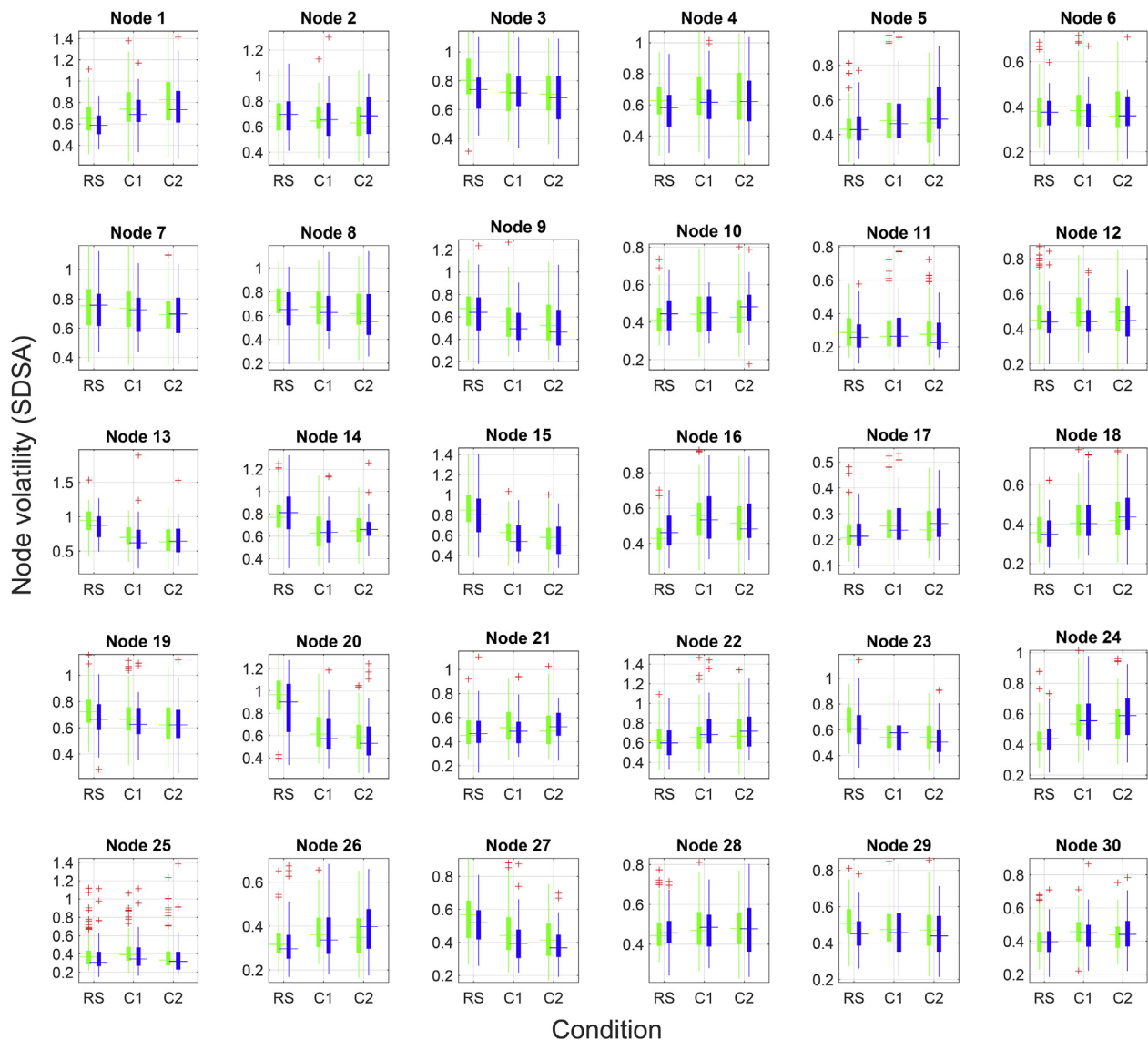


**Figure 6.** Visualization of nodewise SDSA for the 30 non-noise components for stroke patients (blue) and healthy controls (green) during resting state and two load levels of the continuous tracking task.

support this hypothesis as increasing load levels had negligible effect on classification accuracy.

The results obtained using machine learning based classification were largely supported by the univariate edgewise analyses. Edge-level findings revealed strong main effects of condition on a range of edges, only one edge showing significant main effects of group, and no significant interactions between group and condition. The strong effects of experimental condition were corroborated in our node-wise analysis, showing robust modulation of task condition on SDSA in 19 of the 30 nodes, but no significant group differences.

In our previous study (Dørum et al., 2017), multivariate classification using the full set of FC indices yielded robust discrimination between groups of younger and older healthy adults as well as between states of rest and task engagement, thus providing a sensitive framework in which to explore age-related changes in neurobiology and their interactions with cognitive states. Correspondingly - employing the same classification analysis - we expected to find robust discrimination between a group of stroke sufferers and healthy adults. Whereas results in this study indicate high accuracy when classifying between resting state and two levels of attentional demand; group discrimination performed at

chance-level. Machine learning and pattern recognition algorithms enable the capture of multivariate associations beyond traditional univariate analyses and are thus sensitive to differences in spatially distributed patterns of FC, which may serve as noninvasive biomarkers for disease. This methodological approach is congruent with the contemporary view of the brain as an integrative network, and has proven sensitive to distinguish group differences in multiple disease states (Arbabshirani et al., 2013; Craddock et al., 2009; Plitt et al., 2015).

Considering the dependency of FC on cognitive context, we hypothesized that a constrained cognitive task paradigm would comprise a more sensitive context for the study of brain network alterations after a cerebral stroke. In our previous study (Dørum et al., 2017), we found this paradigm to increase classification accuracy between a group of older and a group of younger healthy adults, and thus we expected to find a similar trend in classifying between a group of stroke patients and a matched cohort of healthy adults. Results did not support this hypothesis, however, as group classification accuracy revealed no substantial differences from resting-state to the two load levels of the attention task.

It is possible that the poor group discriminability can be partly explained by the relative high functioning of the stroke sample. The

inherent demands of the study biased patient selection towards less clinically severe strokes – reflected in an average NIHSS score below 1. Further, although healthy controls on average performed better than the stroke group in the cognitive assessment tests as well as during both load levels of the MOT-task, as indexed by response accuracy, these group differences were not found to be statistically significant. Thus, neuropsychological data corroborated the classification analyses with results indicating that clinically mild strokes may result in minimal behavioral and neural network-level effects beyond the area of the lesion. Another, not mutually exclusive aspect of the patient sample is a high level of premorbid functioning. It is possible that patients with higher cognitive capacity are more motivated and able to participate compared with the general stroke population, and that mechanisms related to their premorbid functioning are involved in explaining the apparent null effect. This hypothesis needs to be tested in future studies including lower functioning patients.

Multivariate analysis revealed chance-level discrimination between the stroke group and the healthy controls. Univariate repeated measures ANOVAs probing group differences revealed a significant main effect of group in an edge connecting a temporal and a sensorimotor node where connectivity strength was stronger in the stroke patients than the healthy controls.

Whereas group differences were subtle, a strong network response was observed across groups when participants were engaged in state of effortful attention. The repeated measures ANOVA identified significant main effects of task condition in several edges. The DAN was the network mostly implicated, showing a task-related reduction in connectivity with nodes in the somatosensory, supramarginal and fusiform cortices, as well as a task-related increase in connectivity with a left-lateralized frontoparietal node. Indicating reduced temporal coherence between task-relevant and task-irrelevant networks and stronger coherence within task-relevant networks when participants were in a state of effortful attention. Our analyses revealed no significant interactions between group and task condition, suggesting similar task modulation in FC in the two groups.

Using a similarly heterogeneous sample of stroke patients 1–2 weeks post-stroke incident, Baldassare et al. (2014) found an association between severity of post-stroke deficits and reduction in interhemispheric FC between the DAN and sensorimotor networks as well as higher FC between the usually anticorrelated DAN and DMN. Negative correlation between the internally oriented DMN and the externally focused DAN suggests a competitive relationship between these networks, and reduced anticorrelation or node differentiation has been observed in advancing age (Dørum et al., 2016), Alzheimer's Disease (Weiler et al., 2017) and Parkinson's Disease (Baggio et al., 2015), and might thus reflect neural network degeneration.

Brain signal variability facilitates transition between network configurations and reflects neural network adaptability and efficiency to respond to a greater range of stimuli. Lifespan developmental trajectories conform to an inverted U-shaped curve with less variability in the extremes of age and higher variability during adulthood (Garrett et al., 2010; McIntosh et al., 2008) similar to the quadratic trajectories observed for a range of cerebral health measures such as white matter properties (Westlye et al., 2010; Yeatman et al., 2014) and network modularity (Zuo et al., 2017). Studies have reported a positive association between BOLD signal variability and superior, as well as more consistent performance on a range of cognitive tasks (Garrett et al., 2011, 2012). Thus, we hypothesized higher signal variability for healthy adults compared to stroke patients, reflecting healthier neural dynamics. However, commensurate with edge-level results, our findings revealed no significant group differences in nodal signal variability, further corroborating the notion that clinically mild strokes yield minimal whole-brain neuronal effects.

Whereas group differences were indiscernible, task effects were substantial, reflected in 19 out of 30 nodes showing significant task modulation on node SDSA. Strongest effects were observed in task-

positive frontoparietal networks and the task-negative DMN, as well as the cerebellum. The effects of task were consistent with findings in our previous study, where we observed both task-induced increases and decreases in signal variability for task-positive nodes, and a uniform decrease in SDSA for the DMN.

The present study should be interpreted with certain considerations in mind. The lack of discernable FC alterations between stroke patients and healthy controls might in part be explained by the patient recruitment procedure, specifically the lengthy and demanding task-fMRI session requisite for study participation. Considerable demand was placed on the patients having intact cognitive, motor and visual functions shortly following the stroke incident. As a result, the final patient selection did not reflect a representative cross-section of stroke patients admitted to stroke wards, but rather patients with clinically mild strokes which were exclusively of ischemic etiology, as ischemic strokes are both more common and less debilitating than hemorrhagic strokes (Andersen et al., 2009). Further, the stroke patients had lesions of heterogeneous size and localization, which could lead to effects in the patient group being averaged out and induce variability and bias in the group ICA. To remove common variance with the lesion proper on the network modeling, the individual lesion masks were included as an additional component in the dual regression run which estimated the time series for each node. Hence, the time series that went into the network modeling were independent of the time series of the lesion. A possible methodological explanation for the absence of significant group differences is the dimensionality of the networks derived from the ICA. We estimated networks at a model order of 40 components. The ability to detect group differences in FC may vary as a function of ICA model order (Abou Elseoud et al., 2011), and future studies in larger samples may be able to test the sensitivity to group differences across a range of model orders. Results in this study should be interpreted with care as even mild strokes induce a cascade of neurobiological responses. The absence of group findings on node and edge-level as well as behavioral tests does not infer an absence in neurobiological differences, but reflect the relative insensitivities of the analyses techniques and suggests that for a select subset of patients, the immediate effects of a cerebral stroke can be slight.

In conclusion, the main findings in this study demonstrate that FC patterns between a group of sub-acute stroke patients and a group of healthy controls were indiscernible using multivariate machine learning classification. While we observed high classification accuracy between data obtained during an unconstrained resting state and data obtained during a constrained attentive tracking task, this increase in cognitive demand did not yield an increase in group classification accuracy. Complimentary node-level analyses corroborated the edge-level findings converging on minimal whole-brain neuronal effects of clinically mild ischemic strokes.

## Declarations

### Author contribution statement

Erlend S. Dørum: Conceived and designed the experiments; Performed the experiments; Analyzed and interpreted the data; Contributed reagents, materials, analysis tools or data; Wrote the paper.

Tobias Kaufmann, Dag Alnæs: Conceived and designed the experiments; Performed the experiments; Analyzed and interpreted the data.

Geneviève Richard, Knut K. Kolskår: Conceived and designed the experiments; Performed the experiments; Contributed reagents, materials, analysis tools or data.

Andreas Engvig, Hege Ihle-Hansen: Contributed reagents, materials, analysis tools or data.

Anne-Marthe Saunders, Kristine Ulrichsen: Performed the experiments; Contributed reagents, materials, analysis tools or data.

Jan Egil Nordvik: Conceived and designed the experiments; Analyzed and interpreted the data; Wrote the paper.

Lars T. Westlye: Conceived and designed the experiments; Analyzed and interpreted the data; Contributed reagents, materials, analysis tools or data; Wrote the paper.

#### Funding statement

This work was supported by the Research Council of Norway (204966/F20), the South-Eastern Norway Regional Health Authority (2013054, 2014097, 2015073), the Norwegian Extra Foundation for Health and Rehabilitation (215/FO5146), and the European Research Council under the European Union's Horizon 2020 research and Innovation program (ERC StG, Grant 802998).

#### Competing interest statement

The authors declare no conflict of interest.

#### Additional information

No additional information is available for this paper.

#### References

- Abou Elseoud, A., Littow, H., Remes, J., Starck, T., Nikkinen, J., Nissilä, J., Kiviniemi, V., 2011. Group-ICA model order highlights patterns of functional brain connectivity, 5, 37.
- Adams, H.P., Bendixen, B.H., Kappelle, L.J., Biller, J., Love, B.B., Gordon, D.L., Marsh, E.E., 1993. Classification of subtype of acute ischemic stroke. Definitions for use in a multicenter clinical trial. TOAST. Trial of Org 10172 in Acute Stroke Treatment. *Stroke* 24 (1), 35–41.
- Alnæs, D., Kaufmann, T., Richard, G., Duff, E.P., Sneve, M.H., Endestad, T., Westlye, L.T., 2015. Attentional load modulates large-scale functional brain connectivity beyond the core attention networks. *Neuroimage* 109, 260–272.
- Andersen, K.K., Olsen, T.S., Dehlendorf, C., Kammersgaard, L.P.J.S., 2009. Hemorrhagic and ischemic strokes compared: stroke severity, mortality, and risk factors, 40 (6), 2068–2072.
- Arbabshirani, M.R., Kiehl, K., Pearlson, G., Calhoun, V.D., 2013. Classification of schizophrenia patients based on resting-state functional network connectivity, 7, 133.
- Baggio, H.C., Segura, B., Sala-Llonch, R., Marti, M.J., Valldeoriola, F., Compta, Y., Junqué, C., 2015. Cognitive impairment and resting-state network connectivity in Parkinson's disease, 36 (1), 199–212.
- Baldassarre, A., Ramsey, L., Hacker, C.L., Callejas, A., Astafiev, S.V., Metcalf, N.V., Carter, A.R., 2014. Large-scale changes in network interactions as a physiological signature of spatial neglect. *Brain* awu297.
- Beckmann, C.F., Smith, S.M., 2004. Probabilistic independent component analysis for functional magnetic resonance imaging. *Med. Imag. IEEE Trans.* 23 (2), 137–152.
- Brier, M.R., Mitra, A., McCarthy, J.E., Ances, B.M., Snyder, A.Z., 2015. Partial covariance based functional connectivity computation using Ledoit–Wolf covariance regularization. *NeuroImage* 121, 29–38.
- Bullmore, E., Sporns, O., 2009. Complex brain networks: graph theoretical analysis of structural and functional systems. *Nat. Rev. Neurosci.* 10 (3), 186–198.
- Carter, A.R., Shulman, G.L., Corbetta, M., 2012. Why use a connectivity-based approach to study stroke and recovery of function? *NeuroImage* 62 (4), 2271–2280.
- Compte, A., Brunel, N., Goldman-Rakic, P.S., Wang, X.-J., 2000. Synaptic mechanisms and network dynamics underlying spatial working memory in a cortical network model. *Cerebr. Cortex* 10 (9), 910–923.
- Cordova-Palomera, A., Kaufmann, T., Persson, K., Alnaes, D., Doan, N.T., Moberget, T., Westlye, L.T., 2017. Disrupted global metastability and static and dynamic brain connectivity across individuals in the Alzheimer's disease continuum. *Sci. Rep.* 7, 40268.
- Craddock, R.C., Holtzheimer III, P.E., Hu, X.P., Mayberg, H.S., 2009. Disease state prediction from resting state functional connectivity. *Magn. Reson. Med.* 62 (6), 1619–1628.
- Damoiseaux, J.S., Rombouts, S., Barkhof, F., Scheltens, P., Stam, C.J., Smith, S.M., Beckmann, C.F., 2006. Consistent resting-state networks across healthy subjects. *Proc. Natl. Acad. Sci. U. S. A.* 103 (37), 13848–13853.
- de Haan, B., Clas, P., Juenger, H., Wilke, M., Karnath, H.-O., 2015. Fast semi-automated lesion demarcation in stroke. *NeuroImage: Clin.* 9, 69–74.
- Dickerson, B.C., Agosta, F., Filippi, M., 2016. fMRI in neurodegenerative diseases: from scientific insights to clinical applications. *fMRI Tech. Prot.* 699–739.
- Dørum, E.S., Alnæs, D., Kaufmann, T., Richard, G., Lund, M.J., Tønnesen, S., Gjertsen, Ø., 2016. Age-related differences in brain network activation and co-activation during multiple object tracking. *Brain Behav.* 6 (11).
- Dørum, E.S., Kaufmann, T., Alnæs, D., Andreassen, O.A., Richard, G., Kolskår, K.K., Westlye, L.T., 2017. Increased sensitivity to age-related differences in brain functional connectivity during continuous multiple object tracking compared to resting-state. *NeuroImage* 148, 364–372.
- Ferstl, E.C., Neumann, J., Bogler, C., Von Cramon, D.Y., 2008. The extended language network: a meta-analysis of neuroimaging studies on text comprehension. *Hum. Brain Mapp.* 29 (5), 581–593.
- Friedman, J.H., 1989. Regularized discriminant analysis. *J. Am. Stat. Assoc.* 84 (405), 165–175.
- Garrett, D.D., Kovacevic, N., McIntosh, A.R., Grady, C.L., 2010. Blood oxygen level-dependent signal variability is more than just noise. *J. Neurosci.* 30 (14), 4914–4921.
- Garrett, D.D., Kovacevic, N., McIntosh, A.R., Grady, C.L., 2011. The importance of being variable. *J. Neurosci.* 31 (12), 4496–4503.
- Garrett, D.D., Kovacevic, N., McIntosh, A.R., Grady, C.L., 2012. The modulation of BOLD variability between cognitive states varies by age and processing speed. *Cerebr. Cortex* bhs055.
- Grady, C.L., Garrett, D.D., 2014. Understanding variability in the BOLD signal and why it matters for aging. *Brain Imag. Behav.* 8 (2), 274–283.
- Hampson, M., Peterson, B.S., Skudlarski, P., Gatenby, J.C., Gore, J.C., 2002. Detection of functional connectivity using temporal correlations in MR images. *Hum. Brain Mapp.* 15 (4), 247–262.
- Hanakawa, T., Dimyan, M.A., Hallett, M., 2008. Motor planning, imagery, and execution in the distributed motor network: a time-course study with functional MRI. *Cerebr. Cortex* 18 (12), 2775–2788.
- He, B.J., Snyder, A.Z., Vincent, J.L., Epstein, A., Shulman, G.L., Corbetta, M., 2007. Breakdown of functional connectivity in frontoparietal networks underlies behavioral deficits in spatial neglect. *Neuron* 53 (6), 905–918.
- Helsedirektoratet, 2017. Nasjonal Faglig Retningslinjer. Retrieved from. <https://www.helsedirektoratet.no/retningslinjer/hjerneslag>.
- IBM Corp, R., 2010. IBM SPSS Statistics for Windows. IBM Corp, Armonk, NY.
- Kaufmann, T., Elvsashagen, T., Alnaes, D., Zak, N., Pedersen, P.O., Norbom, L.B., Westlye, L.T., 2016. The brain functional connectome is robustly altered by lack of sleep. *Neuroimage* 127, 324–332.
- Kaufmann, T., Skatun, K.C., Alnaes, D., Doan, N.T., Duff, E.P., Tønnesen, S., Westlye, L.T., 2015. Disintegration of sensorimotor brain networks in schizophrenia. *Schizophr. Bull.* 41 (6), 1326–1335.
- Kelly Jr., R.E., Alexopoulos, G.S., Wang, Z., Gunning, F.M., Murphy, C.F., Morimoto, S.S., Hoptman, M.J., 2010. Visual inspection of independent components: defining a procedure for artifact removal from fMRI data. *J. Neurosci. Methods* 189 (2), 233–245.
- Ledoit, O., Wolf, M., 2003. Improved estimation of the covariance matrix of stock returns with an application to portfolio selection. *J. Empir. Finance* 10 (5), 603–621.
- McIntosh, A.R., Kovacevic, N., Itier, R.J., 2008. Increased brain signal variability accompanies lower behavioral variability in development. *PLoS Comput. Biol.* 4 (7), e1000106.
- Nichols, T., 2009. FDR Implementation provided Online by Tom Nichols at. <http://www-personal.umich.edu/~nichols/FDR/>.
- Nichols, T., Hayasaka, S., 2003. Controlling the familywise error rate in functional neuroimaging: a comparative review. *Stat. Methods Med. Res.* 12 (5), 419–446.
- Nickerson, L.D., Smith, S.M., Öngür, D., Beckmann, C.F., 2017. Using dual regression to investigate network shape and amplitude in functional connectivity analyses, 11, 115.
- Ovadia-Caro, S., Villringer, K., Fiebach, J., Jungehulsing, G.J., Van Der Meer, E., Margulies, D.S., Villringer, A., 2013. Longitudinal effects of lesions on functional networks after stroke. *J. Cerebr. Blood Flow Metabol.* 33 (8), 1279–1285.
- Paulsen, J.S., Zimelman, J.L., Hinton, S.C., Langbehn, D.R., Leveroni, C.L., Benjamin, M.L., Rao, S.M., 2004. fMRI biomarker of early neuronal dysfunction in presymptomatic Huntington's disease. *Am. J. Neuroradiol.* 25 (10), 1715–1721.
- Plitt, M., Barnes, K.A., Martin, A.J.N.C., 2015. Functional connectivity classification of autism identifies highly predictive brain features but falls short of biomarker standards, 7, 359–366.
- Power, J.D., Cohen, A.L., Nelson, S.M., Wig, G.S., Barnes, K.A., Church, J.A., Schlaggar, B.L., 2011. Functional network organization of the human brain. *Neuron* 72 (4), 665–678.
- Raichle, M.E., 2010. Two views of brain function. *Trends Cognit. Sci.* 14 (4), 180–190.
- Richard, G., Kolskar, K., Sanders, A.M., Kaufmann, T., Petersen, A., Doan, N.T., Westlye, L.T., 2018. Assessing distinct patterns of cognitive aging using tissue-specific brain age prediction based on diffusion tensor imaging and brain morphometry. *PeerJ* 6, e5908.
- Salimi-Khorshidi, G., Douaud, G., Beckmann, C.F., Glasser, M.F., Griffanti, L., Smith, S.M., 2014. Automatic denoising of functional MRI data: combining independent component analysis and hierarchical fusion of classifiers. *NeuroImage* 90, 449–468.
- Schäfer, J., Strimmer, K., 2005. A shrinkage approach to large-scale covariance matrix estimation and implications for functional genomics. *Stat. Appl. Genet. Mol. Biol.* 4 (1).
- Siegel, J.S., Ramsey, L.E., Snyder, A.Z., Metcalf, N.V., Chacko, R.V., Weinberger, K., Corbetta, M., 2016. Disruptions of network connectivity predict impairment in multiple behavioral domains after stroke. *Proc. Natl. Acad. Sci.* 201521083.
- Skatun, K.C., Kaufmann, T., Tønnesen, S., Biele, G., Melle, I., Agartz, I., Westlye, L.T., 2016. Global brain connectivity alterations in patients with schizophrenia and bipolar spectrum disorders. *J. Psychiatry Neurosci.* JPN 41 (5), 331.
- Smith, S.M., Fox, P.T., Miller, K.L., Glahn, D.C., Fox, P.M., Mackay, C.E., Beckmann, C.F., 2009. Correspondence of the brain's functional architecture during activation and rest. *Proc. Natl. Acad. Sci. Unit. States Am.* 106 (31), 13040–13045.
- Smith, S.M., Hyvarinen, A., Varoquaux, G., Miller, K.L., Beckmann, C.F., 2014. Group-PCA for very large fMRI datasets. *Neuroimage* 101, 738–749.
- Smith, S.M., Jenkinson, M., Woolrich, M.W., Beckmann, C.F., Behrens, T.E.J., Johansen-Berg, H., Matthews, P.M., 2004. Advances in functional and structural MR image analysis and implementation as FSL. *NeuroImage* 23, S208–S219.

- Smith, S.M., Miller, K.L., Salimi-Khorshidi, G., Webster, M., Beckmann, C.F., Nichols, T.E., Woolrich, M.W., 2011. Network modelling methods for FMRI. *Neuroimage* 54 (2), 875–891.
- Szczepanski, S.M., Pinsk, M.A., Douglas, M.M., Kastner, S., Saalman, Y.B., 2013. Functional and structural architecture of the human dorsal frontoparietal attention network. *Proc. Natl. Acad. Sci. Unit. States Am.* 110 (39), 15806–15811.
- Van Den Heuvel, M.P., Pol, H.E.H., 2010. Exploring the brain network: a review on resting-state fMRI functional connectivity. *Eur. Neuropsychopharmacol* 20 (8), 519–534.
- Weiler, M., de Campos, B.M., de Ligo Teixeira, C.V., Casseb, R.F., Carletti-Cassani, A.F.M.K., Vicentini, J.E., JPN, n., 2017. Intranetwork and internetwork connectivity in patients with Alzheimer disease and the association with cerebrospinal fluid biomarker levels, 42 (6), 366.
- Westlye, L.T., Walhovd, K.B., Dale, A.M., Bjornerud, A., Due-Tonnessen, P., Engvig, A., Fjell, A.M., 2010. Life-span changes of the human brain white matter: diffusion tensor imaging (DTI) and volumetry. *Cerebr. Cortex* 20 (9), 2055–2068.
- Yeatman, J.D., Wandell, B.A., Mezer, A.A. J.N.c., 2014. Lifespan maturation and degeneration of human brain white matter, 5, 4932.
- Yu, Q., Erhardt, E.B., Sui, J., Du, Y., He, H., Hjelm, D., Pearlson, G.J.N., 2015. Assessing dynamic brain graphs of time-varying connectivity in fMRI data: application to healthy controls and patients with schizophrenia, 107, 345–355.
- Zappasodi, F., Olejarczyk, E., Marzetti, L., Assenza, G., Pizzella, V., Tecchio, F.J.P.O., 2014. Fractal dimension of EEG activity senses neuronal impairment in acute stroke, 9 (6), e100199.
- Zuo, X.-N., He, Y., Betzel, R.F., Colcombe, S., Sporns, O., Milham, M.P., 2017. Human connectomics across the life span. *Trends Cogn. Sci.* 21 (1), 32–45.

